Pharmacological Manipulation of Host Macrophage Responses to *Mycobacterium tuberculosis*

Mark Verway

Faculty of Medicine, Department of Physiology

McGill University

August 2014

A thesis submitted to McGill University, Graduate Studies and Research in partial fulfillment of the requirements of the degree of Doctor of Philosophy (PhD).

To Winnipeg

Contents

List of Figures and Tables

Chapter 1

Chapter 2

Chapter 3

Chapter 4

Chapter 5

Supplementary Figures and Data

Abstract

Mycobacterium tuberculosis (*Mtb*) latently infects ~2 billion people and active tuberculosis (TB) represents the leading cause of death from a curable disease. Cases of drug resistant tuberculosis have increased in recent years, driving the demand for new therapies. While antibiotics used for the treatment of tuberculosis target processes in *Mtb* which are critical for its replication and survival, host directed therapies (HDTs) have been suggested in recent years as possible adjunct therapies for the treatment of TB. The primary hypothesis of this thesis is that it is possible to change the host environment so as to make it unfavorable for the bacteria, thus limiting its capacity to replicate. In this thesis we examine two methods of manipulating the host response to infection to aid in the control of the bacteria, namely the use of vitamin D to modulate transcriptional responses and metformin to manipulate host metabolic responses.

Although vitamin D deficiency is a common feature among patients presenting with active tuberculosis, the full scope of vitamin D action during *Mtb* infection is poorly understood. As macrophages are the primary site of *Mtb* infection and are sites of vitamin D signaling, we have used these cells to understand the molecular mechanisms underlying modulation of the immune response by the hormonal form of vitamin D, 1,25-dihydroxyvitamin D (1,25D). We found that the virulent *Mtb* strain H37Rv elicits a broad host transcriptional response. Transcriptome profiling also revealed that the profile of target genes regulated by 1,25D is substantially altered by infection, and that 1,25D generally boosts infection-stimulated cytokine/chemokine responses. We further focused on the role of 1,25D- and infection-induced interleukin 1β (IL-1β) expression in response to infection. 1,25D enhanced IL-1β expression via a direct transcriptional mechanism. Secretion of IL-1β from infected cells required the NLRP3/caspase-1 inflammasome.

Due to the lack of conservation of this VDRE in mice, the impact of elevated IL-1β production was investigated in a novel model wherein infected macrophages were co-cultured with primary human small airway epithelial cells. Co-culture significantly prolonged survival of infected macrophages, and 1,25D/infection-induced IL-1β secretion from macrophages reduced mycobacterial burden by stimulating the anti-mycobacterial capacity of co-cultured lung epithelial cells. These effects were independent of 1,25D-stimulated autophagy in macrophages but dependent upon epithelial IL1R1 signaling and IL-1β-driven epithelial production of the antimicrobial peptide DEFB4/HBD2. These data provide evidence that the anti-microbial actions of vitamin D extend beyond the macrophage by modulating paracrine signaling, reinforcing its role in innate immune regulation in humans.

From a drug screen we identified metformin as being able to prolong survival of infected macrophages and control mycobacterial replication. From this, we have used the *in vitro* model of human macrophage infection with the virulent *M.tb.* strain H37Rv to measure the effects of metformin on cytokine secretion, quantification of cell death and activation of cell death pathways, and bacterial proliferation. Additionally, we have performed GC-MS analysis to characterize the host metabolic response to infection. We have also performed *in vivo* experiments testing the effects of oral metformin administration in the low-dose aerosol model of murine tuberculosis on control of bacterial burden as compared to standard tuberculosis antibiotic therapy. We demonstrate that metformin treatment induces a variety of metabolic changes within the macrophages, such as an increase of glycolysis and depletion of TCA cycle intermediates. When macrophages are faced with mycobacterium, metformin treatment preferentially decreases palmitic acid and cholesterol availability in infected macrophages compared to non-infected. Treatment of infected human and mouse macrophages with metformin

in vitro resulted in a skewing of cell death fate from necrosis to apoptosis, leading to a control of bacterial proliferation. In the *in vivo* murine model of infection, oral dose metformin did not have a significant effect on the course of infection. These results represent the first characterization of the host macrophage metabolomic response to *Mtb*, as well as the successful manipulation *in vitro* of that response for the benefit of the host in the face of infection.

Resumé

Mycobacterium tuberculosis (*Mtb*) infecte de façon latente 2 milliards de personnes à travers le monde et la tuberculose (TB) représente la cause majeure de mort par une maladie curable. Le nombre de cas de résistance aux traitements a augmenté depuis quelques années, accélérant le développement de nouvelles thérapies. Tandis que les antibiotiques utilisés dans le traitement de la tuberculose ciblent des étapes clés de la réplication et de la survie de la mycobactérie, des traitements personnalisés ont récemment suggéré que des thérapies annexes pourraient être envisageables dans le traitement de TB. Dans cette thèse, nous avons étudié deux méthodes permettant le contrôle de la réponse de l'hôte pour contrecarrer l'infection, d'abord l'utilisation de la vitamine D afin de moduler la réponse transcriptionnelle à l'infection et la metformine afin de réguler la réponse métabolique de l'hôte.

Bien que la carence en vitamine D soit une caractéristique commune des patients activement infectés par TB, le large spectre d'action de la vitamine D pendant l'infection reste peu compris et étudié. Comme les macrophages sont le site primaire d'infection par *Mtb* et sont également le site de signalisation par la vitamine D, nous avons utilisé ces cellules afin de comprendre les mécanismes moléculaires sous-jacents à la régulation de la réponse immunitaire par la forme hormonale de la vitamine D, 1,25-dihydroxyvitamin D (1,25D). Nous avons mis en évidence que la souche virulente H37Rv induisait une large réponse transcriptionnelle des macrophages. L'étude du profilage transcriptomique a également révélé que le profil des gènes cibles régulés par 1,25D est en partie altéré par l'infection, et que généralement 1,25D induit l'expression de IL-1β. La sécrétion de IL-1β par les cellules infectées requière l'inflammasome NLRP-3/caspase-1.

Dû à un manque de conservation du motif VDRE chez la souris, l'impact d'une importante sécrétion de IL-1β fût étudié dans un nouveau modèle dans lequel des macrophages infectés sont mis en co-culture avec des cellules humaines primaires d'épithélium des voies aériennes. La co-culture prolonge significativement la survie des macrophages infectés et l'induction de la sécrétion de IL-1β par l'infection et le traitement par 1,25D permet la réduction de la charge bactérienne grâce à la stimulation des capacités anti-mycobacterienne des cellules épithéliales de poumon. Ces effets sont indépendants des mécanismes d'autophagie induits par 1,25D mais dépendent de la signalisation par IL1R1 dans les cellules épithéliales, induisant l'expression de peptides antimicrobien DEFB4/HBD2. L'ensemble de ces données mettent en évidence l'activité anti-microbienne de la vitamine D dans les macrophages induisant une réponse paracrine, renforçant son rôle dans la régulation de la réponse immunitaire chez l'homme.

A partir d'un criblage de drogues, nous avons identifié la metformine comme étant capable de prolonger la survie des macrophages infectés ainsi que de contrôler la réplication mycobacterienne. A partir de ces données, nous avons utilisé un modèle *in vitro* d'infection de macrophages humain avec la souche virulente H37Rv afin de mesurer l'effet de la metformine sur la sécrétion de cytokines, l'induction d'apoptose et la prolifération bactérienne. De plus, nous avons réalisé une analyse par GC-MS (Gaz Chromatographie couplée à la Spectrométrie de Masse) afin de caractériser la réponse métabolique de l'hôte à l'infection. Nous avons également réalisé des expériences *in vivo* afin de tester l'effet de l'administration orale de metformine dans un modèle de souris infectées par aérosol par de faibles doses de TB murine, sur le contrôle de la charge bactérienne comparativement aux traitements classique d'antibiothérapies. Nous avons démontré que la metformine induit une large diversité de changements métaboliques dans les

macrophages, comme l'augmentation de la glycolyse et la suppression d'intermédiaires au cycle de Krebs. Quand les macrophages sont en présence de mycobacterium, la metformine va préférentiellement réduire l'acide palmitique et la disponibilité en cholestérol dans les macrophages infectés comparativement aux macrophages non-infectés. Le traitement *in vitro* des macrophages murins et humains infectés par *Mtb*, résulte en un switch de la mort cellulaire par nécrose vers l'apoptose, conduisant à un contrôle de la prolifération bactérienne. Dans le modèle d'infection *in vivo*, l'administration orale de metformine ne semble pas avoir d'effets sur le contrôle de l'infection. Ces résultats représentent la première caractérisation d'une réponse métabolique à l'infection par *Mtb*, ainsi que la première expérimentation *in vitro* de régulation de cette réponse à l'avantage de l'hôte face à l'infection.

Acknowledgments

I would like to thank my supervisor Dr. John White for his guidance and support, for the opportunity that he gave me to start building a career in research, and for the freedom to chase my ideas. I would also like to thank the past and current members of John's lab who have aided me my in education and improved me for their friendship, including Dr. Mario Calderon, Dr. Ana Palijan, Vassil Dimitrov, Dr. Manuella Bouttier, Ari Bitton, and Dr. Beum-Soo An.

I would like to extend my gratitude to my thesis supervisory committee members Dr. Russell Jones, Dr. Maziar Divangahi, and Dr. Marcel Behr for their encouragement and constructive criticism. I would also like to the thank the members of the Department of Physiology, which has been my home for the last five years, especially Christine Pamplin, who went out of her way to make sure that I could be a graduate student.

My work has taken me through many labs around campus, including that of Dr. Jack Antel, Dr. Behr, Dr. Robert Sladek, and Dr. Divangahi, and I would like to thank them and the members of their lab for their hospitality and assistance. This is especially the case with Dr. Jones and the entire Jones lab, including Brandon Faubert, Said Izreig, Takla Griss, Maya Poffenberger, Eric Ma, and Bozena Samborska, for their mentorship and patience with my ignorance, and to whom I owe the existence of Chapter 4.

Lastly I would like to thank Brandon for making it competitive, even on URTs.

Preface

In accordance with McGill Graduate and Postdoctoral Studies thesis preparation guidelines and approval from the thesis committee and supervisor Dr. John H. White, the results of my doctoral research are presented in manuscript-based format. The text of two original papers is included as chapters for this thesis.

The manuscripts presented in this thesis are the following:

Chapters 2:

Verway M, Bouttier M, Wang T-T, Carrier M, Calderon M, et al. (2013) Vitamin D Induces Interleukin-1β Expression: Paracrine Macrophage Epithelial Signaling Controls *M. tuberculosis* Infection. PLoS Pathogens 9(6): e1003407. doi: 10.1371/journal.ppat.1003407

Chapters 3:

Verway M, Bouttier M, Wang T-T, Carrier M, Calderon M, et al. (2013) Vitamin D Induces Interleukin-1β Expression: Paracrine Macrophage Epithelial Signaling Controls *M. tuberculosis* Infection. PLoS Pathogens 9(6): e1003407. doi: 10.1371/journal.ppat.1003407

Chapter 4:

Verway M, Faubert B, Tzelepis F, Calderon M, Divangahi M, Jones RG, White JH. (2015) Metformin Controls Replication of *M. tuberculosis* by Limiting Macrophage Cholesterol and Palmitate. (Manuscript in Submission)

Other manuscripts published during my PhD training which are not included in this thesis are as follows:

1. Tzelepis F, Verway M, Daoud J, Gillard J, Hassani-Ardakani K, Dunn J, Downey J, Gentile ME, Jaworska J, Sanchez AM, Nédélec Y, Vali H, Tabrizian M, Kristof AS, King IL, Barreiro LB, Divangahi M. (2015) Annexin1 regulates DC efferocytosis and cross-presentation during Mycobacterium tuberculosis infection. Journal of Clinical Investigation: 125(2):752-68. doi: 10.1172/JCI77014.

2. Coulombe F, Jaworska J, Verway M, Tzelepis F, Massoud A, Gillard J, Wong G, Kobinger G, Xing Z, Couture C, Joubert P, Fritz JH, Powell WS, Divangahi M. (2014) Targeted prostaglandin E2 inhibition enhances antiviral immunity through induction of type I interferon and apoptosis in macrophages. Immunity: 40(4):554-68. doi: 10.1016/ j.immuni.2014.02.013.

3. Calderon MR, Verway M, Benslama RO, Birlea M, Bouttier M, Dimitrov V, Mader S, White JH. (2014) Ligand-dependent CoRepressor contributes to transcriptional repression by C2H2 zinc finger transcription factor ZBRK1 through association with KRAB-associated protein 1. Nucleic Acids Research: 42(11):7012-27. doi: 10.1093/nar/gku413.

4. Calderon MR, Verway M, An B-S, DiFeo A, Bismar TA, Ann DK, Martignetti JA, Shalom-Barak T, White JH. (2012) Ligand-dependent Corepressor (LCoR) Recruitment by Krüppel-like Factor 6 (KLF6) Regulates Expression of the Cyclin-dependent Kinase Inhibitor CDKN1A Gene. Journal of Biological Chemistry: 287: 8662-8674.

5. Verway M, White JH, Behr MA. (2011) Vitamin D and Crohn's Disease. Functional Food Reviews: 3(4).

6. Verway M, White JH, Behr MA. (2010) Vitamin D, NOD2, autophagy and Crohn's disease. Expert Review of Clinical Immunology: 6(4), 505-8.

7. Palijan A, Fernandes I, Bastien Y, Tang L, Verway M, Kourelis M, Tavera-Mendoza LE, Li Z, Bourdeau V, Mader S, Yang XJ, White JH. (2009) Function of Histone Deacetylase 6 as a Cofactor of Nuclear Receptor Coregulator LCoR. Journal of Biological Chemistry: 284(44), 30264-30274.

8. Palijan A, Fernandes I, Verway M, Kourelis M, Bastien Y, Tavera-Mendoza LE, Sacheli A, Bourdeau V, Mader S, White JH. (2009) Ligand-dependent Corepressor LCoR Is an Attenuator of Progesterone-regulated Gene Expression. Journal of Biological Chemistry: 284(44), 30275-30287.

Author Contributions

Chapter 1

This chapter was written by Mark Verway and edited by Brandon Faubert

Chapters 2

Mario Calderon performed co-IP experiments presented in Figure S8C on samples prepared by Mark Verway. Marilyn Carrier performed siRNA knockdowns, as well and western blots presented in Figure 2.4 on samples prepared by Mark Verway. Manuella Bouttier performed ChIP experiments presented in Figure 2.3F,G on samples prepared by Mark Verway. All other work presented in this chapter was performed and analyzed by Mark Verway. Mark Verway wrote the chapter, which was edited by Maziar Divangahi, Marcel Behr, and John White. John White supervised the project.

Chapter 3

Manuella Bouttier performed the staining and imaging of cells, which is presented in Figure 3.4, on samples prepared by Mark Verway. All other work presented in this chapter was performed and analyzed by Mark Verway. Mark Verway wrote the chapter, which was edited by Maziar Divangahi, Marcel Behr, and John White. John White supervised the project.

Chapter 4

Brandon Faubert prepared and analysed samples for all GC-MS data presented throughout this chapter. Analysis of GC-MS data was performed by Mark Verway using methods developed by Brandon Faubert. Fanny Tzelepis performed staining, acquisition, and analysis of the FACS data presented in Figure 4.8. Mario Calderon prepared the blots presented in Figure S14 and S16. All other work in this chapter was performed and analyzed by Mark Verway. Mark Verway wrote the chapter. John White and Brandon Faubert edited the chapter. John White supervised the project.

Chapter 5

This chapter was written by Mark Verway and edited by Mario Calderon.

List of Abbreviations

1,25D – 1,25-dihydroxyvitamin D3

25D – 25-hydroxyvitamin D3

5-LO – 5-lipoxygenase

ADP – adenosine diphosphate

AIDS - acquired immune deficiency syndrome

AMP - adenosine monophosphate

AMPK - 5' AMP-activated protein kinase

APC – antigen presenting cell

ASC - apoptosis-associated speck-like protein containing CARD

ATP – adenosine triphosphate

BCG - Bacille Calmette–Guérin

CD4 – cluster of differentiation 4

CD8 – cluster of differentiation 8

CMI – cell-mediated immunity

CTL – cytotoxic T-lymphocyte

DC – dendritic cell

DLN – draining lymph node

DNA – deoxyribonucleic acid

DOTS - directly observed treatment, short-course

ER – endoplasmic reticulum

ETC – electron transport chain

FAD - flavin adenine dinucleotide

GFP – green fluorescent protein

HDT – host-directed therapy

HIV – human immunodeficiency virus

ICE – IL-1 cleaving enzyme

IFN-y – interferon gamma

IL-1 – interleukin 1

IL-12 – interleukin 12

IL-1R – interleukin 1 receptor

LN – lymph node

LPS - lipopolysaccharide

LTA4 – leukotriene A4

MDP – muramyl di-peptide

MDR – multi-drug resistant

MHCI – major histocompatibility complex I

MHCII - major histocompatibility complex II

mRNA – messenger RNA

mROS – mitochondrial ROS

Mtb – Mycobacterium tuberculosis

NADH - nicotinamide adenine dinucleotide

NADPH - nicotinamide adenine dinucleotide phosphate

NLRP3 - NOD-like receptor family, pyrin domain containing 3

NO – nitric oxide

NOD2 - Nucleotide-binding oligomerization domain-containing protein 2

OCT1 – organic cation transporter 1

OXPHOS – oxidative phosphorylation

PAMP – pathogen-associated molecular pattern

PDIM - phthiocerol dimycocerosate

PGE2 – prostaglandin E2

PTGES – prostaglandin E synthase

ROS – reactive oxygen species

RXR – retinoid X receptor

T2DM – type 2 diabetes mellitus

TAP - transporter associated with antigen processing

TB - tuberculosis

TCA – tricarboxylic acid cycle

TCR – T-cell receptor

TDR – totally drug resistant

TLR – Toll-like receptor

TNF-α - tumor necrosis factor alpha

TST – tuberculin skin test

VDR – vitamin D receptor

WHO – world health organization

XDR – extremely drug resistant

CHAPTER 1: Literature Review

1.1 Tuberculosis Introduction and Epidemiology

Approximately two billion people are currently infected with *Mycobacterium tuberculosis* (*Mtb*), the etiological agent of tuberculosis (TB). Despite the availability of antibiotics and the Bacille Calmette–Guérin (BCG) vaccine, eight to ten million new cases are reported every year, and in 2011 TB was responsible for 1.4 million deaths[1], making it the leading cause of death from a curable disease[2]. Eighty percent of all cases occurred in 22 countries, with half of the cases reported coming out of 5 countries in south-east Asia, and the highest rates per capita occurring in African countries, where poor control, lack of access to treatment, and HIV co-infection led to an average mortality rate of 23% in cases of active disease[3] (Figure 2.1).

The success of *Mtb* as a pathogen can be attributed to its capacity to evade the host immune system, as it has evolved numerous virulence mechanisms which delay or inhibit innate and adaptive immune responses[4]. Additionally, it has a life cycle that allows it to persist latently, and it does this in approximately 90-95% of those infected[5]. In the other 5-10% of cases where active disease occurs, or in cases of reactivation where the host immune response is no longer able to contain it, it goes on to induce the lung pathology and inflammation necessary for transmission. Immunodeficiency, especially as a result of HIV co-infection, increases the risk of active disease from 5-10% in a lifetime to ~8% per year[6].

Cases of multi-drug resistant (MDR) and extensively drug-resistant (XDR) TB have been reported in over 84 countries in recent years[7]. MDR cases are defined as those being resistant to the front line antibiotics isoniazid and rifampicin after 6 months of treatment, and XDR cases are those that are resistant to all front line treatment, in addition to any fluoroquinolone or second-line treatment. MDR cases accounted for approximately 3.7% or ~300,000 of all new cases, and

of those cases ~20% had already been treated unsuccessfully[7]. Approximately 60% of all MDR cases reported occurred in Russia, Brazil, China, India, and South Africa[7]. One report from a rural area of South Africa associated XDR with atypically high rate of mortality. The authors identified XDR *Mtb* in 53 cases of HIV positive patients, of which 52 died from the disease, with a median survival of 16 days after diagnosis[8]. Difficulty identifying MDR or XDR strains in the field means that only ~20% of patients with MDR TB are being prescribed the appropriate second-line antibiotics[9]. The declining lack of effectiveness of current treatments, in addition to the first reports of totally drug-resistant (TDR) *Mtb*[10], has made the search for new antibiotic therapies and vaccines an urgent issue.

The BCG vaccine is a live attenuated strain of *Mycobacterium bovis* which has been in widespread use for almost a century, but given the current global burden of disease, it has not proven an effective measure for full control of TB. BCG vaccination strategies have been shown to have variable efficacy, usually requiring multiple vaccinations at a young age to elicit a protective response[11]. Furthermore, the efficacy of the vaccine in preventing active pulmonary disease has been shown to be significantly less in the developing world[12]. Despite recent setbacks[13], progress has been made in development of new vaccines (reviewed in [14]), with a dozen new candidates in stage I to III clinical trials. From this there is hope that we will soon have a vaccine that is able to decrease the incidence of active disease, thus limiting the number of new cases by preventing transmission.

1.2 The History of Tuberculosis

Members of the *M. tuberculosis* complex, which includes *M. tuberculosis*, *M. africanum*,

M. canettii, *M. mungi*, and *M. bovis*, evolved from a common ancestor, *M. prototuberculosis*, about 15,000-35,000 years ago[15,16]. Genetic analysis of clinical samples has determined that there are six major lineages of *M. tuberculosis* that occur with various rates of prevalence in each geographic region[17], and appear to have resulted from an evolutionary bottleneck that occurred 15,000-20,000 years ago[18]. Sequencing has further revealed that most of the diversity currently observed within lineages has occurred within the last 250-1000 years[19].

Records of tuberculosis occur as early in civilization as the ancient Egyptians of 3000 BCE. Evidence of skeletal involvement of tuberculosis, which currently occurs in ~3% of all cases and ~11% of all extra-pulmonary cases of tuberculosis[20], and the presence of *Mtb* DNA has been documented in Egyptian mummies, and the clinical manifestations of TB were depicted in art of that era[21-23]. Tuberculosis was also documented by the ancient Greeks, where Hippocrates identified it as 'phthisis' [24], describing it as a disease of consumption common to young adults. In *Of the Epidemics,* written in 400 BCE, he said that phthisis was,

> the most considerable of the diseases which then prevailed, and the only one which proved fatal to many persons. Most of them were affected by these diseases in the following manner: fevers accompanied with rigors, of the continual type, acute, having no complete intermissions, but of the form of the semi-tertians, being milder the one day, and the next having an exacerbation, and increasing in violence; constant sweats, but not diffused over the whole body; extremities very cold, and warmed with difficulty; bowels disordered, with bilious, scanty, unmixed, thin, pungent, and frequent dejections. The urine was thin, colorless, unconcocted, or thick, with a deficient sediment, not settling favorably, but casting down a crude and unseasonable sediment. Sputa small, dense, concocted, but brought up rarely and with difficulty; and in those who encountered the most violent symptoms there was no concoction at all, but they continued throughout spitting crude matters. Their fauces, in most of them, were painful from first to last, having redness with inflammation; defluxions thin, small and acrid; they were soon wasted and became worse, having no appetite for any kind of food throughout; no thirst; most persons delirious when near death.

In an effort to rebalance the humors, the disruption of which was supposed to have resulted in disease, medical writing from this time contains a wide range of recommendations for the treatment of consumption. These include relocation to dryer and lighter climates, sea journeys, specific changes in diet, regular bathing, and as a last resort, surgical interventions[25]. Even at this time it was clear that consumption affected groups of people and exposure to those groups made

it likely that one would also contract the disease, although prior to the establishment of the germ theory of disease, the idea that it was transmissible remained debateable[25].

The modern era of tuberculosis began on March 24, 1882, when Robert Koch presented *Die Aetiologie der Tuberculose* to the Berlin Physiological Society, in which he demonstrated the tubercule bacilius as the ethological agent of TB, and outlined his postulates for establishing a causative relationship between a microorganism and a disease[26,27]. For this discovery he was awarded the Nobel Prize in Medicine or Physiology in 1905. Specialized facilities for the care of patients with tuberculosis, called sanatoria, opened in central Europe in the late 1800's, and after their early apparent successes in the treatment of TB, similar facilities were opened the world over. Although the exact protocols for treatment varied between institutions, the common approach centered on a regimen of open air and improved nutrition. While this remained the principle public health measure for the management of tuberculosis until the advent of anti-TB antibiotics, comprehensive follow-up studies of German and British sanatoria published in the early 1900's found that the 4-year survival rate of patients that had been discharged, presumably after successful treatment, was approximately 20%[28].

In 1921, Albert Calmette, the founding director of the Pasteur Institute of Lille, successfully trialed his vaccine against tuberculosis[29]. It was an attenuated strain of *M. bovis* which he had developed with his associate Camille Guérin. Following this, the Bacille Calmette–Guérin (BCG) vaccine widely adopted in Europe for the immunization of children against tuberculosis. Streptomycin, the first antibiotic with activity against *Mtb* was identified in 1944 by Schatz, Bugie, and Waksman in a report published in the Proceedings of the Society of the Society for Experimental Biology and Medicine[30]. The first clinical trial with streptomycin for the treatment of TB was not published until 1950[31]. This, in combination with the discovery of

isoniazid in 1952 and rifampicin in 1957, led to a new age of treatment, where even cases of latent TB were treated with the goal of full sterilization of the infection[29].

1.3 Tuberculosis Pathophysiology

In order to develop new vaccines and antibiotics, we must build an understanding of the responses and interplay of the innate and adaptive immune responses to *Mtb* infection. Infection typically begins with the inhalation of droplets containing *Mtb*, which have been aerosolized by the coughing of an individual with active disease (Figure 2.2). *Mtb* is an intracellular pathogen, which, upon inhalation, is able to take up residence in alveolar macrophages in the distal alveoli[32]. The first days of infection are characterized by the induction of innate immune responses, which include the release of cytokines from the infected macrophage to recruit other inflammatory cells to the site of infection, the death of the macrophage, and if these responses are unable to clear the infection, the reuptake of the bacteria by other phagocytic cells[33]. Estimates of the number of bacteria required to form a stable infection range from 1-400[34]. In many cases, the innate responses to this small number of bacteria can be sufficient to clear the infection, and there are reports that clinicians routinely exposed to *Mtb*, as well as individuals living in highly endemic areas, are able to maintain tuberculin skin test (TST) negativity[35].

If the innate responses are not sufficient to contain the infection, *Mtb* is able to take up residence and replicate in a sequence of macrophages and dendritic cells (DCs) in the alveolar space. DCs have the capacity to migrate out of the lungs into proximal draining lymph nodes (LNs) in order to activate T-cell responses, and in doing so carry *Mtb* into the LNs where it is able to develop a secondary site of infection[36-38]. The migration of infected DCs was shown in the mouse model to precede the initiation of antigen-specific $CD4^+$ T-cell responses[36], and it was

later shown that local production of antigen in the LN was required for the initiation of adaptive responses[37]. While it was previously unclear if the antigen used by DCs to prime T-cells originated from the phagocytosed the remains of apoptotic macrophages which were infected in the lung or from bacteria replicating inside the DC itself, this would suggest that the DCs which were responsible for the activation of $CD4^+$ responses were carriers of live bacteria.

Upon the initiation of adaptive responses, antigen-specific T cells migrate back into the pulmonary tissue to the primary site of infection, and in combination with the already present innate cells, form a granuloma which contains the bacteria. There they are able to activate the macrophages in an effort to clear the infection, by either the secretion of interferon-γ (IFN-γ) from $CD4^+$ T-cells, or by the lysis of infected macrophages by $CD8^+$ cytotoxic lymphocytes (CTLs)[39]. Granulomas are dynamic and highly organized structures which contain the infected phagocytic cells surrounded by a number of innate and adaptive immune cells, including $CD4^+$ and $CD8^+$ T-cells[40]. The granuloma contains the infection, and in some cases is able to clear it[41]. *Mtb* has evolved the capacity to survive and thrive in the hypoxic conditions found in the granuloma, and it can use this environment to transition to a stage of latency, while the structures of the granuloma prevent it from being cleared[39]. In this state its rate of replication decreases, which reduces the effectiveness of antibiotics that target bacterial enzymes involved in the active processes of replication. It can maintain dormancy for the remainder of the infected individual's life, or until the granuloma fails to contain it and it becomes reactivated, at which point it will progress to active disease.

1.4 Animal Models in Tuberculosis

A number of animal models have been used to build our understanding of TB and the

pathogenesis of *Mtb* infection. Considerable advances have come from the use of the mouse model of TB, especially with the use of knockout mice. From it we have been able to understand the importance and role of $CD4^+$ and $CD8^+$ T-cells, as well as the relevance of numerous cytokines, including IFN-γ[42] and TNF-α[43], in the course of *Mtb* infection. Additionally, the discovery of foamy macrophages, infected alveolar macrophages which display highly dysregulated lipid metabolism, was first documented in the mice and later confirmed in humans[44]. This led to further work documenting the role of altered lipid metabolism in TB[39,45]. The mouse model is also routinely used as the first step in the evaluation of new potential anti-TB chemotherapy[46].

There are some limitations to the mouse model. For instance, the granulomas formed in mice do not accurately replicate those found in humans, insofar as that they lack the defined structure and central caseating necrosis seen in human lesions[47]. The rabbit model is an improvement in this regard, and it has been successfully used to document the formation and progression of TB granulomas and to model TB meningitis[48-50]. Although they are substantially more expensive, non-human primates develop TB in a manner that accurately replicates human disease[51]. They have been successfully used to model the progression of disease and the dynamics of granulomas[5,41,52]. Infection of non-human primates with multiple independent strains of *Mtb* provided the first evidence that each granuloma can arise from a single mycobacteria[41,53]. Lastly, zebrafish have been used to model the balance of LTA4, TNF-α, ROS, and bacterial burden, providing us with a new understanding of the balance of inflammatory signalling in cases of TB meningitis[54-56].

1.5 Macrophages in Tuberculosis

1.5.1 Introduction

Phagocytes are the principle host to infection, and much of the work focused on understanding the initial stages of infection investigates the host-pathogen interaction that occurs between *Mtb* and macrophages or DCs. In the following we will discuss the role of the macrophage's pattern recognition receptors in the initial detection of the infection, the role of cell death fate on control of the infection and the impact that it has on the formation of adaptive immune responses, and the critical inflammatory cytokines released by innate immune cells in response to infection.

1.5.2 Pattern Recognition Receptors

Toll-like receptors are a family of surface receptors which have the capacity to detect a number of bacterial and viral molecules (Figure 2.3). They are expressed on a range of cells that participate in the innate responses to infection, including macrophages, DCs, neutrophils, and even epithelial cells. Stimulation of TLRs typically leads to a signal cascade through MyD88 which results in changes in gene transcription via modulation of the transcription factors such as NF-κB. *Mtb* produces a large number of lipoproteins that are capable to stimulating TLR2 to induce the secretion of IL-12[57]. In the context of an infected DC, it is able to use this as a mechanism of virulence, as chronic TLR2 stimulation results in a down-regulation of antigen presentation[58]. Although *Mtb* does not produce LPS, the canonical agonist of TLR4, TNF-α secretion in mouse macrophages is inhibited by treatment with a TLR4 antagonist[59]. Mice lacking TLR2, TLR4, or TLR9 have also been shown to have deficits in their long-term control

of *Mtb* infection[60-62], although the validity of these findings has recently been called into question[63].

Mtb also produces muramyl di-peptide (MDP), a molecule which can be recognized by the cytoplasmic PAMP sensor NOD2[64]. NOD2-deficient mice have also been shown to have deficits in their long-term control of mycobacterial infection. Signaling through NOD2 induces secretion of a number of inflammatory cytokines[65] including IL-32[66], induces antimicrobial responses[67,68], and induces the differentiation of monocytes into DCs[66]. This last point is critical for control of *Mtb*, as DCs are important for the generation of $CD4^+$ T-cell responses by presenting *Mtb* antigen on major histocompatibility complex II (MHCII), as well as on MHCI for the activation of $CD8^+$ T-cells. These two processes will be covered in more detail later.

1.5.3 The Importance of Apoptosis

If unable to control the replication of *Mtb*, infected cells will die by necrosis or apoptosis. In necrosis, the integrity of the plasma membrane is lost allowing the bacilli to escape and infect other cells. In apoptosis, the plasma membrane is kept intact while the cell destroys its contents by aggressive proteolytic degradation, threatening the viability of the contained mycobacteria[69].

When macrophage cultures are infected with virulent *Mtb in vitro*, some of the cells die by apoptosis, but most become necrotic[69]. Macrophages infected with avirulent strains are more likely to control the infection and die by apoptosis. In the context of tuberculosis, the mechanism of this change in cell fate is determined by the balance of LXA4 and PGE2 production, two eicosanoid lipid signalling mediators that are derived from arachidonic acid. Arachidonic acid serves as a precursor to two competing pathways, leukotrienes and prostaglandins. Higher levels of PGE2, generated by microsomal PTGES, are associated with elevated levels of apoptosis, and

higher levels of LXA4, catalyzed by 5-LO, are associated with necrosis[70] (Figure 1.4). Accordingly, mice that lack 5-LO are more resistant to infection. These findings have been reproduced in the zebrafish model of tuberculosis and shown to be relevant for understanding infection in humans[54,56].

Pro-apoptotic strains of *Mtb* elicit a larger T-cell response[71]. This has been exploited for vaccination, as the pro-apoptotic mutant strains, or apoptotic bodies from macrophages infected with these mycobacteria successfully generate a protective T-cell response[72]. Furthermore, there is building evidence that DCs can acquire antigen from apoptotic macrophages[69,71,73]. This means that apoptosis in macrophages not only reduces bacterial load in the early stages of infection, but also increases the rate of generating a $CD8^+$ T-cell response. Accordingly, human studies have revealed that genes related to apoptosis are expressed at a higher level in patients with latent TB than in patients with the active disease[74].

1.5.4 Innate Cytokines

In the following section we will discuss the cytokines secreted by macrophages which have been shown to be central to the innate immune response to *Mtb*, namely IL-1β, TNF-α, and IL-12. In addition, we will discuss the role of interferons in the activation of infected macrophages.

- IL-1β

The interleukin-1 (IL-1) family is comprised of IL-1α, IL-1β, IL-18, and IL-33. IL-1α is expressed constitutively by macrophages and epithelial cells, while IL-1β secretion is a process that is tightly controlled. The precursor form of IL-1β is a 31kDa protein which is cleaved into its

active 17kDa form by the inflammasome, a multiprotein complex that includes a range of possible pathogen-associated molecular pattern (PAMP) sensors bound to the apoptosis-associated speck-like protein containing a caspase recruitment domain (ASC), which in turn is bound to catalytically active caspase-1, also known as interleukin-1 cleaving enzyme (ICE)[75] (reviewed in [76]) (Figure 1.5).

The critical nature of IL-1 and IL-1R, the receptor for both IL-1α and IL-1β, has been established in *Mtb* infection[77]. IL-18 knockout studies have determined that it plays a very minor role, if any[78,79], and mice selectively deficient in the capacity to produce functional IL-33R displayed no difference compared to controls in their responses to infection[80]. The first studies demonstrating the importance of IL-1 signaling in control of *Mtb* infection used mice that were double knockouts for IL-1α and IL-1β or IL-1R knockouts, effectively shutting down all IL-1 signaling[81,82]. Follow-up studies demonstrated that mice only lacking IL-1β had an increased severity of infection[83]. Indeed, human genetic studies of polymorphisms associated with a more severe presentation and susceptibility to TB have identified mutations in IL-1 and IL-1R as being risk factors[84,85].

In vitro studies of *Mtb*-infected macrophages have determined that the nod-like receptor family pyrin domain-containing 3 (NLRP3) is critical for the secretion of cleaved IL-1β [78,86]. Despite this, knockout studies have shown that mice deficient in caspase-1, ASC, or NLRP3 do not have any notable deficit in their ability to control infection[78,83,87], suggesting that IL-1β is able to be cleaved by another compensatory process *in vivo*.

- TNF-α

TNF-α is of critical importance for control of *Mtb*. Knockout studies have demonstrated

that mice lacking this cytokine demonstrate an increased severity of disease and rate of mortality[43]. Recent work has shown that TNF-α is able to induce ROS in zebrafish, and that this production of ROS contributes to control of the bacteria[55]. Other reports have documented that TNF-α is critical for macrophage and DC activation, as well as a reduction in the expression of chemokines which were critical for the formation of a granuloma[88]. The balance of TNF-α production has been shown to be of significance, as low levels of TNF-α were associated with a reduced immune response that was unable to control the infection, and excessive levels were associated with a loss of control of infection due to over-inflammation[54,56]. TNF-α is also important for the maintenance of the granuloma, as demonstrated by the reactivation of disease that occurs during anti-TNF therapy in those individuals with a latent infection[89]. For this reason, any patient being evaluated for an anti-TNF therapy, which is commonly used in the treatment HIV and rheumatoid arthritis, is screened by TST to ensure that they are not host to a latent infection.

- IL-12

Macrophages and DCs secrete IL-12 in response to infection. IL-12 stimulates the development and activation of naïve T-cells and induces the secretion of IFN-γ from $CD8^+$ T cells and NK cells. IL-12 can be secreted in two forms, a homodimer of the p40 subunit known as IL-12p80, or as a heterodimer of the p40 and p35 subunits, known as IL-12p70, which signal through the IL-12RB1 and IL-12RB2 respectively[90]. The activation of T-cells is of central importance to the clearance or at least the control of infection, as seen in cases where mutation or decreased production of IL-12p40, or mutations in the IL-12RB1 gene have increased susceptibility to *Mtb* in humans[91,92].

In mouse models of *Mtb* infection, IL-12 secretion is quickly induced and IL-12p80 has been shown to be responsible for the maturation of DCs, giving them the capacity to migrate to the draining lymph node (DLN) and activate T-cells[93]. While IL-12p80 can activate T-cells, it is not sufficient to drive the expression of IFN-γ on its own, leading to susceptibility to infection in IL-12p70 deficient mice[94]. Conversely, IL-12p70 expression is not high in the lungs, but appears to be important for driving antigen-specific T-cell responses from the DLN [95,96], and is required for the maintenance of the protective Th1 response[97]. Overall it would appear that IL-12p80 is important for protective responses in the infected lung tissue, and IL-12p70 is important for activation of T-cells in the DLN[33].

- Interferons

Production of IFN-γ by $CD4^+$ and $CD8^+$ T cells in response to *Mtb* infection has been known to be critical for host defense for decades, demonstrated clearly by the hyper-susceptibility of IFN-γ knockout mice to *Mtb* infection[42,98-100]. Virulence mechanisms identified in *Mtb* have been shown to inhibit IFN-γ responses, allowing it to evade the adaptive immune response[101]. More recently it has been shown that NK cells, NKT cells, and γδ T-cells can also contribute to IFN-γ production in experiments where these cell types were adaptively transferred into deficient mice[102-104]. Specifically, depletion of NK cells from rag-/- mice demonstrated that the IFN-γ produced by these cells was partially responsible for the limited resistance to infection[102]. The relative importance of this is likely limited compared to the production of IFN-γ from $CD4^+$ and $CD8^+$ T cells, as NK depletion of WT mice show no difference in their ability to control their infection compared to the controls[105].

Conversely, Type I interferons, characterized by secretion of IFN-α and IFN-β, have been shown to promote susceptibility to mycobacterial infection[106-108]. Furthermore, mice lacking a Type I IFN receptor were more successful at controlling *Mtb* infection compared to WT mice[108]. Clinical studies have shown that higher serum levels of Type I interferons were documented in patients infected with the active disease as compared to the latently infected controls[109]. The mechanisms of this effect are not fully understood at this time.

1.6 Activation of T-cells in *Mtb* Infection

Stimulation of antigen-specific $CD4^+$ T-cells requires the presentation of *Mtb* antigen on MHC class II by macrophages or DCs[119,120]. As *Mtb* is typically found in the phagosomal compartments of these cells, which is also the natural processing route for MHC class II antigens, mycobacterial peptides are readily available for processing and presentation. In the context of *Mtb* infection, the initial priming of $CD4^+$ T-cells occurs in the DLN when a DC carrying antigen directly activates the T-cell. If an antigen-specific T-cell recognizes the peptide presented, it will undergo clonal expansion, and traffic back into the lungs to begin surveillance of the infected tissue.

Activation of $CD8^+$ T-cells requires the surface presentation of an antigen on an MHC class I molecule by an antigen presenting cell (APC) that is specific to the T cell receptor (TCR) expressed by that T-cell[121]. Similarly to the activation of $CD4^+$ T-cells, this occurs when a DC carrying antigen migrates to a lymph node and presents this antigen to the T-cells that are present[36]. The exact mechanisms underlying the origin and processing of antigen preparation on MHC class I in *Mtb* infection are poorly understood, as it is unclear if the antigen that is

presented is derived from the uptake of apoptotic vesicles from previously infected macrophages or DCs, or from viable *Mtb* that have been phagocytosed by the DC.

There is some evidence that antigen from infected macrophages was not transferred to uninfected DCs, suggesting that infected DCs are required for initiating a $CD8^+$ T-cell response[122]. In accordance with this model, bacteria can be detected in the DLN usually a few days before an antigen-specific $CD8^+$ T-cell response is initiated[123]. Corroborative experiments using a combination of FACS and GFP-labelled *Mtb* demonstrated that the majority of cells infected in the DLN and lungs after two weeks were myeloid DCs[37]. This is advantageous for the mycobacteria, as it has developed mechanisms of impairing DC activation[124], and appears to use DCs migration to disseminate throughout the host.

In opposition to this model, extracellular vesicles, later identified as apoptotic vesicles, were derived from BCG-infected macrophages and DCs *in vitro*, and were found to contain mycobacterial antigen. Incubation of these vesicles with DCs made them capable of activating $CD8^+$ T-cells in a TAP-dependent manner[73]. These vesicles were again used to successfully vaccinate mice against *Mtb* challenge, and cross-presentation of these antigens was shown to require endosomal processing[72]. Furthermore, this strategy resulted in T-cell responses which were detected sooner in transgenic mice expressing TCR for TB antigen 10.4. The same effect was seen when infected pro-apoptotic (5LO-/-) macrophages were adoptively transferred to WT mice, when compared to the rate of activation after transfer of infected WT macrophages[70]. These results suggest that the effective pathways of antigen presentation and $CD8^+$ T-cell activation do not require the migration of an infected cell to the DLN, but whether this occurs during the normal course of infection has yet to be established.

1.7 Antigen Processing and Cross Presentation

Almost all MHC class I antigens are derived by intracellular proteolysis[125,126]. Cytosolic proteins are cleaved into smaller antigenic peptides by the proteasome. Each of these peptides must be cleaved to a particular length as the structure of the binding groove of MHC class I protein requires that the protein antigen presented is 8-10 amino acids in length[127]. These proteins are then transported into the endoplasmic reticulum (ER) by transporter associated with antigen processing (TAP), where they are trimmed and loaded into the binding groove of MHC class I molecules[128], although this is not always the case[129,130]. The chaperones and loading complexes of this pathway are mostly confined to the ER[125], therefore trimming must be completed before surface presentation.

The cytosolic localization of the proteasome raises a problem for processing antigenic peptides which, in the case of *Mtb* infection, are contained in the phagosome. Despite this, it is possible for endocytosed and phagocytosed antigen to be processed and presented on MHC class I[131], in a process that has been named 'cross-presentation'[132,133], although the mechanisms of cross presentation are poorly understood[134,135].

As stated previously, it is not mechanistically clear if the DCs which activate $CD8^+$ T-cells acquire antigen from uptake of apoptotic vesicles or from phagocytosed *Mtb* (Figure 1.6). Across a number of antigenic sources, cross presentation has been shown to be more efficient for particulate antigens than soluble antigens[136], and so research on cross-presentation has focused on antigen uptake by phagocytosis instead of endocytosis. Mechanisms explaining the translocation of antigen out of the phagosome have not been identified. Most MHC class I presentation appears to be from proteins that localize to the cytosol at some point, as it has been shown to be TAP-dependent[128]. Proteases have been identified in the endosomal/vacuolar

pathway which can make small cleavage products[137,138], although their limited expression and catalytic specificity have been deemed insufficient to fully explain the preparation of antigen independent of the cytoplasmic proteasome.

Virulent *Mtb* has been shown to reduce membrane integrity via expression of ESX-1[139], a Type VII secretory system, and inhibit plasma membrane repair[69], presumably also compromising the integrity of the phagosome that contains it. This, in addition to the secretion of mycobacterial antigenic peptides (which are overrepresented as antigens[140]), would serve as a simple explanation for the cytosolic localization of antigen without invoking the presence of protein export channels located in the phagosomal membrane. Furthermore, recent evidence has shown that virulent, but not avirulent, strains of *Mtb* are able to escape the phagosome, and after 96 hours can be detected in the cytoplasm by a mechanism that is ESX-1 dependent[141]. Translocation may not be the main mechanism of antigen escape as antigen presentation has been shown to occur much faster than *Mtb* have been seen to translocate[142,143]. Additionally, antigen-specific $CD8^+$ T-cell priming in *Mtb* infection can occur independent of ESX-1 expression[144], although it is unclear if this is the result of antigen processing by an alternative pathway only available due to a decrease in virulence.

1.8 Adaptive Immune Responses in Tuberculosis

1.8.1 Introduction

Cell mediated immunity (CMI) is critical for the long-term control of *Mtb* infection in the granuloma. The granuloma contains a number of different cell types, including macrophages, neutrophils, $CD4^+$ T-cells, $CD8^+$ T-cells, and B-cells. In the following we will focus primarily on

the activation of $CD4^+$ and $CD8^+$ T-cells, their role in controlling infection, and the methods by which antigens are processed and presented.

1.8.2 The Role of $CD4^+$ and $CD8^+$ T-cells

Mouse studies have demonstrated that $CD4^+$ cells are critical for control of infection[110]. When activated, they produce IFN-γ and TNF-α, two cytokines which are important for the activation of infected macrophages. Additionally, the direct contact of $CD4^+$ T-cells with infected myeloid cells has recently been shown to be a necessary for $CD4^+$ effector function[111]. Loss of $CD4^+$ T-cells in humans, especially in cases of HIV co-infection, substantially increases the risk of active TB[112], and a decreased $CD4^+$ T-cell count is a predictor of extra-pulmonary TB[113].

While $CD4^+$ T-cells form the principle adaptive response to *Mtb* infection, $CD8^+$ T-cell have also been shown to provide a form of protection in response to infection[114]. Furthermore, *ex vivo* $CD8^+$ T-cells specific for *Mtb* antigens have been shown to be able to lyse infected macrophages, leading to control of the bacteria[115,116]. Lysis of infected macrophages may have the unintended consequence of disseminating the infection, although if the bacteria are phagocytosed by activated macrophages, it could lead to clearance of the infection[117]. Additionally, inducing the apoptosis of infected macrophages produces apoptotic bodies that contain *Mtb* and *Mtb* antigens, which are taken up by other macrophages and DCs in a process termed efferocytosis[118]. As mentioned previously, this transfer of antigen may be important for the full initiation of $CD8^+$ T-cell responses.

1.9 Host Directed Therapies

Host-directed therapies (HDTs) have been suggested as supportive measures for the treatment of TB. There are two principle strategies in the development of HDTs. Firstly, that the treatment leads to an improved rate of *Mtb* clearance, and secondly, that it reduces inflammation under circumstances where it can be deleterious to organs. With regard to the second strategy, a handful of successful clinical trials were conducted in the late 1990's where prednisolone was administered in combination with anti-*Mtb* chemotherapy[119]. Similarly, etanercept and thalidomide, both administered with the goal of decreasing TNF-α, were trialed in TB patients with positive results[120,121]. Activation of immune responses by IL-2[122] or delivery of IFN-γ by aerosol[123], along with others, have met with limited success. The timing of this administration is critical, otherwise the use of inflammatory cytokines might trigger a 'cytokine storm'. In the case of IFN-γ, patients needed to receive treatment within a window in order to see a benefit.

Recent studies in the zebrafish model of TB demonstrated that LT4A high or low status correlated with high or low levels of TNF-α[54]. This finding was extended to a human clinical population of TB meningitis where LT4H and TNF-α status, either in cases where it was very high or too low, corresponded to a less favorable disease outcome[56]. From this it was suggested that any HDT looking at modulating L4TH or TNF-α levels should be tailored to the patient's status. This work was expanded upon in the zebrafish model with the finding that high TNF-α levels produced an increased microbicidal effect, but that it led to a secondary wave of necrosis which was detrimental[55]. The authors also demonstrated that they were able to inhibit this secondary necrosis, leaving the zebrafish with the benefits of increased TNF-α while avoiding the later detriments associated with an overactive inflammatory response[55]. This approach has not yet been tested in humans.

In the following we will focus on the two methods of manipulating the host macrophage response to *Mtb* infection that are explored in chapters 3, 4, and 5, namely the modulation of the gene expression profile with 1,25-dihydroxyvitamin D and the host metabolic program with metformin.

1.10 Vitamin D

1.10.1 Vitamin D Physiology

While discovered as the cure for nutritional rickets and studied mostly for its role in calcium homeostasis, work over the last 20-25 years has revealed that vitamin D has a broad range of activities, including a role as a cancer chemopreventive agent [124], and as a regulator of immune system function [125].

Vitamin D is obtained from limited dietary sources, including fish oil and supplemented dairy products [126], as well as from the photochemical conversion of 7-dehydroxycholesterol in the skin in the presence of sufficient solar ultraviolet B radiation (295-320nm). With increasing latitude, surface solar UVB irradiation is insufficient to induce cutaneous vitamin D3 synthesis for periods around the winter solstice of 6 months or even more at the latitudes of northern Europe or Scandinavia, a period that is known as vitamin D winter. UVB-induced vitamin D synthesis is also strongly influenced by skin colour[126]. Lack of cutaneous vitamin D synthesis because of lack of sun or sun avoidance, coupled with vitamin D-poor diets, has contributed to widespread vitamin D insufficiency or deficiency[127].

The term 'vitamin D' refers collectively to vitamin D_2 (ergocalciferol), which is fungal in origin, and vitamin D_3 (cholecalciferol), which is obtained from animal sources or irradiation of skin[127] (Figure 1.7). Vitamin D compounds are constitutively hydroxylated largely in the liver by

CYP2R1 or CYP27A1 to form 25-hydroxyvitamin D (25D), the major circulating form and marker of vitamin D status. The hormonal form of vitamin D, 1,25-dihydroxyvitamin D (1,25D), is generated by 1α-hydroxylation of 25D by the enzyme CYP27B1[128-130]. With regard to vitamin D's role in calcium homeostasis, this modification occurs primarily in the kidneys. In addition to this, CYP27B1 is also expressed in several other cell types throughout the body, including cells of the immune system. Signaling by 1,25D occurs via binding to the vitamin D receptor (VDR), a member of the nuclear receptor family of ligand-regulated transcription factors. A canonical target gene of ligand-bound VDR is CYP24A1, the enzyme that catabolizes 1,25D in a negative feedback loop. The catabolic products of vitamin D are then secreted in the urine[128-130].

Ligand-bound VDR is a nuclear receptor, a class of transcription factors including the estrogen receptor (ER) and retinoic acid receptor (RAR). Ligand binding induces a conformational change in the VDR which triggers dimerization with the retinoid X receptor (RXR). The VDR, as with other nuclear receptors, recognizes and binds to highly conserved DNA binding motifs termed vitamin D response elements (VDREs)[128,131,132]. A consensus sequence for VDREs has been identified as two half sites of PuG(G/T)TCA separated by 3, 6, or 8 nucleotides[133,134]. The VDR/RXR heterodimer has the capacity to recruit other transcriptional regulators to this site, and depending on the location and context of the VDRE, this may function to enhance or suppress gene expression.

Vitamin D has been classically associated with calcium homeostasis. The renal production of 1,25D is stimulated by parathyroid hormone (PTH) and suppressed by high serum calcium. Thus vitamin D is responsible for the mineralization of bone, and accordingly, severe vitamin D deficiency can lead to rickets. Chronic vitamin D deficiency can also lead to

chronically elevated PTH, which will drive the resorption of bone, resulting in osteoporosis and an elevated risk of bone fractures.

1.10.2 Vitamin D in Immune Responses

A number of studies have been published in recent decades suggesting a link vitamin D status and susceptibility to pulmonary infectious disease, both viral and bacterial in etiology. For example, vitamin D deficiency correlated with the incidence of severe lower respiratory tract infections in India[135]. Based on this and other evidence, it has been suggested that supplementation of vitamin D might be able to reduce the incidence of infectious disease. Double-blind randomized control trials (DB-RCTs) have been conducted to test this, although they have demonstrated variable efficacy. In a Japanese study, children on 1,200 IU/day vitamin D supplementation showed a reduction in the incidence of seasonal influenza[136], although another similar study found no improvement in adults given 2000IU/day[137]. The incidence of pediatric pneumonia in Ethiopia correlated with vitamin D deficiency[138], although a DB-RCT of quarterly bolus supplementation of vitamin D in Afghani children showed no decrease in the incidence of pneumonia[139]. A difficulty in interpreting these studies is that they are inconsistent in design, they utilize different definitions of vitamin D sufficiency, and employ large differences in the dosage and timing of intervention.

Recent research has begun to unravel the mechanisms of vitamin D action in the regulation of innate and adaptive immunity[125]. Stimulation of innate immune cells triggers the release of cytokines and chemokines, which are important for the culmination of the innate immune response, as well as recruiting and activating cells of the adaptive immune system to the site of infection. In response to bacterial pathogens, the innate immune responses include the

production and release of antimicrobial peptides (AMPs)[140]. In data first published by our group, treatment of several cell lines or primary cell cultures with 1,25D induced the expression of two AMPs, human β-defensin 2 (DEFB2/DEFB4/HBD2) and cathelicidin AMP (CAMP)[141]. Moreover, conditioned media from 1,25D-treated cells acquired the capacity to kill bacteria, including the pathogen *Pseudomonas aeruginosa*. While the effect of 1,25D alone on DEFB4/HBD2 was only modest, recent work has shown that 1,25D in combination with other signaling pathways leads to robust stimulation of DEFB4/HBD2 expression. By contrast, induction of CAMP was particularly strong and subsequent follow-up studies have shown that CAMP expression is widely regulated by 1,25D both *in vitro* and *in vivo*[142-144].

The innate immune system uses pattern recognition receptors to detect the presence of conserved molecular motifs characteristic of certain families of pathogens. Importantly, TLR2/1 stimulation by *Mycobacterium tuberculosis* lipoprotein induces the expression of both the VDR and CYP27B1. Stimulated macrophages thus acquire the capacity to respond to circulating levels of 25D, underlying the central role of vitamin D signaling in human innate immune responses[143]. The observation that *NOD2* is a 1,25D target gene also links vitamin D signaling to autophagy. Stimulation of NOD2 expression by 1,25D implies that 1,25D would boost autophagy at least in part by enhancing NOD2 function. In addition, recent work has shown that 1,25D-stimulated CAMP production enhanced autophagy in mycobacteria-infected macrophages [145]. Previous work had shown that CAMP expressed in 1,25D-treated cells colocalized with mycobacterial in phagolysosomal structures. Ablation of CAMP expression decreased the number of autophagosomes in 1,25D-treated cells [145]. While this study is intriguing, it is not clear whether CAMP functioned to enhance autophagy directly or indirectly by reducing bacterial viability due to its AMP activity.

1.10.3 Vitamin D in Tuberculosis

Historically, there is a correlation between vitamin D deficiency and active TB[125,146]. Epidemiologic studies have documented a higher clinical incidence of active TB during winter months when sunlight exposure is reduced [147] and vitamin D deficiency has been identified as a common feature of patients with active TB [148-150]. In addition, certain VDR polymorphisms have been shown to be associated with a higher risk of developing TB[151]. Despite this, recent clinical trials where vitamin D was administered in combination with the standard antibiotic regimen have not revealed a substantial benefit of vitamin D in the treatment of active disease[152,153]. However, the mechanisms underlying vitamin D signaling and control of *Mtb* infection are not well understood, and the possibility remains that vitamin D deficiency predisposes one towards having active disease.

1,25D synthesis is induced in macrophages and dendritic cells upon exposure to pathogen, and the 1,25D-bound vitamin D receptor (VDR) directly induces transcription of genes encoding AMPs DEFB4/HBD2 and CAMP[141-143,154-156], both of which have demonstrated anti-mycobacterial activity[157,158]. In addition, CAMP is able to induce autophagy, and in doing so leads to the degradation of *Mtb* in autophagosomes[159]. Furthermore, human serum from vitamin D deficient individuals is not able to support the expression of normal levels of CAMP mRNA in response to TLR2 stimulation[143] and antibacterial activity in response to IFN-γ[160].

1.11 Immunometabolism

1.11.1 Introduction

The maintenance of ATP levels is critical for the functioning of all cellular life. Starting with glycolysis, glucose can be broken down into two molecules of pyruvate yielding a net 2 molecules of ATP, generated by the phosphorylation of ADP. In cells capable of oxidative phosphorylation (OXPHOS), the molecules of pyruvate can be converted into acetyl-CoA, where they can feed into the tricaboxylic acid (TCA) cycle. The chemical conversion of acetyl-CoA throughout that cycle generates NADH and $FADH_2$, two electron carriers which donate their electrons to the mitochondrial electron transport chain (ETC). The flow of the electrons from complex I or II to complex IV in the ETC generates a proton gradient across the inner mitochondrial membrane, which drives the rotation of ATP synthase to generate an additional ~36 ATP from ADP. Cells can also fuel carbon flow through the TCA cycle by the modification of glutamine in a process called glutaminolysis, and the breakdown of fatty acid chains by β-oxidation. O_2 serves as the final electron acceptor for complex IV in the ETC, and in its absence under hypoxic conditions, the flow of electrons is limited. This means that all of the ATP required for cellular processes must be generated by glycolysis, and the pyruvate produced by glycolysis is modified into lactic acid in order to regenerate NAD^+ in order for glycolysis to continue[161]. Under certain circumstances, cells can preferentially use glycolysis to generate ATP even though O_2 is available. This aerobic glycolysis was identified by Otto Warburg as a feature of cancer cells, and this pattern of cellular metabolism is now termed 'the Warburg effect' (Figure 1.8). Cells with large biosynthetic and energetic demands can switch to this less efficient method of ATP production in order to generate molecules to meet both of these requirements[162].

The study of the metabolic state of immune cells, and the impact of metabolic pathways on the ability to generate specific immune responses, as well as the impact of immune responses on metabolic pathways, has only begun to be understood[163]. The metabolic pathways used by cells to produce energy and build amino acids or fatty acids are very complex and interconnected, and the flow of carbon through one pathway or the decreased availability of another precursor can have long reaching effects. The capacity of a cell to modulate its energy production and carbon flow is critical for its ability to meet specific biosynthetic demands, and in many immune cells these demands can change rapidly depending on activation by certain triggers. In the following we will focus what is currently known about the interactions between immune responses and cellular metabolism in macrophages.

1.11.2 Macrophage Metabolism

In recent years macrophage activation programs have been categorized into two major subgroups: M1, the inflammatory IL-1 and TNF-α secreting macrophage, and M2, the anti-inflammatory IL-10 secreting macrophage. Each of these has been shown to have separate metabolic states, with M1 macrophages demonstrating Warburg metabolism with high glycolysis and decreased OXPHOS compared to unstimulated macrophages, and M2 macrophages demonstrating the opposite, with higher OXPHOS and lower glycolysis[164]. This reprogramming of cellular metabolism was shown to be important for the inflammatory responses of M1 macrophages, as overexpression of CARKL, which inhibits the pentose-phosphate pathway (PPP), led to a decrease in the secretion of inflammatory cytokines in response to LPS stimulation[165]. The PPP is also important for the generation NADPH, which can be oxidized by

NADPH oxidase to produce reactive oxygen species (ROS), and is necessary for nitric oxide (NO) production[166].

The decrease in OXPHOS seen in M1 macrophages has also been shown to be important for increasing production of ROS. ROS has been shown to play an important role in the control of intracellular bacteria[167], and in macrophages activated by TLR agonists, mitochondria were found to co-localize with phagolysosomes. The ROS produced from inhibition of TCA flow was also shown to activate the NLRP3 inflammasome, leading to an increase in IL-1β secretion[168,169]. This is notable as the cleavage of IL-1β in the context of *Mtb* infection also occurs via the NLRP3 inflammasome.

1.11.3 *Mtb M*etabolism

The metabolic networks of *Mtb* have been extensively characterized in an effort to understand how it is able to meet its biosynthetic needs, which sources of carbon it is able to use, which sources of carbon it preferentially uses, and how an understanding of these pathways might produce new targets for antibiotic or host-directed therapy. *In vitro* studies have demonstrated that *Mtb* is able to replicate using a range of carbon sources[170,171], including fatty acids, glycerol, D-glucose, and acetate. A recent paper using ^{13}C labeling of carbon sources reported that the principle source of carbon feeding *Mtb*'s central metabolism while in a host macrophage was a 2-carbon (2C) source, most likely the product of β-oxidation of fatty acids imported from the host cell[172]. This corroborated previous reports which suggested that *Mtb* was primarily using host fatty acids for energy and replication[173,174]. A 3C source was also identified, and the authors speculated that it had originated from glycerol, although this was not demonstrated. The 3C could have also originated from the processing of cholesterol by *Mtb*[175]. A

1C source was identified[172], and further experiments determined that it origination from the fixation of CO_2, confirming earlier *in vitro* reports that showed incorporation of CO_2 into *Mtb* under limited culture conditions[170,176].

With regard to amino acids, mutation studies have determined that *Mtb* which lack the capacity to produce their own leucine, proline, tryptophan, or glutamine are attenuated in *in vivo* models of infection[177-180]. Mycobacteria lacking the capacity to synthesize methionine, isoleucine, or valine showed no attenuation in *in vitro* macrophage infections[181,182], indicating that while *Mtb* may be able to synthesize some of its own amino acids, it requires the uptake of others from the host cell. Utilization of host alanine, glutamate, and aspartate was also demonstrated[172]. The uptake of alanine is notable, as alanine is used in the biosynthesis of peptidoglycan, a principle cell wall component of *Mtb*, and *Mtb* that lack the ability to process alanine demonstrate attenuation of growth[181].

1.11.4 Cholesterol Regulation in *Mtb*-Infected Macrophages

The import of cholesterol from the host has recently been shown to be of critical importance for the ability of *Mtb* to form a persistent infection[174]. Accordingly, multiple reports have established that *Mtb* can accumulate and utilize cholesterol as a carbon source[183,184], although the metabolism of cholesterol leads to the accumulation of toxic metabolites, which require the import of host fatty acids to neutralize in a pathway that generates PDIM[175], a cell wall component and virulence factor of *Mtb*. Infection with virulent, but not avirulent, *Mtb* is able to induce the formation of lipid-laden macrophages named 'foamy macrophages'[185]. This dysregulation of cellular cholesterol and fatty acids is a critical component of *Mtb* virulence. The incidence of these cells in a granuloma is associated with more severe outcomes[39], and elevated

cholesterol levels in patients with active TB has been associated with a less favorable prognosis[186].

1.11.5 Metformin

Metformin is an oral drug commonly prescribed as a first-line therapy in the management of type II diabetes mellitus (T2DM). It inhibits complex I of the ETC (Figure 1.9), reducing OXPHOS which leads to an increase in the AMP:ATP ratio[187,188]. For this reason it is commonly used experimentally as an activator of AMPK, a central regulator of cellular metabolism. It is classified as a biguanide and is used therapeutically to reduce hepatic glucose production, reduce intestinal absorption of glucose, and increase glucose utilization. It has few side effects, although it can induce lactic acidosis in cases of overdose[189]. As metformin is not metabolized, it is excreted unchanged into urine with a half-life of approximately 5 hours[190]. Soluble in water, it is transported in and out of cells and organs by a number of transporters, although SLC22A1 (encoded by OCT1) is primarily responsible for hepatic uptake[191]. As T2DM has been identified as a risk factor for active TB[192], and the rates of T2DM are rising in many countries in the developing world where TB is prevalent[193], an understanding of the impact of metformin, if any, on the progression of disease needs to be addressed.

1.12 Thesis Hypothesis and Objectives:

"**As *Mtb* is an intracellular pathogen which has evolved to exploit specific aspects of the host response, we aim to limit bacterial viability by changing that environment via modulation of the host transcriptome or metabolome."**

Specific Objectives:

i) To characterize the effect of 1,25D on the transcriptome of *Mtb*-infected macrophages.

ii) To determine the secondary effects of 1,25D in the broader innate immune response to *Mtb*.

iii) To characterize the global metabolic response of the host macrophage to *Mtb*

iv) To determine if modulation of host cell metabolism with metformin is effective at limiting bacterial replication *in vitro* and *in vivo*.

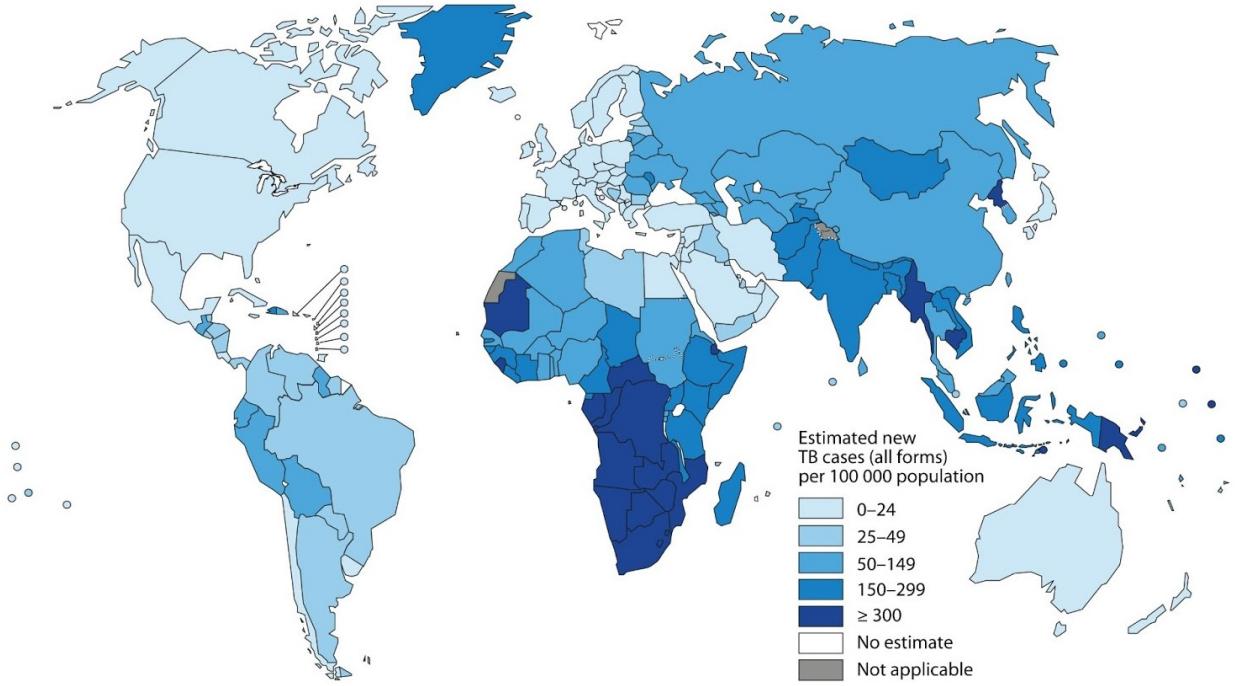

Figure 1.1 - Estimated TB incidence by country in 2011.
Reproduced from the WHO Global Tuberculosis Report 2012, (2012)[194].

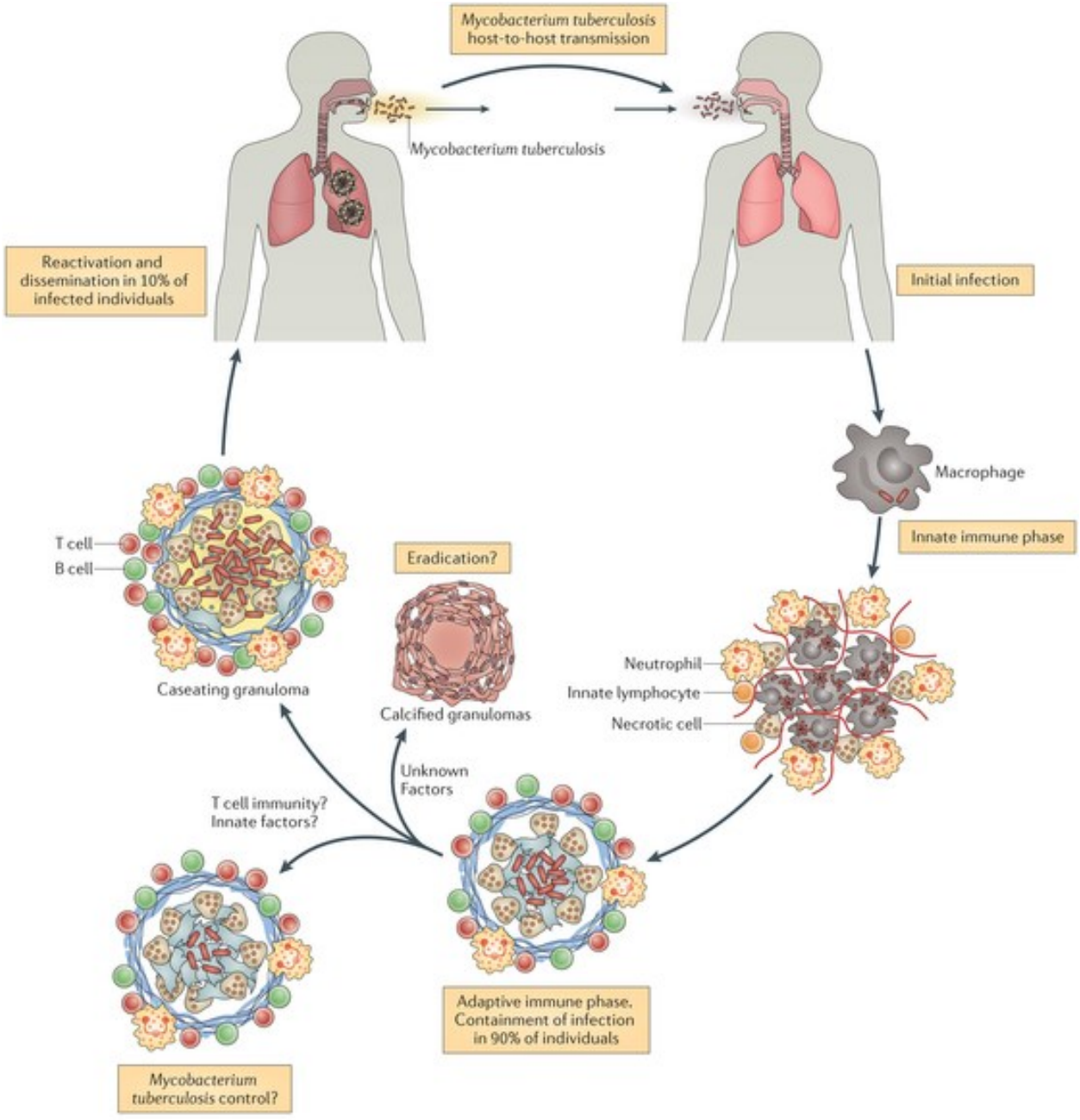

Figure 1.2 - The transmission cycle of *M. tuberculosis*.
Mtb is transmitted by aerosolized droplets from individuals with active disease (top). Upon infecting a macrophage, the innate immune responses recruit other innate immune cells, including neutrophils, to the site of infection (right). Upon activation of antigen-specific adaptive immune responses, the infection is effectively contained within the granuloma (bottom). In most cases these responses are sufficient to contain or clear the infection, but in ~10% of the population, the granuloma becomes caseous and *Mtb* is able to disseminate into the pulmonary space, where it is able to be transmitted. Reproduced from Nunes-Alves et al (2014)[195].

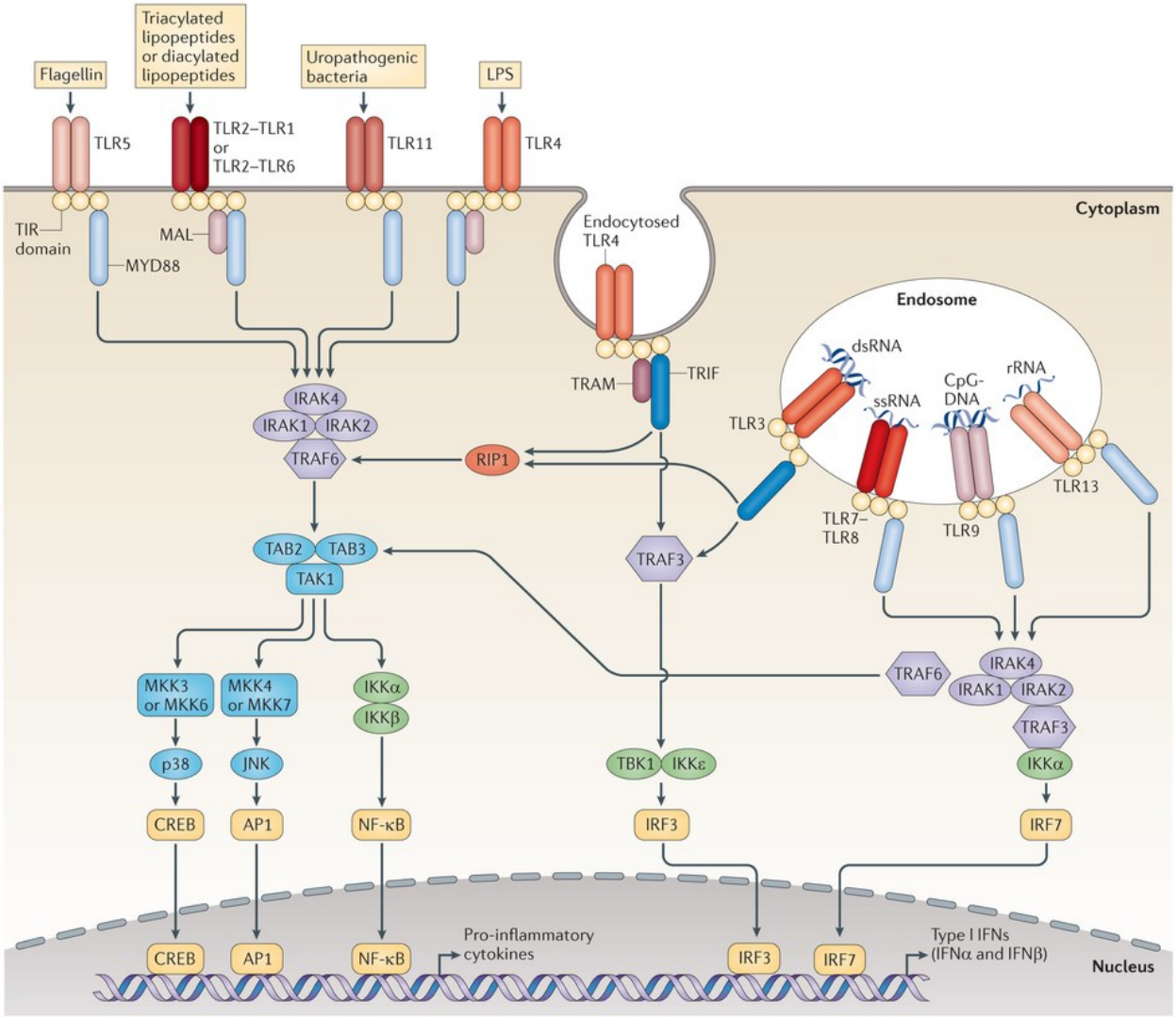

Figure 1.3 - Signaling pathways of the TLR receptors.
Toll-like receptors (TLRs) are a class of surface and endosomal proteins which recognize ligands commonly produced by bacteria and viruses. Upon detection of pathogen-associated molecular patterns (PAMPs), TLRs initiate a signaling cascade which activates transcription factors, including AP1, NF-κB, and IRFs, in order to modulate the expression of inflammatory cytokines. Upon secretion, these cytokines activate proximal cells and recruit other immune cells to the site of infection. Reproduced from O'Neill et al (2013)[196].

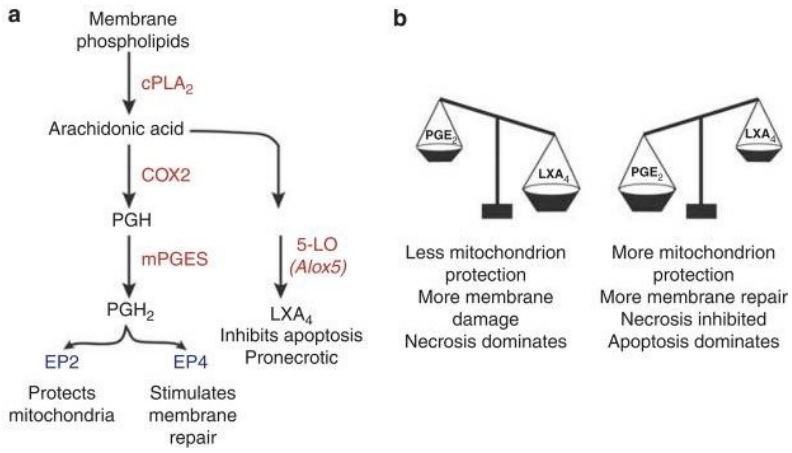

Figure 1.4 - The balance of eicosanoid signaling directs cell death fate in *Mtb* infection.
(a) Schematic of arachidonic acid processing. Enzymes responsible for each catalytic step are indicated in red. (b) The competitive balance between PGE2 and LXA4 result in either an apoptosis or necrosis respectively. Reproduced from Behar et al (2011)[197].

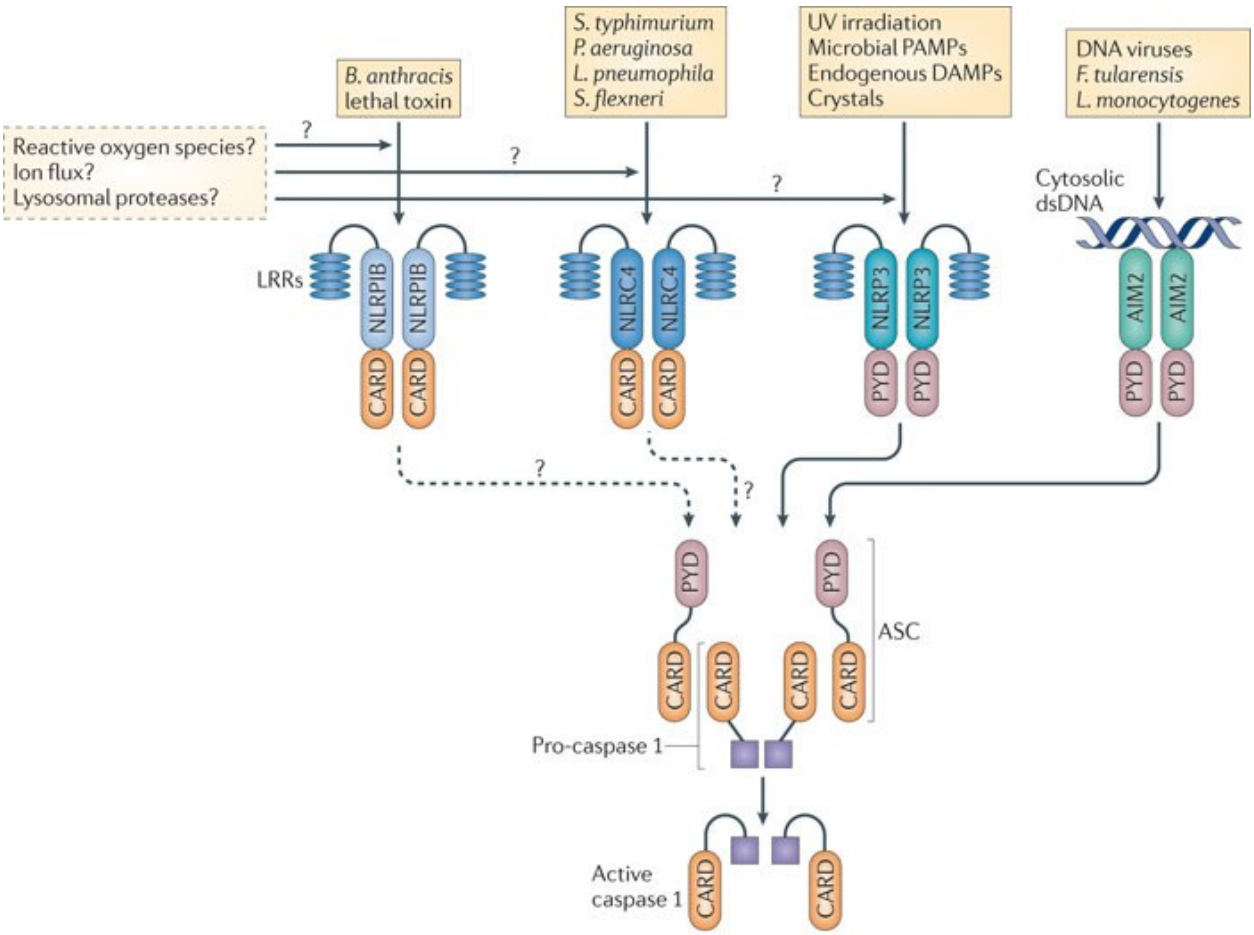

Figure 1.5 – Components of the inflammasome.
The inflammasome is a multiprotein complex that assembles a range of cytoplasmic pathogen-associated molecular pattern (PAMP) and damage-associated molecular pattern (DAMP) sensors (top), including NLRP3, to catalytically active caspase-1 in response to stimulus. Active caspase-1 enzymatically cleaves pro-IL-1β into active IL-1β. IL-1β is a powerful inflammatory cytokine, and this complex allows for its activation to be tightly controlled in cells participating in innate immune responses. Reproduced from Lamkanfi et al. (2011)[198].

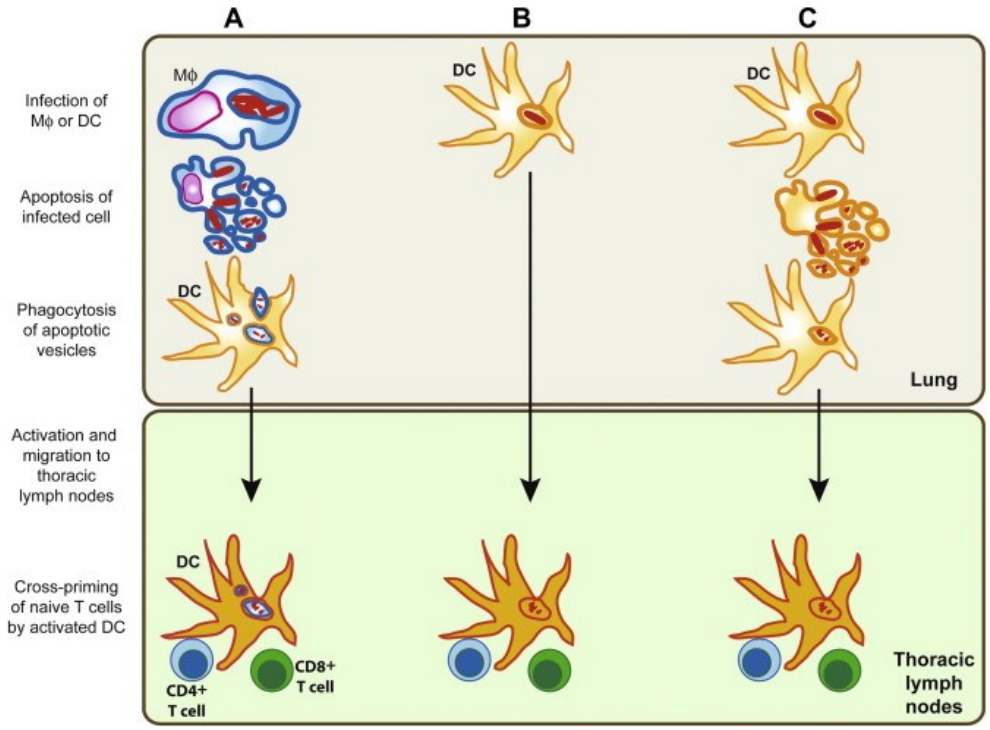

Figure 1.6 - Models of the derivation of antigen in *Mtb* infection.
In A, apoptotic vesicles are phagocytosed by DCs which traffic to the LNs. In B, infected DCs migrate to the lymph node containing the mycobacteria, from which it is able to derive antigen. In C, the apoptotic vesicles are derived from DCs, and activation occurs as described in A. Reproduced from Behar et al (2011)[199].

Figure 1.7 - Biosynthesis of 1,25-dihydroxyvitamin D3.
Provitamin D3 (7-dehydrocholesterol) is converted to vitamin D3 (cholecalciferol) by UVB exposure in the skin. It can then be 25-hydroxylated in the liver to generate 25-hydroxyvitamin D3 (calcifediol). 25-hydroxyvitamin D3 can then be α-hydroxylated in the kidney, skin, and some immune cells to form the hormonally active 1,25-dihydroxyvitamin D3 (calcitriol).

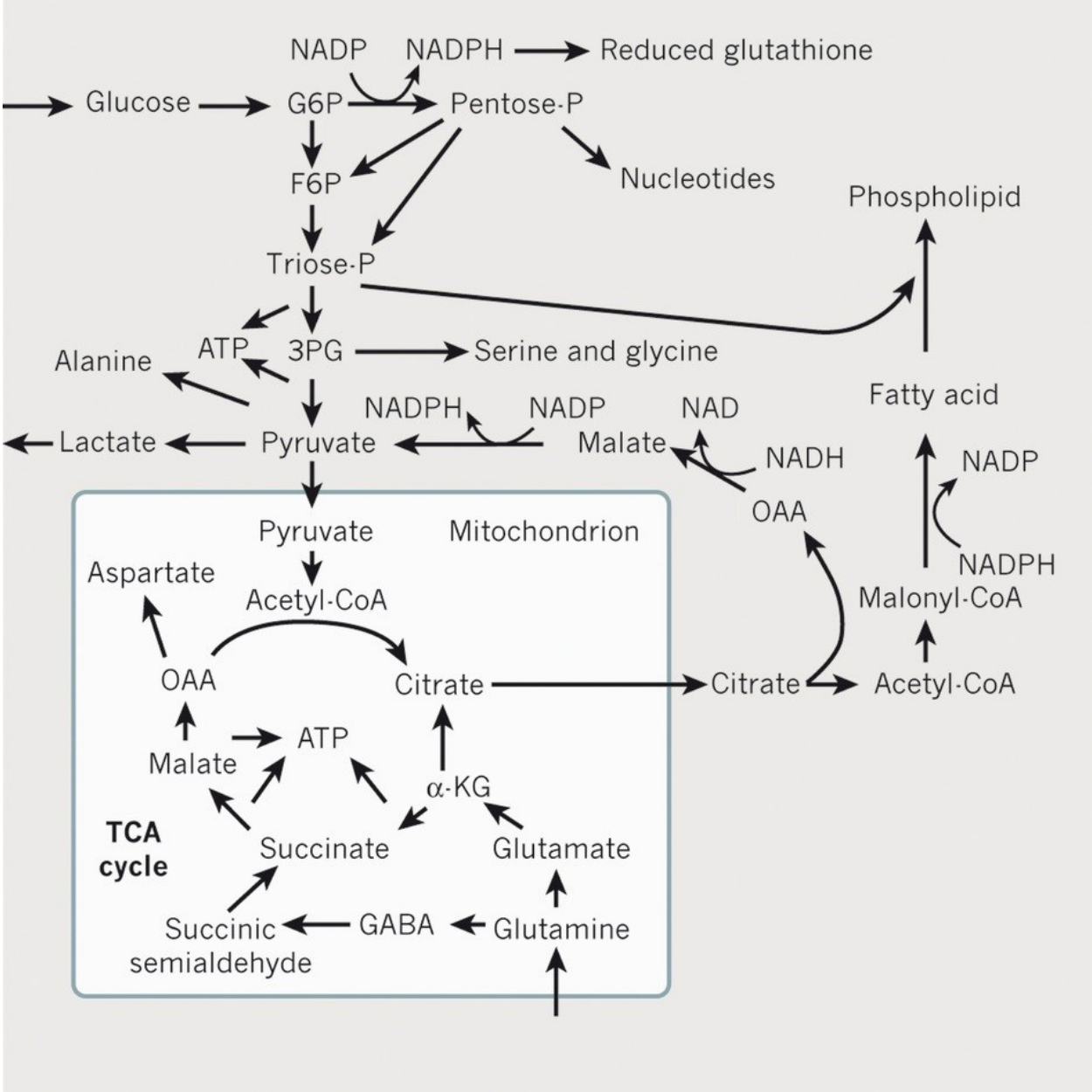

Figure 1.8 – The central metabolic network participating in the Warburg effect.
Glucose is processed via glycolysis to form 2 molecules of pyruvate. Pyruvate feeds into the TCA cycle in the form of acetyl-CoA. Under anaerobic or Warburg conditions, the rate of its conversion to lactate increases. Citrate from the TCA can be exported from the mitochondria for the biosynthesis of fatty acids. Glutamine can feed into the TCA by conversion to glutamate via glutaminolysis. It can also feed into the TCA via the GABA shunt. Reproduced with modification from O'Neill et al (2013)[200].

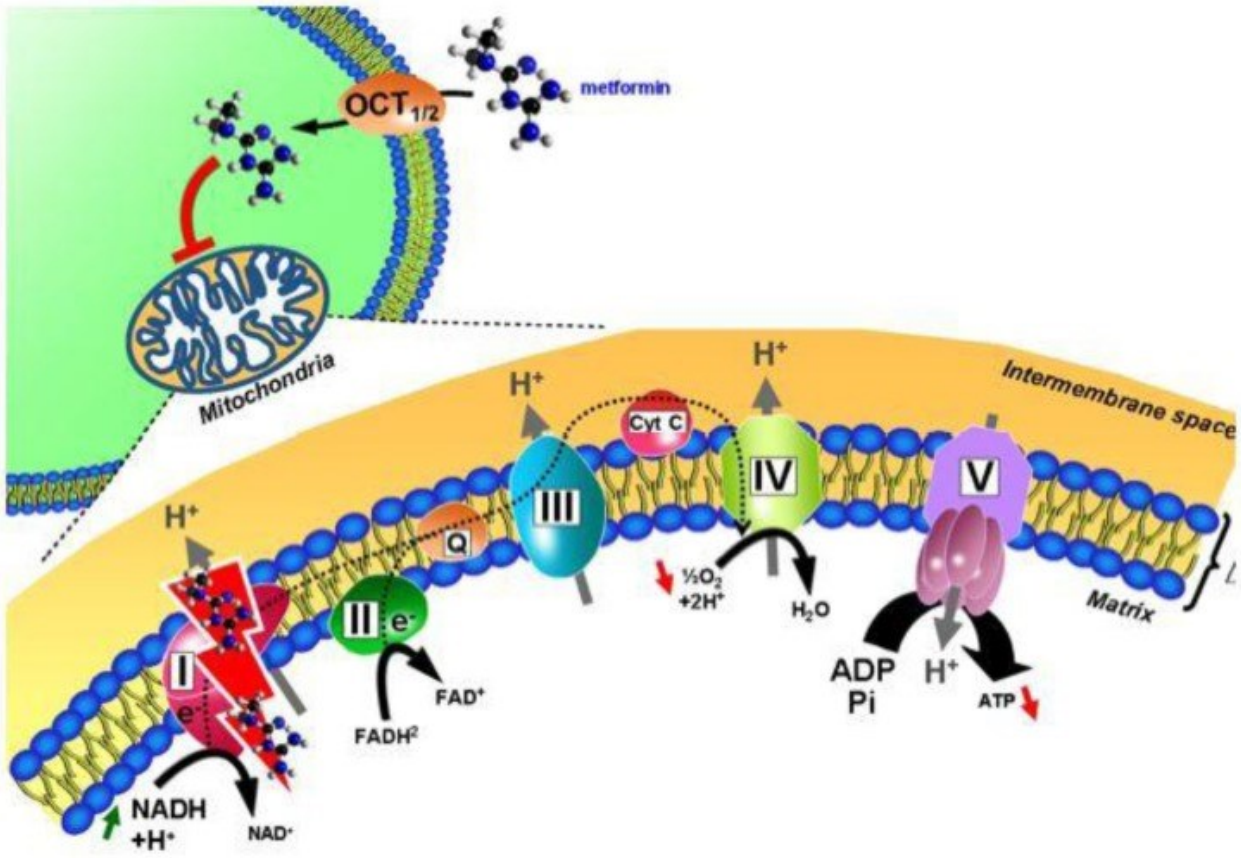

Figure 1.9 – Metformin inhibits the mitochondrial electron transport chain at complex I. Metformin is actively transported into cells by organic cation transporters 1 and 2 (OCT1/2). Although the mechanism of metformin action is not currently understood, once inside the cell it acts by inhibiting complex I of the ETC. This limits the capacity of NAD^+ to be regenerated, as NADH donates electrons to complex I. Reproduced from Viollet et al (2012)[201].

CHAPTER 2: Vitamin D Induces the Expression and Secretion of Cytokines in *Mtb*-Infected Macrophages

2.0 Preface to Chapter 2

Clinical studies have documented that most patients with active TB are also vitamin D deficient. While this alone does not demonstrate causation, it raises the possibility that vitamin D serum status may predispose individuals to active disease. At the time of the initial publication of the data in this chapter, clinical studies were being conducted which were investigating the effects of vitamin D supplementation in the clinical treatment of TB.

Given the possibility that 1,25D treatment was a viable option for the treatment of TB, we hypothesized that 1,25D induced changes during the early stages of infection. Prior to the publication of the paper that contained the data in this chapter (Verway et al. PLoS Pathogens, 2013), no effort had been made to determine the global host transcriptomic response to 1,25D in *Mtb*-infected cells. While previously published work had demonstrated that 1,25D was able to limit bacterial replication in *Mtb*-infected macrophages, these efforts had largely focused on the regulation of anti-microbial peptides CAMP and DEFB4. As the macrophage is the primary site of infection, we used this system investigate the effects of 1,25D. Upon finding that the single largest family of genes regulated was cytokines, we characterized the secretion profile of these cells.

2.1 Abstract

Although vitamin D deficiency is a common feature among patients presenting with active tuberculosis, the full scope of vitamin D action during *Mycobacterium tuberculosis* (*Mtb*) infection is poorly understood. As macrophages are the primary site of *Mtb* infection and are sites of vitamin D signaling, we have used these cells to understand the molecular mechanisms underlying modulation of the immune response by the hormonal form of vitamin D, 1,25-dihydroxyvitamin D (1,25D). We found that the virulent *Mtb* strain H37Rv elicits a broad host transcriptional response. Transcriptome profiling also revealed that the profile of target genes regulated by 1,25D is substantially altered by infection, and that 1,25D generally boosts infection-stimulated cytokine/chemokine responses. We further focused on the role of 1,25D- and infection-induced interleukin 1β (IL-1β) expression in response to infection. 1,25D enhanced IL-1β expression via a direct transcriptional mechanism. Secretion of IL-1β from infected cells required the NLRP3/caspase-1 inflammasome.

2.2 Introduction

Mycobacterium tuberculosis (*Mtb*) infects ~2 billion people [202] and active tuberculosis (TB) represents the leading cause of death from a curable disease [203]. The typical *Mtb* life-cycle involves entry into the host via inhalation (exposure), survival and replication of bacteria in the lungs and associated lymph nodes where they resist host elimination (infection), and ultimately promotion of host immunopathology resulting in aerosol transmission via coughing to the next host (disease). While current treatments aim to control active disease or prevent progression from infection to disease, an attractive point of intervention would be at the transition from exposure to infection by enhancing innate pathogen control at the time of exposure.

IL-1β is critical for host resistance to *Mtb* infection, demonstrated by the substantially reduced survival of IL-1β-/- or IL1R-/- mice after infection [77,81,83,204]. Caspase-1 cleaves a precursor of IL-1β to generate its active form. Catalytically active caspase-1 binds to the apoptosis-associated speck-like protein containing a caspase recruitment domain (ASC) subunit of inflammasomes, multiprotein complexes containing pattern recognition receptors (PRRs), which detect infection by pathogens or cellular stress. A number of PRRs have been implicated in the detection of intracellular pathogens, and the resulting IL-1β secretory response. For example, AIM2 is a cytoplasmic sensor for double stranded DNA (dsDNA) and has recently been implicated as a component of the caspase-1 inflammasome in cells infected with viral and intracellular bacterial pathogens [205-209]. Similarly, NOD2 is a cytoplasmic sensor for muramyl dipeptide [64], which stimulates NF-κB signaling to induce IL-1β expression [210], plays an important role in immunity against *Mtb* [65], and associates with the NALP1-containing inflammasome [211]. Lastly, the NLRP3 pattern recognition receptor is activated by a wide range

of signals [212]. It is of particular importance for IL-1β secretion from macrophages after infection with *Mycobacteria marinum* (*M. marinum*) [86] and *Mtb* [87].

Given the critical role of innate immunity in initiating an effective response to *Mtb* infection, we determined in detail the host macrophage transcriptomic and cytokine responses to virulent H37Rv infection and modulation of this response by the hormonal form of vitamin D, 1,25-dihydroxyvitamin D (1,25D). Historically, there is a correlation between vitamin D deficiency and TB susceptibility [125,146]. Epidemiologic studies have documented a higher occurrence of active TB during winter months when sunlight exposure is reduced [147] and vitamin D deficiency has been identified as a common feature of patients with active TB [148-150]. However, the mechanisms underlying vitamin D signaling and control of *Mtb* infection are not well understood. 1,25D synthesis is induced in macrophages and dendritic cells upon exposure to pathogen, and the 1,25D-bound vitamin D receptor (VDR) directly induces transcription of genes encoding AMPs DEFB4/HBD2 and cathelicidin antimicrobial peptide (CAMP) [141-143,154-156], both of which have demonstrated anti-mycobacterial activity [157,158]. Despite this, the direct effects of 1,25D on *Mtb* bacterial burden in infected macrophages have been modest [159,213], posing the question of whether these findings alone could account for the clinical and epidemiological observations, if they are indeed causally associated.

Here, we show that one of the primary macrophage responses to *Mtb* infection is a broad cytokine/chemokine response, which is generally enhanced by 1,25D. Importantly, 1,25D directly stimulates *IL1B* gene transcription, a critical component of the macrophage response to *Mtb* infection [214]

2.3 Results

1,25D enhances expression and secretion of cytokines and chemokines in *Mtb*-infected macrophages. In order to understand the host macrophage transcriptional response to *Mtb* infection, we performed expression profiling studies in PMA-differentiated human THP-1 macrophage cells. Cells were infected with virulent *Mtb* strain H37Rv (I) or left uninfected (NI), and treated with vehicle (DMSO) or 100nM 1,25D (+D) for 24 hours. 1,25D treatment of *Mtb*-infected macrophages produced broad changes in mRNA profiles (**Table S1, Figure S1**), in which expression of 328 genes was altered at least 5-fold by either infection or 1,25D (**Figure 2.1A, Table S2**). A heat map of highly induced transcripts identified three major groups of genes: those that were regulated by 1,25D in uninfected cells, but not in infected cells (group 1), those that were regulated in the same direction in infected cells treated with vehicle or 1,25D (group 2), and those that were regulated in infected cells in either the vehicle or 1,25D treated condition, but not both (group 3). From this it is clear that about half of all 1,25D target genes in uninfected macrophages (NI+D) are not regulated in infected cells, as they do not belong to group 1. Infection resulted in broad changes in transcription, which substantially changed the cohort of genes regulated by 1,25D, indicated by group 3, and the columns that change in intensity in group 2 (**Figure 2.1A**).

To understand the dominant effects of 1,25D in *Mtb*-infected macrophages, the 328 genes regulated more than 5-fold by infection were filtered to retain those whose expression was altered at least a further 1.5-fold by 1,25D (**Figure 2.1B**). Functional clustering of the resulting 94 genes revealed that the largest classification of these encoded cytokines (**Fig. 2.1B)**, and Ingenuity IPA network clustering strongly implicated a role in inflammatory responses, immune cell trafficking, and signaling (**Figure 2.1C, Figure 2.2**). IPA Pathway clustering of these

revealed the strongest effects were on secreted factors, many of which were further induced by 1,25D (**Figure 2.1D**). To confirm the transcriptional changes at the translational levels, the supernatants from the cells used for microarray were subjected to Milliplex Human Cytokine Assay for a wide range of cytokines and chemokines analysis. We found that, in agreement with microarray data, 1,25D significantly enhanced secretion of IL-1β, CCL3/MIP1α, CCL4, CCL8, TNFα, IL-8/CXCL8, and CCL20 from macrophages infected with *Mtb* (**Table 2.1**).

To understand if the changes in transcription resulting from infection with H37Rv after 24 hours were specific to infection with this virulent strain, we compared it to samples infected with H37Ra at an equivalent MOI and found no global differences in the trends of regulation (**Figure S2**). An analysis of the genes differentially regulated between these conditions showed no large deviations, although the fold expression of some inflammatory cytokines was slightly higher in conditions infected with H37Ra (**Figure S3**).

Production of mature 1L-1β requires caspase-1 and NLRP3 in *Mtb* infection. Considering the critical role of IL-1β in immunity to *Mtb* infection [33,83,204], we next investigated the mechanisms by which 1,25D increased the expression and secretion of IL-1β in *Mtb*-infected macrophages. Consistent with the microarray data, RT/qPCR analysis showed that 1,25D up-regulated the expression of *IL1B* transcripts in uninfected and *Mtb*-infected macrophages (**Figure 2.3A**). Essentially identical results were obtained with two independent cultures of primary human macrophages (**Figure 2.3B**). Although the levels of pro-IL-1β were elevated in both 1,25D-treated macrophages as well as *Mtb*-infected macrophages treated with 1,25D, mature IL-1β was only detected in extracts of *Mtb*-infected cells treated with 1,25D (**Figure 2.3C**). Results of western blotting were consistent with analysis of IL-1β released from THP-1

cells or primary human macrophages, where secretion was observed only in supernatants of infected cells, and significantly elevated upon treatment with 1,25D (**Figures 2.3D, E**).

Previous *in silico* studies [215] identified a promoter-proximal sequence corresponding to a consensus vitamin D response element (VDRE) in the *IL1B* gene (**Fig. S4**). To further investigate the mechanisms of *IL1B* gene expression by 1,25D, we evaluated the VDR binding to this element by chromatin immunoprecipitation (ChIP) assay. VDR binding was 1,25D-dependent, and significantly enhanced by infection (**Figure 2.3F**). 1,25D-dependent binding of the VDR may be due in part to its elevated expression, which was stimulated by 1,25D (**Figure S2**), consistent with the *VDR* being a 1,25D target gene [216]. A similar profile was observed with RNA polymerase II (polII) binding at the *IL1B* transcription start site (TSS) (**Figure 2.3G**). Collectively, these experiments show the 1,25D-bound VDR stimulates transcription of the *IL1B* gene. To determine the extent of conservation of this mechanism, we performed a comparison of the *IL1B* VDRE loci across mammalian species using the UCSC genome browser [217]. The VDRE and the surrounding regions are well conserved in the genomes of non-human primates, but not in the mouse, rabbit, or guinea pig (**Figure S6**), which are commonly used to model *Mtb* infection *in vivo* [218]. Indeed, while 1,25D significantly enhanced *cyp24* expression in mouse macrophages, no regulation of *il1b* was seen (**Figure S7**), in contrast to the 6-8-fold induction of *IL1B* expression seen in uninfected THP-1 cells or primary human macrophages (**Figures 2.3A, B**) indicating that mice would not serve as a viable *in vivo* model to understand this effect.

Pro-IL-1β can be cleaved into its mature form by caspase-1 [198]. Western blots of lysates from infected macrophages revealed that neither 1,25D nor infection altered expression of caspase-1 in its pro-form (**Figure S8A**). Caspase-1 enzymatic activity was significantly higher in cytosolic lysates from *Mtb*-infected cells treated with 1,25D (**Figure S8B**). Catalytically active caspase-1

is a component of inflammasomes, of which ASC is a core component. We found that while the 23kD form of ASC was predominant in THP-1 cells, the 20kD splice variant [219,220] coimmunoprecipitated with caspase-1, an association only seen in infected cells and found to be slightly higher in infected cells treated with 1,25D, consistent with elevated cytosolic caspase-1 activity under these conditions (**Figure S8C**). Inflammasomes also contain pattern recognition receptors (PRR) that detect infection or cellular stress [198,221]. To understand which inflammasome PRR, or combination of PRRs, was responsible for the 1,25D-driven secretion of IL-1β, we investigated the potential roles of NOD2, NLRP3, and AIM2 in regulating IL-1β maturation in infected cells. Each of these has been previously implicated in detection of *Mtb* or other intracellular pathogens and in stimulating inflammasome-mediated IL-1β maturation [86,222,223]. Notably, expression of AIM2, a cytoplasmic sensor for dsDNA [206,208], was induced ~30-fold in *Mtb*-infected macrophages by RT/qPCR and western blotting (**Figure 2.4A**), suggesting that the AIM2 inflammasome may contribute to IL-1β cleavage and secretion.

Expression of *AIM2*, *NOD2* or *NLRP3* was strongly reduced by siRNA-mediated knockdown (**Figure S9**), along with positive controls *IL1B* and *CASP1*, in *Mtb*-infected macrophages. None of the knockdowns of PRRs had any effect on expression of pro-IL-1β protein or on expression of caspase-1 (**Figure 2.4B**). Depletion of NOD2 or AIM2 expression had no significant effect on IL-1β secretion (**Figure 2.4C**). In contrast, knockdown of NLRP3 essentially abolished IL-1β secretion from *Mtb*-infected macrophages (**Figure 2.4C**). These findings suggest that induced AIM2 expression is not primarily responsible for driving IL-1β maturation, but are consistent with other studies showing that IL-1β production during *Mtb* infection is largely controlled by NLRP3 [86,87]. In contrast, they are not consistent with the finding that NOD2 function is of primary importance [223].

2.4 Discussion

In this study we have presented the first large scale microarray profile to determine the host macrophage transcriptomic responses to *Mtb* infection and the effect of 1,25D on those responses. Analysis of this data demonstrated that infection markedly changed the profile of genes regulated by 1,25D. ChIP studies also revealed that infection enhances DNA binding by the VDR. These data suggest infection induces large-scale changes in chromatin that modify the availability of VDREs for binding by the VDR throughout the genome. Additionally, it is clear from this work that studies of 1,25D target genes in uninfected macrophages are not an accurate depiction of its contribution to host responses in the face of an active infection. A potential limitation of this study was our initial use of THP-1 cells for microarray analysis of target genes. As this is cell line is derived from a monocytic leukemia, not all of the genes identified as being regulated may be found under similar experimental conditions using primary human alveolar macrophages.

Pathways analysis of genes differentially regulated by 1,25D in infected THP-1 cells revealed that the dominant function of 1,25D in the context of the innate immune response to *Mtb* is the up-regulation of specific components of the broad cytokine response induced by infection. Previous computational analysis identified VDREs proximal to the *IL1B, CCL3*, *CCL4*, *CCL8* genes, but not *IL-8* or *TNF-a* [215]. Probing 1,25D modulation of these cytokines *in vivo* is complicated by our results showing that these VDREs are not conserved in mouse, rabbit, or guinea pig, the model organisms typically used to study *Mtb* infection. Despite the fact that IL-1β signaling also is critical for innate immune responses to *Mtb* in these animal models, it would appear that they would not be appropriate for *in vivo* modeling of the modulatory effects of vitamin D on the early innate immune responses to infection.

1,25D markedly enhanced mRNA levels and secretion of IL-1β in *Mtb*-infected macrophages. Our data reveal that 1,25D is acting primarily at the level of *IL1B* gene transcription without affecting the levels of inflammasome, as substantial levels of pro-IL-1β were seen in uninfected macrophages after 1,25D treatment, whereas secretion required infection. Furthermore, of the cytokines whose secretion was elevated by 1,25D treatment after infection (CCL3, CCL4, CCL8, IL-8, and TNF-α), treatment did not induce their secretion from uninfected cells. This would suggest that 1,25D is acting to prime and potentiate inflammatory innate immune responses, without inducing any unwanted inflammation in a resting state.

IL-1β and IL1R1 are essential for survival in mouse models of *Mtb* infection [77,81,83,204]. IL-1β is also of critical importance during the early stages of infection as shown by *in vitro* infections using macrophages from these knockout mice [81]. Additionally, it has been demonstrated that *Mtb* expresses *zmp1*, a metalloproteinase that prevents phagolysosomal maturation by inhibiting inflammasome-mediated IL-1β cleavage, a mechanism of virulence that suppresses the host response [214]. siRNA-mediated knockdowns of various inflammasome sensors demonstrated that the NLRP3 inflammasome is responsible for IL-1β secretion under all conditions, in agreement with previously published data looking at mycobacterial infection in mouse and human macrophages [86,87]. While mouse genetic models have revealed that IL-1β signaling plays a key role in *Mtb* resistance, *nlrp3*-/- and *casp1*-/- mice showed no deficiency in the production of IL-1β, control of bacterial burden, or survival [87]. Even though ASC was important in this model, this may be because ASC-null mice are deficient in antigen presentation and DC trafficking due to a loss of Dock2 expression [224]. It is therefore unclear at this time whether the NLRP3 inflammasome is required *in vivo* for control of *Mtb* infection.

2.5 Materials and Methods

Ethics Statement. Intraperitoneal macrophages were acquired from C57BL/6 mice as outlined in an animal use protocol approved by McGill University (Permit #2010-5860) according to Canadian Council on Animal Care guidelines. De-identified human peripheral blood was purchased from Research Blood Components (Boston, MA). Following informed written consent, blood was collected by venipuncture from healthy adult volunteers, recruited by Research Blood Components. Protocols for the collection of whole blood for research purposes were approved by New England Institutional Review Board.

Tissue Culture. THP-1 cells (TIB-202, ATCC) were cultured in RPMI-1640 (Wisent) with 10% FBS. H37Rv was cultured to mid-log phase in a rolling incubator at 37°C in Middlebrook 7H9 (Difco) with .05% Tween-80 and 10% ADC enrichment (BD Biosciences).

Macrophage Infections. $1x10^6$ THP-1 cells were terminally differentiated by $2x10^{-8}$M PMA for 24 hours in RPMI with 10% charcoal stripped FBS, inducing cell cycle arrest. H37Rv cultures were centrifuged and pellets were resuspended in RPMI-1640 with 10% charcoal stripped FBS and .05% Tween-80 and clumping was disrupted by repeated passage through a 27-gauge needle. Media was removed from THP-1 cells and replaced with media containing *Mtb* in the indicated multiplicity of infection (MOI) for 4 hours. THP-1 cells were then vigorously washed three times with RPMI to remove extracellular bacteria, followed by incubation in RPMI with 10% charcoal stripped FBS containing either vehicle (DMSO) or 1,25D at a final concentration of 10^{-7} M.

RNA extraction and qPCR/Microarray. RNA extraction was performed with TRIzol and chloroform (Invitrogen) as per manufacturers' instructions. RT was performed with iScript cDNA Synthesis Kit (Bio-Rad) and qPCR was performed with SsoFast Eva Green with low ROX (Bio-Rad) on an Eco qPCR cycler (Illumina), normalizing expression to β-actin and 18S. Primers used are listed in Table S3. Human Gene 1.0 ST arrays (Affymetrix) were used to measure samples from two independent experiments, each performed in biological triplicate. Microarray data presented is from one triplicate set, which is representative of the other.

Western Blots and Immunoprecipitation. Protein extracts from THP-1 cells were prepared in lysis buffer (10 mM Tris, pH 7.5, 150 mM NaCl, 1% Triton X-100, 1 mM phenylmethylsulfonyl fluoride, 0.2 mM sodium orthovanadate, 0.5% Nonidet P-40) and processed for Western blotting and separated on Tris-HEPES-SDS gradient protein gels (Pierce) using standard transfer and blotting protocols. Immunoprecipitation was performed as described in [225], using 2μg of either rabbit serum IgG (sc-2027) or α-caspase-1 p10 (sc-515, Santa Cruz) antibody for each sample.

Reagents, ELISAs, and Western blot antibodies. Antibodies: α-IL-1β (MAB601, R&D Systems), α-AIM2 (ab93015, abcam), α-caspase-1 p20 (sc-1780, Santa Cruz), α-actin (sc-1616, Santa Cruz), α-VDR (sc-1008, Santa Cruz), α-ASC (sc-271054, Santa Cruz), murine serum IgG (Sigma).

Human macrophage isolation. Following informed consent, blood was drawn from healthy adults. Buffy coats were isolated from whole blood by Ficoll density-gradient centrifugation using Ficoll-Paque Premium (GE Healthcare), and thrice resuspended in PBS and centrifuged to

remove platelets. Monocytes were purified from the total leukocyte population by sorting of adherent cells after 2 hours, by washing the culture plates twice with RPMI-1640 with 20% human serum. Cells were allowed to differentiate into naïve macrophages over 6 days in RPMI-1640 with 20% human serum before infection, with media changes every two days throughout.

Mouse macrophage isolation. Intraperitoneal macrophages were elicited from C57BL/6 mice (Jackson) by intraperitoneal injection of 2ml of 3% thioglycolate solution. Three days later, macrophages were collected by lavage of the peritoneal cavity. Macrophages were purified using CD11b Microbeads (Miltenyi Biotech) and allowed to adhere for 24 hours before infection.

siRNA-mediated knockdowns. One day after PMA-induced differentiation, siRNAs targeting *CASP1*, *AIM2*, *IL1B*, *NLRP3*, *NOD2*, and the non-targeting scrambled control (NC1) (Integrated DNA Technologies) were transfected into THP-1 cells using Transductin (Integrated DNA Technologies) in 10% Q-serum, according to manufacturer's instructions. After 4 hours, media was replaced with RPMI with 10% charcoal stripped FBS. After another 48 hours, cells were infected with H37Rv in accordance with the above protocol.

Caspase-1 Activity Assay. Total caspase-1 activity was assayed using ICE/Caspase-1 Colorimetric Protease Assay Kit (Millipore) as per manufacturers' instructions. Cell lysates were incubated with YVAD-pNA and read in a spectrophotometer at 405nM.

Secreted Cytokine and Chemokine Quantification. Media from THP-1 cells was collected 24 hours after treatment and sterilized by passage through .20μm filters. Levels of secreted

cytokines and chemokines were assayed by Milliplex Human Cytokine Panels 1, 2 and 3 (Millipore) and read on a BioPlex (Bio-Rad).

ChIP Assays. Infected and uninfected THP-1 cells were collected after 24 hours of treatment. Cells were fixed for 20 minutes with 1% formaldehyde, and washed with 1.25μM glycine. Following cell and nuclei lysis, chromatin was sonicated for 75 cycles of 10s ON / 20s OFF on a Bioruptor Sonicator (Diagenode). IPs were then performed with either normal rabbit IgG, 6μg of anti-VDR (Santa Cruz sc13133) or 6μg of anti-RNA Polymerase II (Abcam anti-polIICTD #ab5131). Primers used for region amplification are listed in Table S3. Quantification of immunoprecipitated material was performed by qPCR and normalized for input DNA.

Statistical Analysis. Student's t-test, ANOVA, or a two-tailed Fisher's exact test was performed where indicated using GraphPad software. For microarray samples, Flexarray v1.6 software was used to normalize overall chip signal using the Affymetrix Power Tools (APT) Robust Multi-Array Average (RMA) algorithm. The EB (Wright and Simon) algorithm was used for statistical analysis to calculate fold transcript expression and significance between of each experimental condition relative to the uninfected, untreated condition (NI). A 5-fold cutoff was used as this was sufficient to bring the false-discovery rate below 5%.

2.6 Figures

Figure 2.1. 1,25D alters the host macrophage transcriptomic response to *Mtb* infection.

(**A**) Intensity heat map of genes regulated 5-fold or more during infection in the absence or presence of 1,25D. THP-1 cells were either not infected (NI) or infected with H37Rv (I) and treated with vehicle (DMSO) or 100nM 1,25D (+D) for 24 hours. Each vertical line represents one gene that was either up-regulated (red), down-regulated (blue) or not affected (white) under each of the conditions relative to uninfected cells not treated with 1,25D, as indicated in the scale. Group 1 represents those genes that were only detected in the NI+D condition, group 2 were those genes that were commonly expressed in both infected conditions, and group 3 represents those genes that were expressed in only one of the infected conditions as a result of 1,25D treatment. (**B**) Functional clustering heat map of genes selected for a >5-fold change in either the I or I+D condition relative to the NI control as well as having a >1.5-fold difference between the two. Increasing brightness for red and blue denote up- and down-regulation respectively. (**C**) Highest-rated functions associated with relative expression of I+D/I in genes from **B**, with a Fisher's exact test p-value threshold set at 0.01 (red line) using Ingenuity Pathways Analysis (IPA) software. (**D**) Network clustering analysis of genes from **B** using IPA software. Solid and hashed lines denote known direct and indirect actions between two proteins as determined by IPA. Red and blue denote relative up- or down-regulation of their expression in the I+D condition as compared to the I condition, respectively. Data is derived from analysis of Affymetrix Human Gene 1.0ST microarray chips. mRNA samples for analysis were prepared in triplicate, and data presented is representative of two independent replicates.

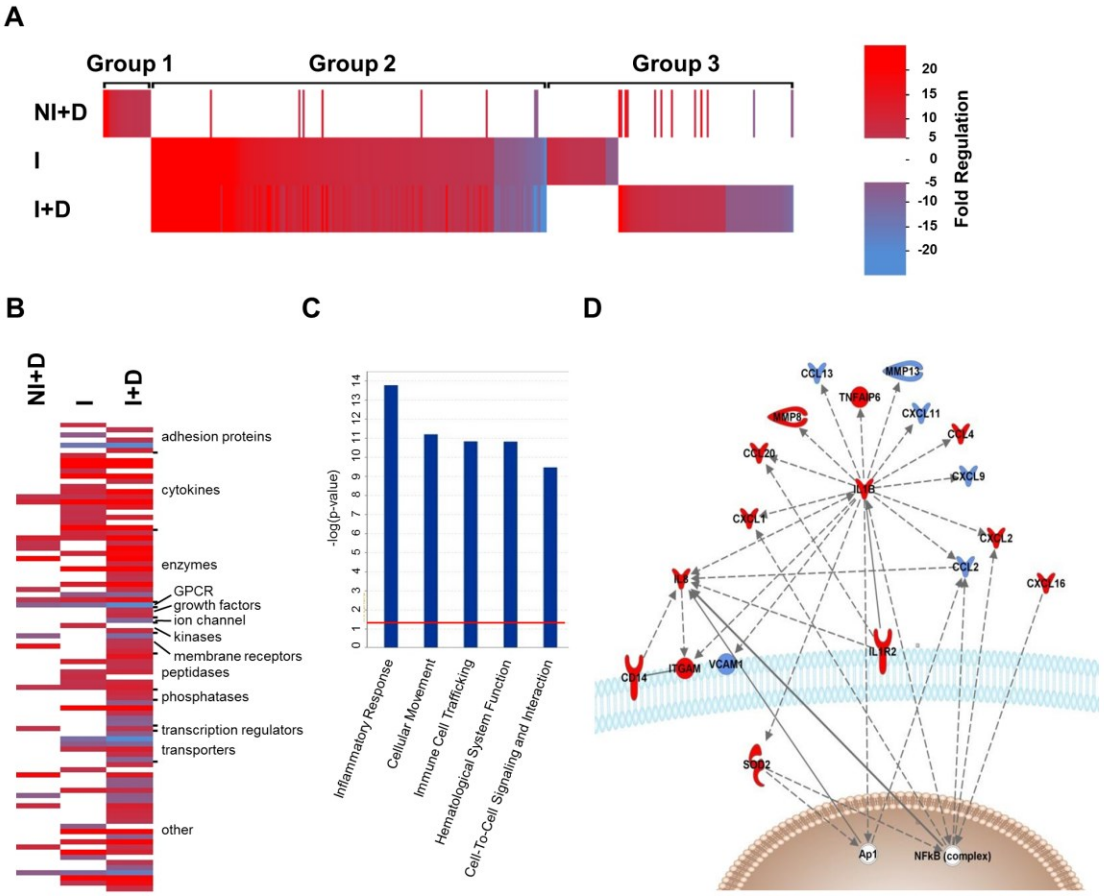
A
Group 1
Group 2
Group 3
NI+D
I
I+D
20
15
10
5
0
-5
-10
-15
-20
Fold Regulation
B
NI+D
I
I+D
adhesion proteins
cytokines
enzymes
GPCR
growth factors
ion channel
kinases
membrane receptors
peptidases
phosphatases
transcription regulators
transporters
other
C
-log(p-value)
0 1 2 3 4 5 6 7 8 9 10 11 12 13 14
Inflammatory Response
Cellular Movement
Immune Cell Trafficking
Hematological System Function
Cell-To-Cell Signaling and Interaction
D
CCL13
MMP13
TNFAIP6
MMP8
CXCL11
CCL4
CCL20
CXCL9
IL1B
CXCL1
CXCL2
CCL2
IL6
CXCL16
IL1R2
CD14
ICAM
VCAM1
SOD2
Ap1
NFkB (complex)

Figure 2.2 Clustering Analysis of Functional Groups

IPA functional clustering of genes regulated at least 5 fold by microarray in the specified comparisons. Genes identified as being regulated are displayed in bold, with arrows indicating the relative rate of expression as being higher or lower. (**A**) Uninfected macrophages vs. uninfected macrophages treated with 1,25D. (**B**) Uninfected macrophages vs. macrophages infected with H37Rv. (**C**) Macrophages infected with H37Rv vs. macrophages infected with H37Rv and treated with 1,25D.

A

Molecules in Network	Top Functions
ACPP, ↑**ADAM28,** ↑**ADAMDEC1,** ↑**CD14,** ↓**CX3CR1,** CXCR2, CXCR4, ↑**CYP19A1,** DEFB4A, ↑**DPP4,** ERK1/2, ↑**FN1,** FSH, ↑**G0S2,** ↑**GEM,** Gm-csf, HAS1, ↑**HSD11B1,** IL2, ↑**IL8,** IL13, ↑**IL1B,** IL1F8, Lh, MBD2, MT2A, NFkB (complex), NR5A1, PGF, PTHLH, ↑**SLC16A6,** TACR1, TIRAP, TPT1 (includes EG:7178), ↑**TREM1**	Cell-To-Cell Signaling and Interaction, Hematological System Development and Function, Immune Cell Trafficking
CASP3, CASP8, CD44, CTNNB1, ↑**CYP24A1,** EGFR, ERBB2, Histone h3, IDO1, IgG, IL1R1, IRS1, MMP2, MMP9, MT1L, MUC1, MYC, NOS2, PI3K, PROC, PSEN1, SAA1, ↑**SAT1,** ↑**SEMA3C,** SMAD3, ↑**THBD,** TNF, TP53	Cancer, Inflammatory Response, Cellular Growth and Proliferation
↑**APBB3,** C14ORF156, NCOA1	Cancer, Drug Metabolism, Endocrine System Development and Function

B

Molecules in Network	Top Functions
Ap1, ↓**CCL2,** ↑**CCL4,** ↑**CCL8,** ↓**CCL13,** ↑**CCL20,** ↑**CD14,** Creb, ↑**CXCL1,** ↑**CXCL2,** ↓**CXCL9,** ↓**CXCL11,** ↑**CXCL16,** ↑**DUSP1,** ERK1/2, Fibrinogen, Gm-csf, hCG, ↑**IL8,** IL12 (complex), ↑**IL1B,** ↑**IL1R2,** Immunoglobulin, ↑**ITGAM,** Jnk, Mapk, ↑**MMP8,** ↓**MMP13,** NFkB (complex), P38 MAPK, PI3K, SAA, ↑**SOD2,** ↑**TNFAIP6,** ↓**VCAM1**	Cell-To-Cell Signaling and Interaction, Hematological System Development and Function, Immune Cell Trafficking
↑**ADAMDEC1,** ↑**CCL20,** CD69, ↑**CD226,** ↑**CD274,** ↑**CLEC4E,** ↓**CX3CR1,** ↑**CXCL1,** CXCL5, ↓**CXCL13,** ↑**DMXL2,** Eotaxin, Gm-csf, IL2, IL13, IL21, IL12 (complex), IL18RAP, ITGAL, ↓**LAMP3,** NFATC1, NFATC2, NFKB2, ↓**PTX3,** ↑**SAT1,** SELE, SELL, ↑**SEMA3C,** SOCS1, ↓**SORT1,** TLR8 (includes EG:51311), TNF, TPT1 (includes EG:7178), ↓**VCAM1,** WNT5A	Inflammatory Response, Cellular Movement, Hematological System Development and Function
AREG, ↑**C1S,** CCL5, CCNB1, CDH1, CTNNB1, ↑**CYP19A1,** ↑**CYP24A1,** ↑**EREG,** ERK1/2, FSH, ↑**GEM,** HELZ, HNF1A, IgG, IL6, ↓**KLF4,** Lh, ↑**MET,** MMP7, ↑**MMP19,** NR5A1, NR5A2, ↑**ORM1,** PTHLH, RAB33B, RNA polymerase II, ↑**RND3,** ↓**S100A4,** ↓**SERPING1,** ↓**SMYD3,** SNAI1, ↑**SPTBN1,** TP53, ↓**VCAN**	Cellular Development, Cellular Movement, Cancer

C

Molecules in Network	Top Functions
↑**CD40,** ↑**CD80,** ↑**CD274,** ↑**CXCL2,** ↑**CXCL9,** ↑**CXCL10,** ↑**CXCL11,** ↑**EBI3,** ↑**GCH1,** Gm-csf, ↑**IDO1,** ↑**IFIT3,** Ifn gamma, ↑**IL1B,** Immunoglobulin, Interferon alpha, Jnk, ↑**KYNU,** ↑**LAMP3,** ↑**OAS1,** ↑**OAS2,** ↑**OASL,** PI3K, ↑**PLSCR1,** ↑**PTX3,** ↑**RND3,** ↑**SAT1,** ↑**STAT1,** ↑**STAT2,** ↑**TAP1*,** ↑**TDRD7,** ↑**TLR3,** ↑**TNF*,** ↑**TNFAIP3,** ↑**XAF1**	Organismal Injury and Abnormalities, Cellular Movement, Hematological System Development and Function
Akt, Ap1, ↑**BIRC3,** Caspase, ↑**CCL2,** ↑**CCL3,** ↑**CCL4,** ↓**CCR2*,** ↑**CCR7,** ↑**CXCL1,** ERK, ERK1/2, Estrogen Receptor, Fibrinogen, hCG, Histone h3, ↑**ICAM1,** ↑**IGFBP3,** IKK (complex), ↑**IL8,** IL12 (complex), ↓**ITGAM,** LDL, Mapk, ↑**MMP13,** ↑**NAMPT*,** NFkB (complex), ↑**NFKBIA,** P38 MAPK, SAA, ↑**SOD2,** ↑**SRC,** ↑**TNFSF10,** ↑**VCAM1,** ↑**VEGFC**	Cell-To-Cell Signaling and Interaction, Hematological System Development and Function, Immune Cell Trafficking
↑**CCL2,** ↑**CCL4,** CCL5, ↑**CCRL1,** CD44, ↑**CXCL13,** ↑**DDX58,** ERK1/2, ↑**GBP5,** ↑**IFI35,** IFNB1, IFNG, IgG, ↑**IL8,** IL10, IL21, IL12 (complex), ↑**IL1B,** IRF3, MMP9, ↑**MMP19,** NMI, P38 MAPK, PLAUR, ↑**SERPING1,** SMAD3, SP3, ↑**STAT1,** TGFB1, ↓**TGFBR1,** ↓**TGFBR2,** TIRAP, TLR4, ↑**TNF*,** ↑**TNFAIP6**	Inflammatory Response, Cellular Movement, Hematological System Development and Function
AGER, ↑**AIM2,** ↑**APOL1,** CD69, ↑**CXCL9,** ↑**CXCL10,** ↑**DHX58,** HMGB1 (includes EG:3146), ↑**IFI6,** ↑**IFI27,** ↑**IFIH1,** ↑**IFIT1,** ↑**IFIT2,** IFN Beta, IL4, IL5, IL10, IL29, IL1R1, Interferon alpha, ↑**IRAK2,** IRF3, LBP, ↑**MX1,** MYD88, P38 MAPK, ↑**PDE4B,** PI3K, ↑**SLAMF7,** SOCS1, TLR4, TLR7, TLR9, TLR8 (includes EG:51311), ↑**USP18**	Inflammatory Response, Infectious Disease, Antimicrobial Response
↑**ADA,** ↑**ADAMDEC1,** AKT1, ↑**AMPD3,** ANG, ↑**ATF3,** ↑**CCL8,** ↑**CCL13,** ↑**CCL20,** ↑**CD38,** ↑**CXCL10,** CXCR4, ↑**DLL4,** ↑**ENPP2,** Eotaxin, FASLG, HMGB1 (includes EG:3146), IL6, IL13, IL29, IL1A, ↑**IL1B,** IL1F8, IL1R2, ↑**LGALS3BP,** ↑**PML,** RNASE1, RNASE2, S100A8, TLR4, TLR9, TP53, TXN, ↓**VCAN,** VEGFA	Inflammatory Response, Cellular Movement, Hematological System Development and Function
ACPP, ↑**AXL,** C1q, CDC42EP4, CDH1, CFLAR, Creb, ↓**CX3CR1,** CXCR4, ↑**CYP19A1,** FSH, ↑**HERC5,** ↑**IFITM1,** ↑**IFITM3,** IgG, IL2, ↑**IL1RN,** ↑**ISG20,** KRT18, Lh, ↑**MT2A*,** MYC, NR5A1, PTGER2, PTGER4, RNA polymerase II, SMARCA4, SNAI1, ↓**SPTBN1,** ↑**TNFAIP3,** ↑**TNFRSF9,** TNFSF9, ↑**TNFSF13B,** TOB1, VEGFA	Cellular Growth and Proliferation, Cancer, Cell Death

Table 2.1. Secretion profile of media samples taken from cells used for microarrays.

THP-1 cells were either not infected (NI) or infected with H37Rv (I) and treated with vehicle or 100nM 1,25D (+D) for 24 hours. All units are in pg/ml, and empty boxes represent no detectable increase above background. Data are from three experiments (mean and s.e.m.). The following were not detected: IFNγ, IL-2, IL-3, IL-5, IL-10, IL-15, IL-17, INFβ, IL-11, IL-29, XCL1, CXCL5, CXCL6, CXCL7, CCL14a**.**

	NI		NI+D		I		I+D	
Protein	mean	s.e.m.	mean	s.e.m.	mean	s.e.m.	mean	s.e.m.
CCL2	19.76	3.12	8.63	0.44	3777.66	99.65	2629.93	32.62
CCL3	190.00	15.68	161.76	9.91	9125.36	1416.96	40257.15	721.02
CCL4	24.81	1.17	34.62	1.73	2267.37	203.19	4911.99	160.92
CCL8					145.60	80.41	751.90	64.22
CCL19					7.33	0.42	14.92	2.07
CCL20					43.62	9.35	269.35	49.68
CXCL11					210.18	37.87	144.17	26.97
CXCL9					897.26	82.85	1385.54	72.30
Eotaxin	17.80	0.67	26.33	1.39	135.69	0.31	152.41	2.06
G-CSF					5.68	1.00	11.97	2.24
GM-CSF	3.92	0.33	4.07	0.14	35.56	0.74	39.92	3.02
IFNα2	3.38	0.31	4.27	0.26	15.67	0.85	20.73	1.63
Il-1α					27.85	2.14	26.02	1.28
Il-1β	5.24	0.57	16.49	1.65	145.58	5.94	751.93	54.70
Il-4					11.66	1.20	8.87	0.66
Il-6					6.95	0.93	10.69	0.26
Il-7	4.44	0.22	4.64	0.41	22.23	3.02	36.02	2.64
Il-8	314.19	29.63	619.37	54.81	2659.95	295.76	16184.26	2899.75
IL-12 (p40)					11.48	1.49	11.12	2.81
IL-12 (p70)					4.35	0.45	7.02	0.69
Il-13					4.98	0.70	4.92	0.76
IP-10	3.79	1.15	3.30	0.66	11335.31	184.79	10192.62	144.57
TNFα	11.04	1.05	8.28	0.44	116.89	9.30	220.30	6.35

Figure 2.3. 1,25D directly regulates IL-1β expression in *Mtb*-infected macrophages.

A. Expression of *IL1B* transcripts as assessed by RT/qPCR in control or H37Rv-infected THP-1 cells 24 hours after infection. Data are normalized to the uninfected, untreated control (NI, uninfected cells; NI+D, uninfected cells treated with 1,25D; I, H37Rv-infected cells; I+D, infected cells treated with 1,25D). **B.** Expression of *IL1B* transcripts in two independent cultures of H37Rv-infected primary human macrophages, analyzed as in A. **C.** Protein expression and processing of IL-1β in uninfected and infected THP-1 cells. **D.** Secretion of IL-1β from uninfected and infected THP-1 cells. **E.** Secretion of IL-1β from uninfected and infected primary human macrophages. **F.** ChIP analysis of association of the VDR with the *IL1B* VDRE and transcription start site (TSS). **G.** ChIP analysis of recruitment of the large subunit of RNA PolII to the VDRE and TSS of the *IL1B* gene. ChIP values are normalized to input for each condition and expressed as a fold relative to non-specific IgG control. All data are from one experiment and representative of at least three independent experiments (n=3, mean, s.d.). *P<0.05, **P<0.01, ***P<0.001 as determined by Student's t-test.

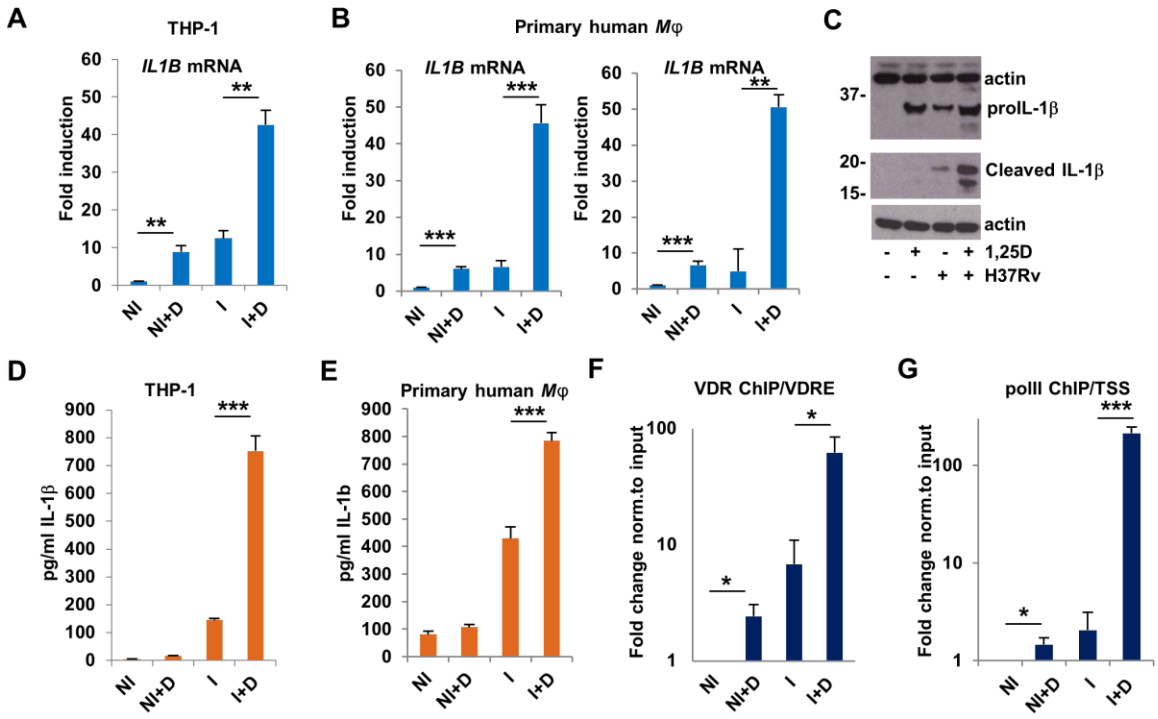
A
THP-1
IL1B mRNA
Fold induction
NI
NI+D
I
I+D
B
Primary human Mφ
IL1B mRNA
IL1B mRNA
C
37-
actin
proIL-1β
20-
15-
Cleaved IL-1β
actin
- + - + 1,25D
- - + + H37Rv
D
THP-1
pg/ml IL-1β
E
Primary human Mφ
pg/ml IL-1b
F
VDR ChIP/VDRE
Fold change norm.to input
G
polII ChIP/TSS
Fold change norm.to input

Figure 2.4. **1,25D-induced IL-1β secretion requires NLRP3.**

A. Expression of AIM2 transcripts and protein in control and infected cells 24 hours after infection. (NI, uninfected cells; NI+D, uninfected cells treated with 1,25D; I, H37Rv-infected cells; I+D, infected cells treated with 1,25D). Values are expressed as fold relative to NI. **B.** Western blots of pro-IL-1β, caspase-1, and β-actin from THP-1 cells transfected with siRNAs indicated and infected for 24 hours with H37Rv. **C.** IL-1β secretion from uninfected (NI) or infected (I) THP-1 cells transfected with siRNAs indicated. 1,25D (D) was added as indicated. All data are from one experiment and representative of at least three independent experiments (n=3, mean, s.d.). **P<0.01 as determined by Student's t-test relative uninfected (A) or respective siCTL (C) control.

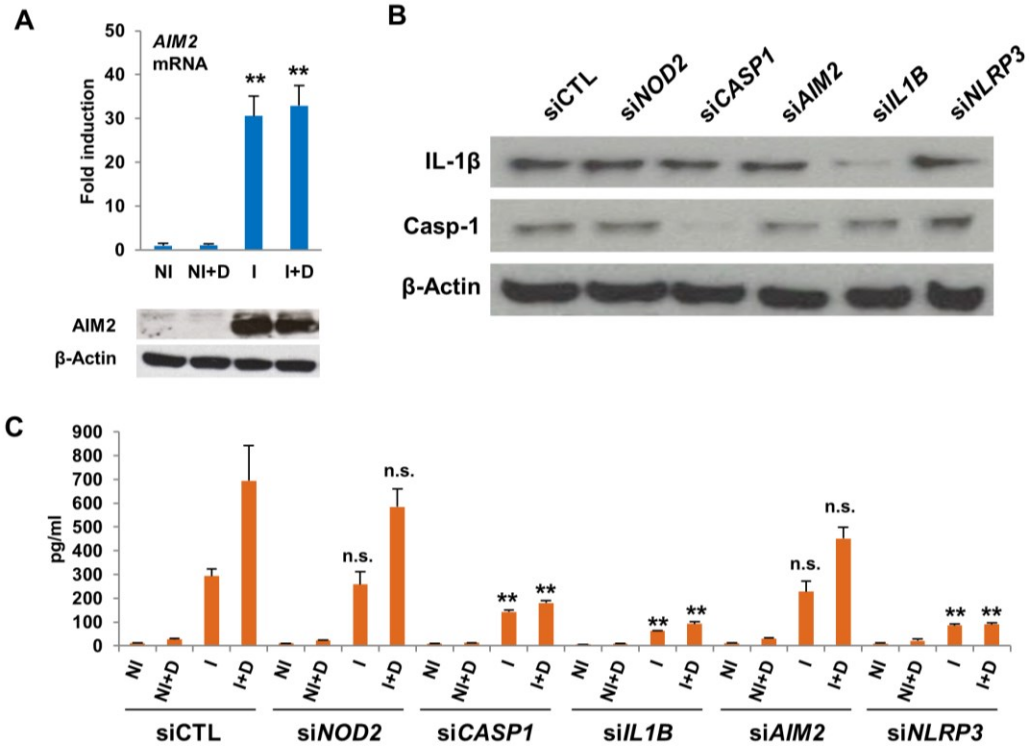
A
AIM2 mRNA
Fold induction
50
40
30
20
10
0
**
**
NI
NI+D
I
I+D
AIM2
β-Actin
B
siCTL
siNOD2
siCASP1
siAIM2
siIL1B
siNLRP3
IL-1β
Casp-1
β-Actin
C
pg/ml
900
800
700
600
500
400
300
200
100
0
n.s.
n.s.
n.s.
**
**
**
**
**
**
NI
NI+D
I
I+D
siCTL
siNOD2
siCASP1
siIL1B
siAIM2
siNLRP3

Table S1. Microarray results and statistical analysis from NI+D, I, and I+D conditions measured relative to NI.
THP-1 cells were either not infected (NI) or H37Rv-infected (I) and treated with vehicle (DMSO) or 100nM 1,25D (D) for 24 hours before RNA extraction. Samples were prepared in triplicate and run on Human Gene 1.0ST microarrays from Affymetrix. Overall chip signal was normalized using RMA. Fold expression and significance relative to NI was calculated using EB (Wright and Simon).

Processed data is available for download from :
http://s3-eu-west-1.amazonaws.com/files.figshare.com/1077275/Table_S1.xlsx

Raw files used for the analysis are available on the Gene Expression Omnibus:
http://www.ncbi.nlm.nih.gov/geo/query/acc.cgi?acc=GSE52819

Figure S1. Heatmap of microarray data using a 5-fold cutoff

Intensity heat map of the >5-fold cut off gene list (N-, uninfected cells; N+, uninfected cells treated with 1,25D; A- H37Ra-infected cells; A+ H37Ra-infected cells; V-, H37Rv-infected cells; V+, H37Rv-infected cells treated with 1,25D). Each vertical line represents one gene that was either up-regulated (red), down-regulated (blue) or not affected (white) under each of the conditions relative to the uninfected, untreated control condition. Group 1 represents those genes that were only detected in one condition, group 2 includes those only regulated by either H37Ra or H37Rv infection, group 3 are those regulated in either infection, group 4 are those that are regulated or no longer regulated in infected cells treated with vitamin D, and group 5 represents those genes regulated in other patterns, including those genes which are differentially regulated under a number of conditions.

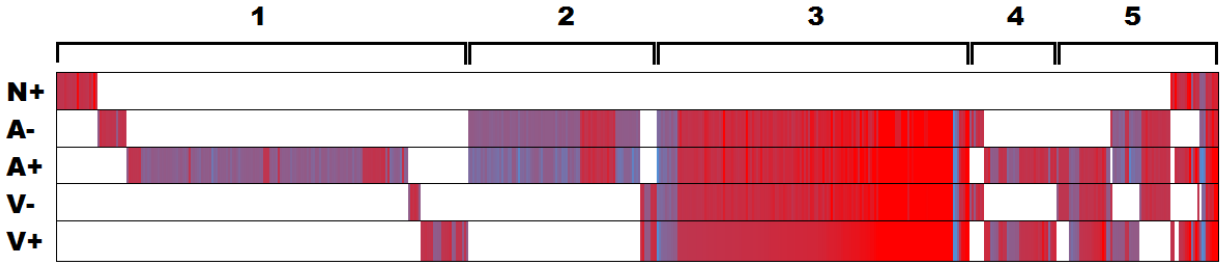

Table S2. Population of genes regulated in each condition measured by microarray.
Number of genes detected by microarray that were up- or down-regulated at least 5-fold relative to the uninfected, vehicle-treated control. THP-1 cells were not infected vehicle control (NI) or infected with H37Rv (I) and treated with vehicle or 100nM 1,25D (D) for 24 hours before RNA isolation.

Cutoff	2-Fold			5-Fold		
Condition	Up Regulated	Down Regulated	Total	Up Regulated	Down Regulated	Total
NI	237	382	619	39	4	43
Ra	953	979	1932	194	96	290
Ra+D	1188	1327	2515	253	224	477
Rv	874	1037	1911	191	29	220
Rv+D	1016	1099	2115	215	55	270
			3197			560

Figure S2. Comparison of fold gene expression in H37Ra and H37Rv infection.
Plot of fold gene expression of macrophages infected with H37Ra (x-axis) vs H37Rv (y-axis), both at an MOI of 5 for 24 hours, relative to the uninfected control.

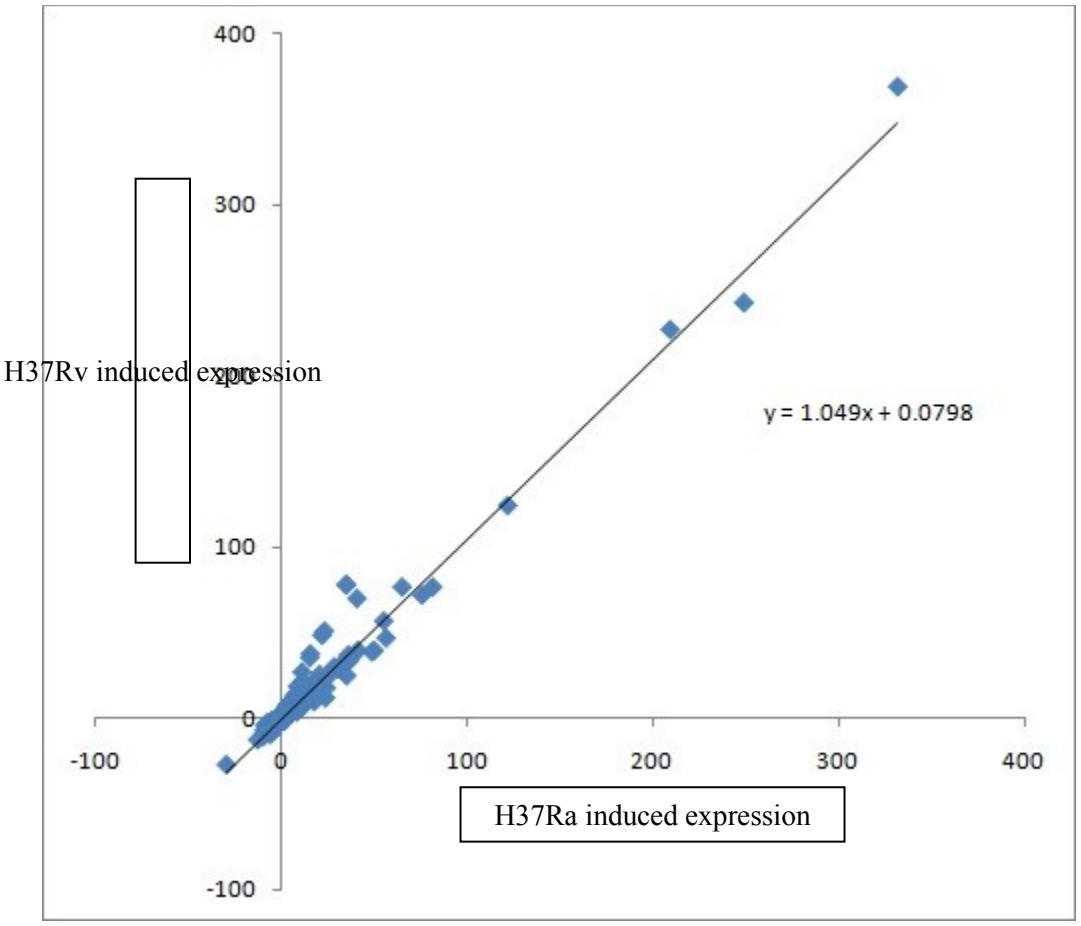

Figure S3. Top genes differentially regulated in H37Ra and H37Rv infected macrophages.

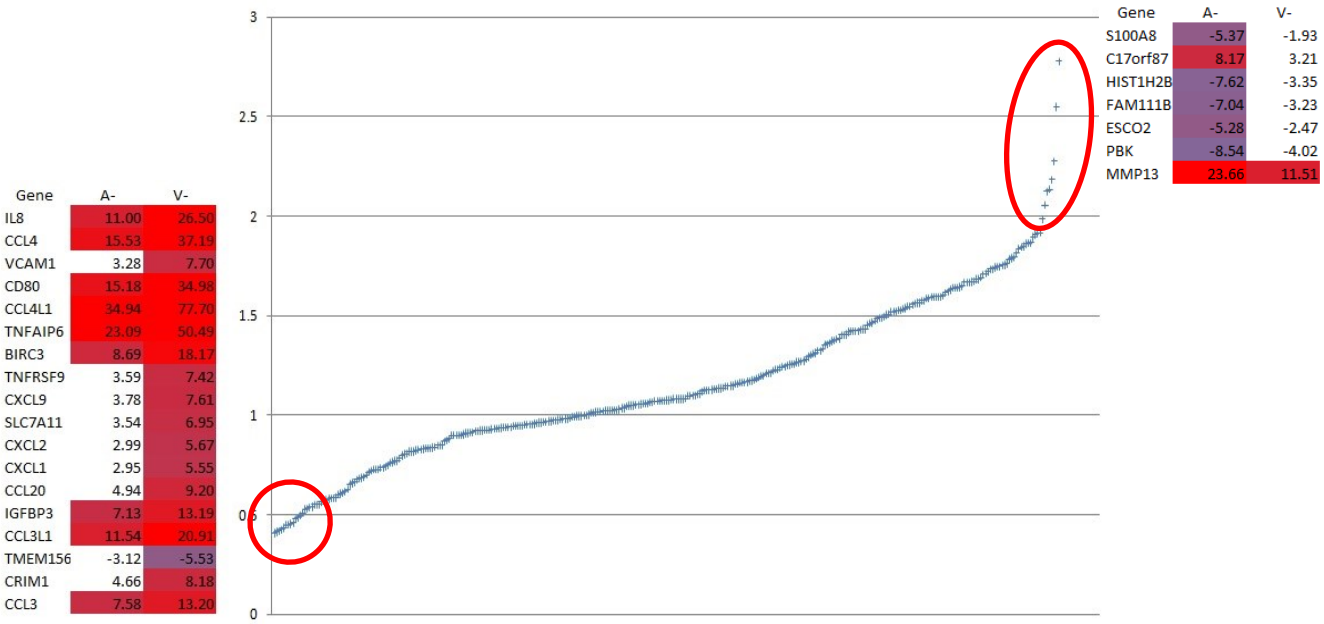

Figure S4. Sequence and position of the *IL1B* VDRE in the human genome relative to the *IL1B* transcription start site.
Each half site of the VDRE is indicated by the nucleotides which are capitalized.

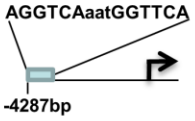

Figure S5. VDR protein expression in *Mtb*-infected macrophages.
Western analysis of VDR expression in THP-1 cells that were not infected (NI) or H37Rv-infected (I) and treated with vehicle or 100nM 1,25D (+D) for 24 hours. Data are from one experiment and representative of two.

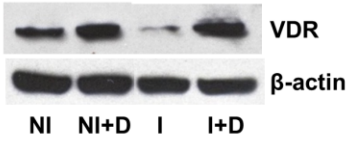

Figure S6. Evolutionary conservation of the *IL1B* VDRE in mammals.
Comparison of the *IL1B* VDRE loci (4287 bases upstream of the human *IL1B* transcription start site) across various mammalian species, as aligned by the UCSC Genome Browser. Agreement with the human sequence is indicated by the nucleotide base appearing in red. Both VDRE half-sites are indicated by the position of the black boxes.

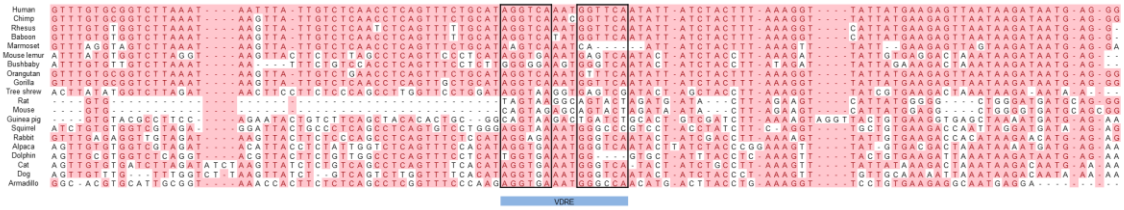

Figure S7. Regulation of *il1b* gene expression by 1,25D in primary cultures of mouse macrophages measured after 24 hours.
Regulation of the VDR target gene cyp24 is provided as a positive control for 1,25D signaling. Values are normalized to untreated control for each time point. All data are from one experiment and representative of two independent experiments (n=3, mean, s.d.). **P<0.01 as determined by Student's t-test relative to untreated.

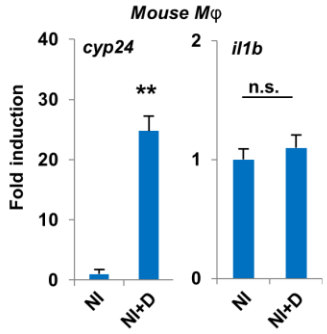

Figure S8. Caspase-1 expression and activity in control and infected THP-1 cells.
(**A**) Expression of caspase-1 analyzed by western blotting in THP-1 cells that were not infected (NI) or H37Rv-infected (I) and treated with vehicle or 100nM 1,25D (+D) for 24 hours. Data is from one experiment and representative of at least five. (**B**) Enzymatic activity of caspase-1 in cell lysates as measured by cleavage of YVAD-pNA substrate. Data are from four experiments (mean and s.e.m.). Indicated p-values were calculated using Student's t-test relative to respective uninfected controls. (**C**) Western blot of ASC in cell lysates where caspase-1 p10 antibody was used for immunoprecipitation. Protein lysates from infected THP-1 cells were collected 24 hours after infection, and data are representative of two independent experiments.

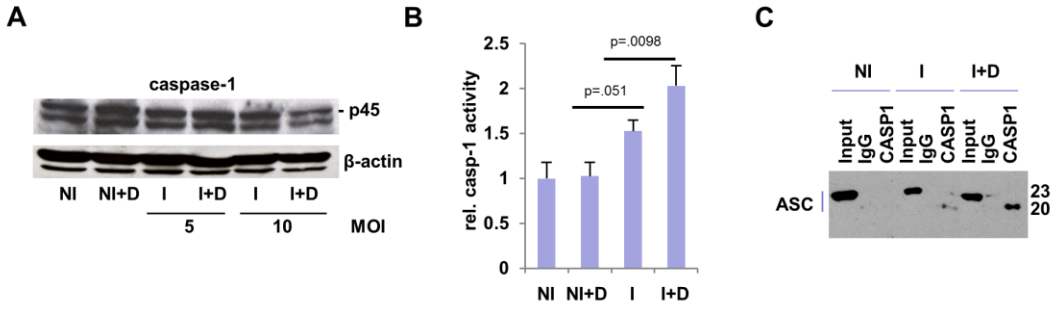

Figure S9. Control experiments for effects of knockdown of pattern recognition receptor expression on IL-1β secretion from infected THP-1 cells.
A. siRNA-mediated knockdown of *AIM2* expression in uninfected and infected THP-1 cells as quantified by RT/qPCR. **B.** qPCR quantification of NOD2 and NLRP3 gene expression in *Mtb*-infected THP-1 cells after transfection with control or specific siRNAs. Values are expressed as fold relative to control siRNA. All data are from one experiment and representative of at least three independent experiments (n=3, mean, s.d.).

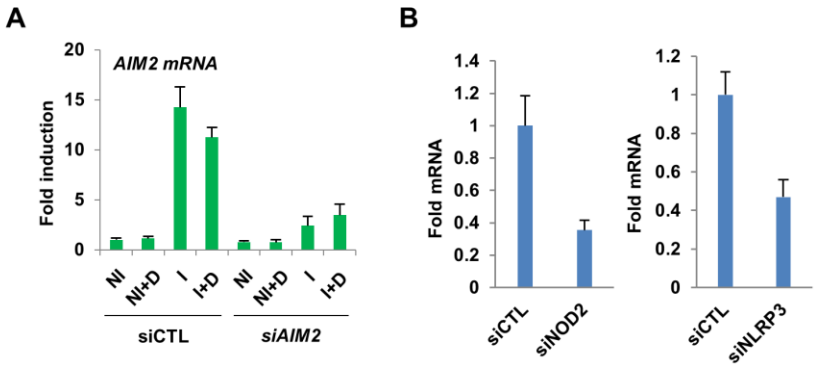

Table S3. Primer sets used for ChIP and qPCR assays.

ChIP Primers		
IL1B VDRE	GGGAAAGCCATTGGAGACT	GAGGGCTTAGATATATGAGCAGGT
IL1B TSS	CCTCAGAGGCTCCTGCAAT	GGGTCTCTACCTTGGGTGCT
qPCR Primers		
AIM2	GTCGCAAAGCAACGTGCTGCA	TGGCAAACAGCGCTTCTGAAACC
18S	CCGAAGCGTTTACTTTGA	GCCGTCCCTCTTAATCAT
B-Actin	GCTGGGGTGTTGAAGGTCTC	GGCATGGGTCAGAAGGATTCC
CAMP	GGACCCAGACACGCCAAA	GCACACTGTCTCCTTCACTGTGA
CYP24	GGCAACAGTTCTGGGTGAAT	TATTTGCGGACAATCCAACA
DEFB4	AAGCTCCCAGCCATCAGCCA	TCCGCATCAGCCACAGCAGC
IKBA	TCCACTCCATCCTGAAGGCTAC	CAAGGACACCAAAAGCTCCACG
NOD2	GGAGCGGGGTTTCGTCAGCC	CCGTGGTCCTCAGCTTGGCC
NLRP3	CTTCTCTCTGATGAGGCCCAAG	GCAGCAAACTGGAAAGGAAG
IL1B	CAAGGGCTTCAGGCAGGCCG	TGAGTCCCGGAGCGTGCAGT
mouse b-actin	CCAGGCATTGCTGACAGGATGCA	CGCAGCTCAGTAACAGTCCGCCT
mouse cyp24	GAGTGTCACGGGTCGCCTGC	CACGGACCTTGGGGGTTGCC
mouse il1b	TCCAGCCAAGCTTCCTTGTGCAA	GCTGCTGCGAGATTTGAAGCTGG

CHAPTER 3: IL-1β Paracrine Signaling Enhances DEFB4 Secretion from Alveolar Epithelial Cells

3.0 Preface to Chapter 3

In the previous chapter we investigated the global changes that 1,25D induced in *Mtb*-infected macrophages, and found that the largest change was in the production of cytokines, especially IL-1β. While previously published work had demonstrated that 1,25D was able to limit bacterial replication in *Mtb*-infected macrophages, these efforts had largely focused on the regulation of anti-microbial peptides CAMP and DEFB4, and their local production and action in the macrophages themselves. From the data presented in Chapter 2, we hypothesized that a macrophage-only culture system was insufficient for trying to determine the effects of 1,25D during the acute stages of infection. As we had also determined that the VDREs proximal to the cytokines regulated by 1,25D in humans were not present in mice, we proceed to first determine the effect of this changed secretion profile on alveolar epithelial cells, and secondly, to co-culture infected macrophages with these cells so that their dynamic interaction could be investigated.

3.1 Abstract

In the previous chapter we identified the global transcriptional effects of 1,25D on *Mtb*-infected macrophages. From this we found that one of the most prominent groups of genes induces was that of cytokines, and further characterization demonstrated that IL-1β secretion was elevated due to a direct effect of regulation of gene expression. Due to the lack of conservation of this VDRE in mice, the impact of elevated IL-1β production was investigated in a novel model wherein infected macrophages were co-cultured with primary human small airway epithelial cells. Co-culture significantly prolonged survival of infected macrophages, and 1,25D/infection-induced IL-1β secretion from macrophages reduced mycobacterial burden by stimulating the anti-mycobacterial capacity of co-cultured lung epithelial cells. These effects were independent of 1,25D-stimulated autophagy in macrophages but dependent upon epithelial IL1R1 signaling and IL-1β-driven epithelial production of the antimicrobial peptide DEFB4/HBD2. These data provide evidence that the anti-microbial actions of vitamin D extend beyond the macrophage by modulating paracrine signaling, reinforcing its role in innate immune regulation in humans.

3.2 Introduction

Innate immunity to *Mtb* infection is critical for determining disease outcome, and it has long been recognized that during TB outbreak investigations, only 30-50% of those with an equivalent exposure develop a productive infection, as demonstrated by a tuberculin skin-test conversion [226]. The primary site of *Mtb* infection is alveolar macrophages, which lie within the alveolar space, adjacent to the epithelial lining [227]. Lung epithelial cells are generally not considered part of the innate immune responses to *Mtb* infection. However, they represent both a physical and an immunological barrier to infection by contributing to the maintenance of mucosal integrity, promoting phagocytosis, and producing several antimicrobial peptides, vanguards of innate immune responses to infection [227,228]. For example, antimicrobial peptide (AMP) DEFB4/HBD2 is expressed in upper airway epithelial cells, is inducible by interleukin-1β (IL-1β), and has been detected in bronchoalveolar lavage fluid from normal healthy humans [229]. It has been shown to have direct antimicrobial activity against *Mtb* and drug-resistant *Mtb* [230] .

Here, we show that IL-1β secreted from infected macrophages initiates a paracrine signaling cascade with proximal airway epithelial cells. As this mechanism of *IL1B* regulation explored in Chapter 2 was not conserved in mice, we developed a co-culture system between macrophages and primary small airway lung epithelial cells to model the effects of elevated IL-1β secretion. In these co-culture experiments, 1,25D potentiated IL-1β signaling from macrophages resulting in the secretion of DEFB4 from primary lung epithelial cells. Taken together these results suggest that the effects of 1,25D extend beyond the macrophage and involve the modulation of paracrine signaling to enhance the innate immune responses to *Mtb* infection.

3.3 Results

1,25D enhances IL-1β secretion from *Mtb*-infected macrophages, inducing *DEFB4* gene expression in primary lung epithelial cells. Upon infection, alveolar macrophages initially phagocytose *Mtb.* Importantly, alveolar macrophages are also in direct contact with the respiratory epithelial surface [227]. Although the immunological contribution of lung epithelia is well studied in other contexts [231], it is poorly characterized during the course of *Mtb* infection. IL-1β induces expression of genes encoding AMPs in epithelial cells through its capacity to stimulate the activity of transcription factor, NF-κB, leading to secretion of antimicrobial proteins [232,233]. Thus, to understand the potential crosstalk between alveolar macrophages and the human respiratory epithelial surface, we conducted a series of experiments using an *in vitro* co-culture system between macrophages and human primary cultures of non-polarized small airway epithelial cells (SAECs) from multiple donors. In cultures of SAECs alone, recombinant IL-1β induced expression of the gene encoding DEFB4, while 1,25D had no significant effect (**Figure 3.1A**). Conversely, induction of *CAMP* gene expression was largely 1,25D-dependent (**Figure 3.1A**). Essentially identical results seen when using CaLu3 cells, a lung epithelial cell line (**Figure S10A**). Media supernatants from these treated SAECs were assayed for DEFB4 and CAMP secretion by ELISA. DEFB4 was detected under control conditions, and was found to be elevated when SAECs were treated with rIL-1β, but not 1,25D (**Figure 3.1B)**. In contrast, the cleaved C-terminal of CAMP, LL-37, was not detected above background signal under any of the conditions (**Figure 3.1B**). In comparison, neither DEFB4 nor LL-37 was detected in media supernatants from THP-1 cells infected with *Mtb* using this assay (data not shown). Media supernatant isolated from CaLu3 cultures from these experiments demonstrated direct antimicrobial activity against *Mtb* after 24 hours (**Figure S10B**).

SAECs were then cultured with conditioned media from control or H37Rv-infected macrophages to test for effects of 1,25D and secreted factors on AMP expression. In addition, as IL-1β has been shown to induce NF-κB signaling through IL1R1 [233], we investigated the expression of NF-κB target gene *DEFB4* [232,233] in lung epithelial cells. Media from infected macrophages induced expression of *DEFB4* (**Figure 3.1C**) in SAECs. Importantly, pre-incubation of the transferred media with IL-1β-neutralizing antibody abolished *DEFB4* gene induction. Given that *DEFB4* expression levels are driven by IL-1β, the combined effects of 1,25D and infection on *DEFB4* transcription are consistent with levels of IL-1β secretion induced in 1,25D-treated, infected macrophages (**Figure 2.3D,E**). As expected, *CAMP* expression in SAECs was dependent on 1,25D (**Figure 3.1D**). Essentially identical results were seen when media was transferred onto CaLu3 cells instead of SAECs (**Figure S10C,D**).

Co-culture of macrophages and SAECs enhances macrophage survival and helps control *Mtb* infection. Next, to model the consequences of the real-time interaction between infected macrophages and the alveolar epithelia during the initial round of infection, we established a transwell co-culture system between *Mtb*-infected macrophages and SAECs (**Figure 3.2A**). Macrophages were infected with *Mtb* for 4 hours and washed extensively to eliminate any remaining extracellular mycobacteria. A transwell bucket containing co-cultured lung epithelial cells was then added to the tissue culture plate containing the infected macrophages. The two cell populations were separated by a 0.4μm filter to allow for the exchange of secreted proteins but prevent migration of mycobacteria. Note that in control experiments no mycobacteria were detected in the transwell bucket 4 days after infection (data not shown). Co-culture of macrophages infected at an multiplicity of infection (MOI) of 5 with

SAECs dramatically extended macrophage cell survival at three days post-infection, as measured by cytoplasmic lactate dehydrogenase (LDH) release (**Figure 3.2B**), a marker of plasma-membrane compromise and necrosis. After 3 days of infection, the relative amount of LDH release was comparable to that seen 24 hours after infection under macrophage-only conditions. 1,25D treatment had no effect on the survival of infected cells cultured in the absence or presence of SAECs. When macrophages infected at an MOI of 10 were co-cultured with SAECs, LDH release was slightly higher, but a similar protective effect of SAECs was observed (**Figure 3.2B**). The protective benefit of the SAECs in co-culture was also clear by the relative amount of adherent cells remaining as visualized by phase-contrast microscopy (**Figure 3.2C**); most of the macrophages co-cultured with SAECs were still adherent, whereas infected macrophages cultured in the absence of SAECs had detached from the plate.

To determine any effects of co-culturing with and without 1,25D on mycobacterial burden, colony forming unit (CFU) assays were performed with cells co-cultured as above. We determined changes in total *Mtb* burden after 72 hours of infection. The addition of SAECs resulted in a halving of mycobacterial burden at this time point, and addition of 1,25D to the co-culture system produced a further significant reduction in mycobacteria (**Figure 3.3A**). A similar magnitude of effect was generated when co-culturing infected THP-1 cells with CaLu3 cells (**Figure S11**). To confirm the contribution of epithelial signaling by infection- and 1,25D-induced IL-1β towards the reduction in mycobacterial burden, we knocked down IL1R1 receptor expression in SAECs 36 hours prior to their co-culture. Control experiments showed that expression of epithelial IL1R1 was reduced for at least 72 hours after siRNA-mediated knockdown (**Figure 3.3B**). Mycobacterial burden was sharply elevated 72 hours after infection in the absence or presence of 1,25D when macrophages were co-cultured with IL1R1-depleted

SAECs. In contrast, co-culture of SAECs transfected with control siRNAs eliminated net mycobacterial growth in the presence of 1,25D (**Figure 3.3C**), consistent with experiments described above. To determine if epithelial secretion of DEFB4 was responsible for the increased control of mycobacterial proliferation, we transfected SAECs with either siRNA against *IL1R1* or *DEFB4* transcripts 36 hours prior to their co-culture with infected macrophages. Reduced expression of *DEFB4* was verified by qPCR in samples collected 72 hours after the initiation of their co-culture (**Figure 3.3D**). CFU assays were performed at 72 hours after infection and demonstrated that siRNA-mediated knockdown of *DEFB4* expression permitted levels of bacterial proliferation similar to what was observed in knockdown of *IL1R1* (**Figure 3.3E**). Taken together, these data reveal that IL-1β secreted from infected macrophages drives a paracrine signaling cascade which contributes to control of mycobacterial burden in our culture system.

The contribution of 1,25D to reducing mycobacterial burden in macrophages arises at least in part from its capacity to enhance autophagy in infected macrophages in a CAMP-dependent manner [213,234], a critical mechanism for control of intracellular pathogens. To understand if epithelial CAMP or DEFB4 secretion was helping to control bacterial burden by enhancing autophagy in macrophages, even if CAMP was undetected in the media supernatant in control experiments, we probed for colocalization of *Mtb* and LC3 protein, a marker of autophagosomes, in (1,25D-treated) infected macrophages 3 days after infection. Using bright-field fluorescence microscopy, we visualized *Mtb* and the presence of any colocalized LC3 (**Figure 3.4A**). Quantification of the number of times in which mycobacteria were found in LC3-containing membrane structures in confocal imaging revealed that the frequency of colocalization increased when infected macrophages were treated with 1,25D; however, the presence of SAECs in co-

culture had no impact on the degree of colocalization, both in the absence and presence of 1,25D (**Figure 3.4B**). Finally, analysis of 3-dimensional stacks of confocal images taken from 1,25D-treated conditions confirmed that the signal from *Mtb* colocalized with LC3-containing structures (**Figure 3.4C**). Taken together, these data reveal that the decrease in CFU observed in co-culture experiments was not a consequence of an increase in autophagy in macrophages.

3.4 Discussion

Previous studies on the role of IL-1β in the innate immune response to infection have focused on its capacity to control infection by autocrine signaling from infected macrophages. While epithelial cells are known to have important immunologic function in other diseases and contexts [227,235,236], they are usually not considered to be an important part of the innate immune response to *Mtb* infection. Primary upper respiratory epithelial cells express DEFB4 in response to IL-1β stimulation *in vitro* [229]. Our data demonstrate that the IL-1β secreted from infected macrophages has the capacity to elicit an antimycobacterial response from small airway epithelial cells. Importantly, siRNA-mediated knockdown of epithelial IL1R1 or DEFB4 expression significantly negated the control of *Mtb* growth in co-cultured macrophages. Modeling of these findings *in vivo* will be necessary to fully understand the extent of the contribution of epithelial cells to the innate immune response in this context. Doing so in primates would pose a major undertaking, and it would be difficult to assess the contribution of the reciprocal signaling cascade between alveolar macrophages and epithelial cells in such a model, as it would likely occur in the acute response to a very low dose exposure.

Macrophage-epithelial cell co-culture controls mycobacterial burden but did not induce autophagy, and epithelial knockdown of IL1R1 expression negated any protective benefit. Taken together, our data suggest that paracrine secretion of DEFB4 from epithelial cells provides a more substantial level of protection against infection than DEFB4 production by macrophages. Previous studies have provided evidence for a reduction in bacterial burden when *Mtb*-infected macrophages are treated with 1,25D *in vitro* [159,213]. We find that this effect is limited, and that bacterial burden is elevated 3 days after infection with virulent *Mtb*, representing a failure to

control the infection. From this study it is clear that more complete models of the innate immune response are required to understand the full effect of 1,25D.

Correlations between vitamin D deficiency and a higher incidence of TB have repeatedly been observed [148-150]. Clinical trials did not reveal a substantial benefit of vitamin D in the treatment of active disease [152,153], although a recent study showed that vitamin D supplementation accelerated the resolution of inflammatory responses during treatment for *Mtb* disease in some patients [237]. Our results would suggest that the optimal point of treatment would be vitamin D supplementation to bolster innate responses and prevent infection. Such a program would be economically viable considering the negligible cost of vitamin D supplementation as compared to antibiotic chemotherapy, and a useful prophylactic measure against drug-resistant tuberculosis. Our mechanistic data supports the idea that serum levels of vitamin D may be causally important for defense against *Mtb* exposure, but clinical trials would be required to understand this.

3.5 Materials and Methods

Ethics Statement. De-identified human peripheral blood was purchased from Research Blood Components (Boston, MA). Following informed written consent, blood was collected by venipuncture from healthy adult volunteers, recruited by Research Blood Components. Protocols for the collection of whole blood for research purposes were approved by New England Institutional Review Board.

Tissue Culture. THP-1 cells (TIB-202, ATCC) were cultured in RPMI-1640 (Wisent) with 10% FBS. SAEC cells were acquired following informed consent, permission, and ethical approval by Lonza, and were cultured in SAGM (Lonza), as directed by manufacturer. These cells were isolated by a proprietary method from the 1mm bronchiole of the lung, which includes alveoli. H37Rv was cultured to mid-log phase in a rolling incubator at 37°C in Middlebrook 7H9 (Difco) with .05% Tween-80 and 10% ADC enrichment (BD Biosciences). CaLu3 cells were cultured in EMEM with 15% FBS and 1% penicillin/streptomycin.

Macrophage Infections. $1x10^6$ THP-1 cells were terminally differentiated by $2x10^{-8}$M PMA for 24 hours in RPMI with 10% charcoal stripped FBS, inducing cell cycle arrest. H37Rv cultures were centrifuged and pellets were resuspended in RPMI-1640 with 10% charcoal stripped FBS and .05% Tween-80 and clumping was disrupted by repeated passage through a 27-gauge needle. Media was removed from THP-1 cells and replaced with media containing *Mtb* in the indicated multiplicity of infection (MOI) for 4 hours. THP-1 cells were then vigorously washed three times with RPMI to remove extracellular bacteria, followed by incubation in RPMI with 10% charcoal stripped FBS containing either vehicle (DMSO) or 1,25D at a final concentration of 10^{-7} M.

RNA extraction and qPCR. RNA extraction was performed with TRIzol and chloroform (Invitrogen) as per manufacturers' instructions. RT was performed with iScript cDNA Synthesis Kit (Bio-Rad) and qPCR was performed with SsoFast Eva Green with low ROX (Bio-Rad) on an Eco qPCR cycler (Illumina), normalizing expression to β-actin and 18S. Primers used are listed in Table S3.

Reagents, ELISAs, and antibodies. Antibodies: α-IL-1β (MAB601, R&D Systems) murine serum IgG (Sigma). Recombinant IL-1β was purchased from Millipore. ELISAs for DEFB4 (Abnova) and LL-37 (Hycult Biotech) were performed in accordance with the manufacturer's instructions.

CaLu3 Media Transplant Three days prior to treatment, CaLu3 cells were cultured in RPMI with 10% charcoal stripped FBS. THP-1 cells were not infected or infected with H37Rv followed by treatment with DMSO or 1,25D at a final concentration of 10^{-7} M for 24 hours. Media was filter sterilized by passage through 0.20μm filters. Media was then incubated with anti-IL-1β or non-specific murine IgG for 30 minutes before transfer to CaLu3 cultures. Cells were harvested after 24 hours for RNA extraction.

Macrophage CFU Assay. At the indicated time points, tissue culture plates were centrifuged to pellet any liberated mycobacteria and non-adherent cells. Media was aspirated and macrophages were lysed with water for 5 min, after which an equal volume of 2x 7H9 with .1% Tween-80 was

added. Samples were vigorously resuspended and plated in serial dilution on Middlebrook 7H10 (Difco) with 10% OADC enrichment (BD Biosciences).

siRNA-mediated knockdowns. One day after PMA-induced differentiation, siRNAs targeting *IL1R,1 DEFB4*, or the non-targeting scrambled control (NC1) (Integrated DNA Technologies) were transfected into SAEC cells using Transductin (Integrated DNA Technologies) in 10% Q-serum, according to manufacturer's instructions. After 4 hours, media was replaced with RPMI with 10% charcoal stripped FBS. After another 48 hours, cells were cocutured with THP-1 cells infected with H37Rv.

Statistical Analysis. Student's t-test, ANOVA, or a two-tailed Fisher's exact test was performed where indicated using GraphPad software..

THP-1 to SAEC or CaLu3 Media Transplant. THP-1 cells were not infected or infected with H37Rv followed by treatment with DMSO or 1,25D at a final concentration of 10^{-7} M for 24 hours. Media was filter sterilized by passage through 0.20μm filters. Media was then incubated with anti-IL-1β or non-specific murine IgG for 30 minutes before transfer to epithelial cell cultures. Cultures were harvested for RNA after 24 hours.

Transwell Co-culture. Epithelial cells were seeded in transwell buckets with 0.4μm pores (Corning) and cultured in RPMI with 10% charcoal stripped FBS 48 hours before infection of the THP-1 cells. After the THP-1 cells were infected for 4 hours at a MOI of 5 and washed, SAECs were placed in co-culture with H37Rv-infected THP-1 cells by transferring the buckets

containing the epithelial cells to the plates containing the infected macrophages, and then treated with DMSO or 1,25D (10^{-7} M). At indicated time points, plates were centrifuged and both cell populations were lysed with water and pooled for CFU assay, performed as described above.

Immunofluorescence and image acquisition. Following 4% paraformaldehyde fixation over 10 minutes, cells on coverslips were washed with 100mM glycine and then PBS. Cells were then permeabilized with 0.1% Triton X-100 for 5 minutes. Cells were incubated in PBS-0.2% BSA during 5 minutes. Primary antibody against LC3 (Novus Biological, dilution 1/300) was incubated with coverslips for 1 hour at 37°C in a humidified chamber in phosphate-buffered saline with 1% BSA. Following 3 washes, cells were incubated with the secondary antibody anti-rabbit Alexa-647 (Life Technologies, dilution 1/1000) and with the anti-*Mtb* antibody coupled to FITC (Abcam ab20962, dilution 1/100) for 45 minutes at RT in the dark. Slides were mounted in Vectashield containing DAPI (Vector) and observed with a Zeiss Axiovert X100 bright field microscope or a Zeiss LSM510 X100 confocal microscope. Images were acquired with LSM510 software. Stacks of confocal images, 3D reconstitution, and quantification of percent of colocalization were performed with Imaris 7.4 and the figures were assembled with Photoshop (Adobe).

LDH Assay

Cell-free media supernatant was collected from infected macrophages with and without SAECs in co-culture. Cytotoxicity Detection Kit (LDH) from Roche was used in accordance with manufacturer's instructions.

3.6 Figures

Figure 3.1. *DEFB4* and *CAMP* genes are regulated by IL-1β and 1,25D in SAECs.

A. Expression of *DEFB4* and *CAMP* in SAECs as measured by RT/qPCR. Cells were incubated with IL-1β (10ng/ml) or 1,25D (100nM) for 24h. **B.** Media supernatants from cells in (A) were tested for DEFB4 and LL-37 protein secretion by ELISA. **C and D.** Expression of *DEFB4* (C) and *CAMP* (D) genes in SAECs incubated with conditioned media from uninfected (NI) or H37Rv-infected (I) THP-1 cells treated with vehicle or 100nM 1,25D (+D) for 24 hours. Media was treated with neutralizing antibody against IL-1β (α-IL-1β), or normal serum IgG, as indicated, for 30 minutes prior to incubation with cells. Values are expressed as a fold of the NI control. All data are from one experiment and representative of three independent experiments using separate donors of SAECs (n=3, mean, s.d.). *P<0.05, **P<0.01 as determined by Student's t-test relative untreated (A, B) or respective IgG (C) control.

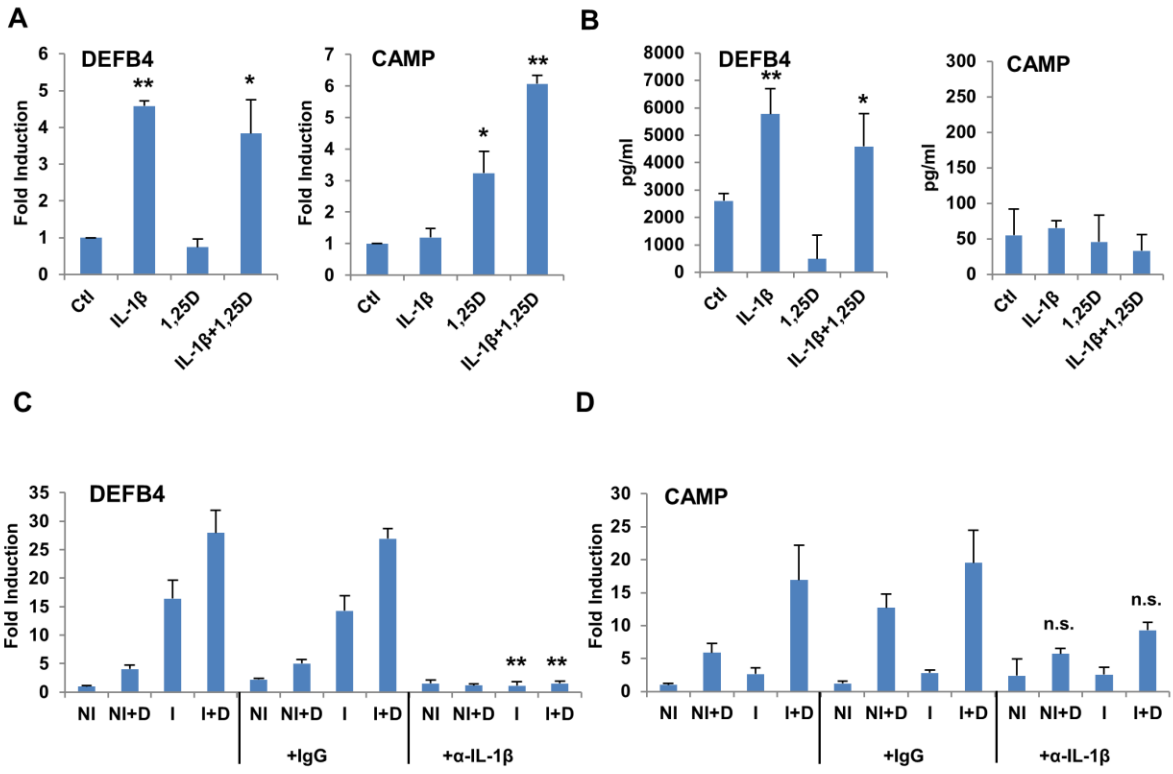
A
DEFB4
Fold Induction
Ctl
IL-1β
1,25D
IL-1β+1,25D
CAMP
B
pg/ml
C
NI
NI+D
I
I+D
+IgG
+α-IL-1β
D
n.s.

Figure 3.2. Co-culture with SAECs enhances survival of *Mtb*-infected macrophages.

A. Schematic representation in profile of co-culture system. THP-1 cells were cultured and infected in the lower well and SAECs were seeded in the upper transwell bucket. **B.** LDH activity measured in the media supernatant from macrophages (Mφ) infected with H37Rv at an MOI of 5 or 10, as indicated, and treated with vehicle control or 100nM 1,25D (+D), with and without the presence of SAECs in transwell co-culture (CC). Signal was normalized to spontaneous LDH release levels from uninfected macrophages, as measured from media supernatant collected from cells at each day. All data is expressed relative to LDH activity of the Mφ condition infected at an MOI of 5 at 24 hours post-infection. Data are from one experiment and representative of two independent experiments using separate donors of SAECs (n=3, mean, s.d.). **P<0.01 as determined by two-way ANOVA comparing Mφ to CC conditions. **C**. Representative phase-contrast microscopy of macrophages 3 days after infection with and without 1,25D treatment in the presence or absence of SAECs in co-culture. In the macrophage only condition, most of the cells visible appear round and out of focus as they are floating freely in the media, while cells co-cultured with SAECs are almost all adherent and exhibit normal macrophage morphology.

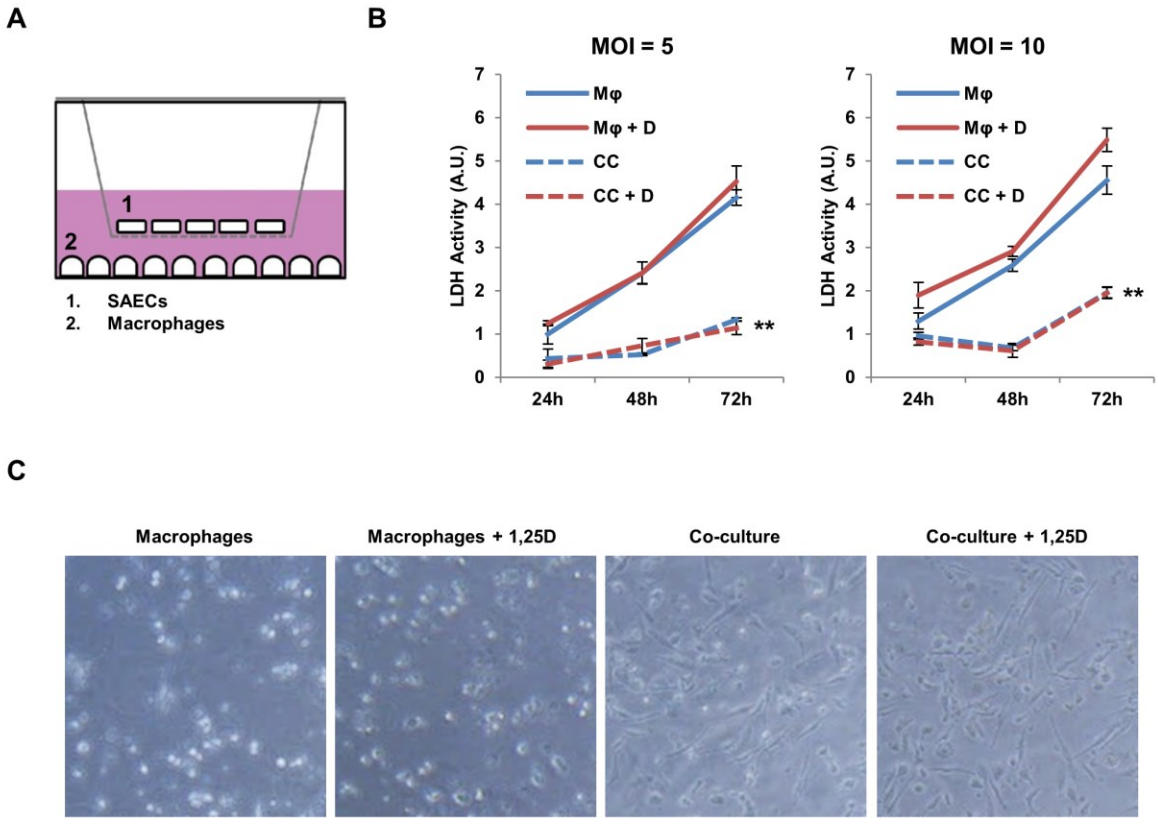
A
1
2
1. SAECs
2. Macrophages
B
MOI = 5
MOI = 10
LDH Activity (A.U.)
Mφ
Mφ + D
CC
CC + D
24h
48h
72h
**
C
Macrophages
Macrophages + 1,25D
Co-culture
Co-culture + 1,25D

Figure 3.3. Control of *Mtb* infection by co-cultured epithelial cells is dependent on epithelial IL1R1 and DEFB4 expression.

A. CFU of macrophages (Mφ) infected with H37Rv at an MOI of 5 for 4 hours and treated with vehicle control or 100nM 1,25D (+D), with and without the additional presence of SAECs in transwell co-culture (CC). Data are from three experimental replicates (mean and SD) and representative of three independent experiments using different donors of primary cells. Statistical significance was determined by one-way ANOVA. (*P<0.05). **B.** Validation of siRNA-mediated knockdown of *IL1R1* expression in SAECs. RNA was extracted from SAECs cells 3 days after the initiation of co-culture and 4.5 days after transfection of control siRNA (siCTL) or siIL1R1. Data are from three experimental replicates (mean and SD), **P<0.01 as determined by student's T-test relative to respective siCTL controls. **C.** CFU quantification of *Mtb* in THP-1 cells infected at an MOI of 5 for 4 hours after 72 hours of co-culture with SAEC cells transfected with control siRNA (siCTL) or siRNA specific to *IL1R1*. 1,25D (D) was added as indicated. Data are from three experimental replicates (mean and SD) and representative of two independent experiments. Statistical significance was determined by one-way ANOVA. (**P<0.01). **D.** Validation of siRNA-mediated knockdown of *DEFB4* expression in SAECs. RNA was extracted from SAECs cells 3 days after the initiation of co-culture and 4.5 days after transfection of control siRNA (siCTL) or siDEFB4. Data are from three experimental replicates (mean and SD) and representative to two independent replicates. **P<0.01 as determined by student's T-test relative to siCTL control. **E.** CFU quantification of *Mtb* in THP-1 cells infected at an MOI of 5 for 4 hours after 72 hours of co-culture with SAEC cells transfected with control siRNA (siCTL) or siRNA specific to *IL1R1* or *DEFB4*. Data are from three experimental replicates (mean and SD) and representative of two independent experiments using separate donors of SAECs. Statistical significance was determined by one-way ANOVA. (*P<0.05).

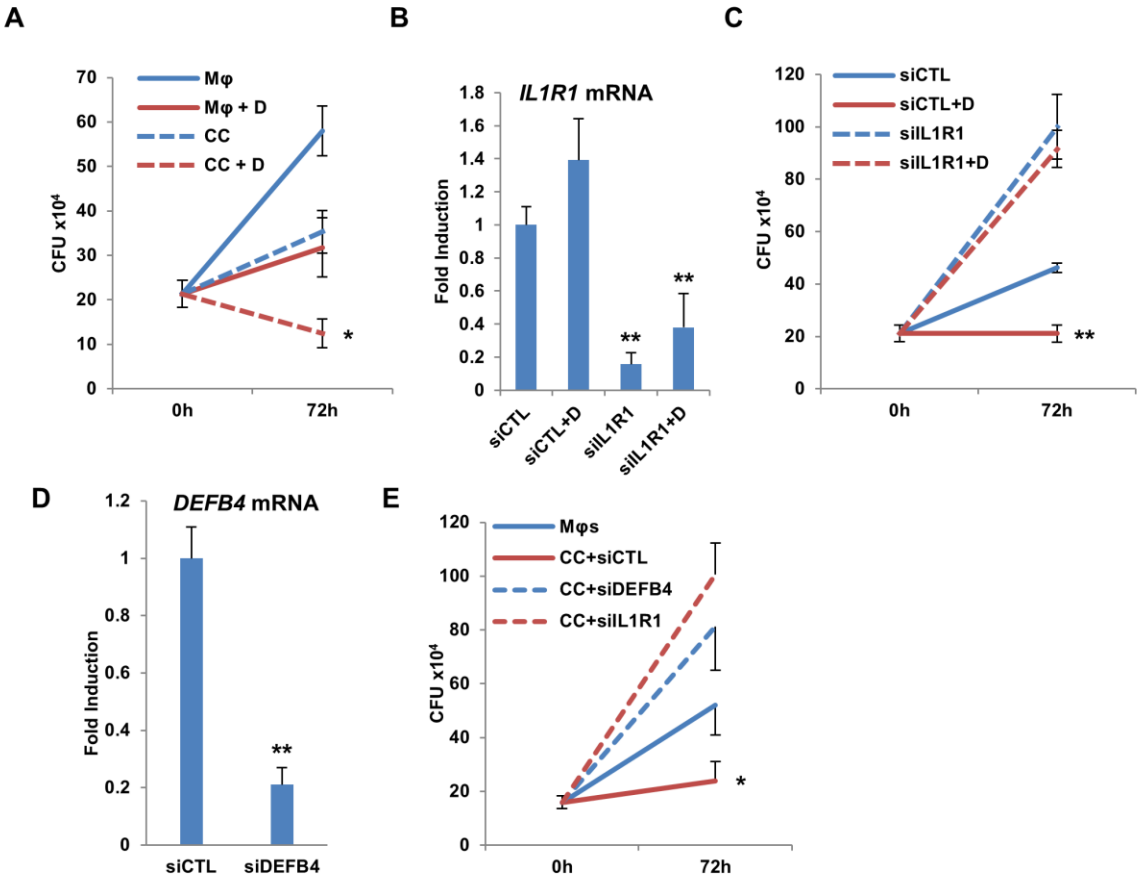
A
Mφ
Mφ + D
CC
CC + D
CFU x10⁴
0h
72h
*
B
IL1R1 mRNA
Fold Induction
siCTL
siCTL+D
siIL1R1
siIL1R1+D
**
C
siCTL
siCTL+D
siIL1R1
siIL1R1+D
CFU x10⁴
0h
72h
**
D
DEFB4 mRNA
Fold Induction
siCTL
siDEFB4
**
E
Mφs
CC+siCTL
CC+siDEFB4
CC+siIL1R1
CFU x10⁴
0h
72h
*

Figure 3.4. Co-culture with SAECs does not enhance autophagy in *Mtb*-infected macrophages.

A. Representative bright-field microscopy of infected macrophages cultured in the absence or presence of 1,25D and/or a transwell containing SAECs. Cells were fixed and probed with an antibody against *Mtb*, LC3, and the nuclear stain DAPI. **B.** Percent of *Mtb* that colocalized with LC3 signal under each condition as determined by counting populations of infected macrophages across at least 10 confocal images, with at least two infected cells per image. Statistical significance was determined by a two-tailed Fisher's exact test (**P<0.01). **C**. 3-dimensional rendering of confocal stacks of infected macrophages treated with 1,25D to demonstrate colocalization of LC3 and *Mtb* signal.

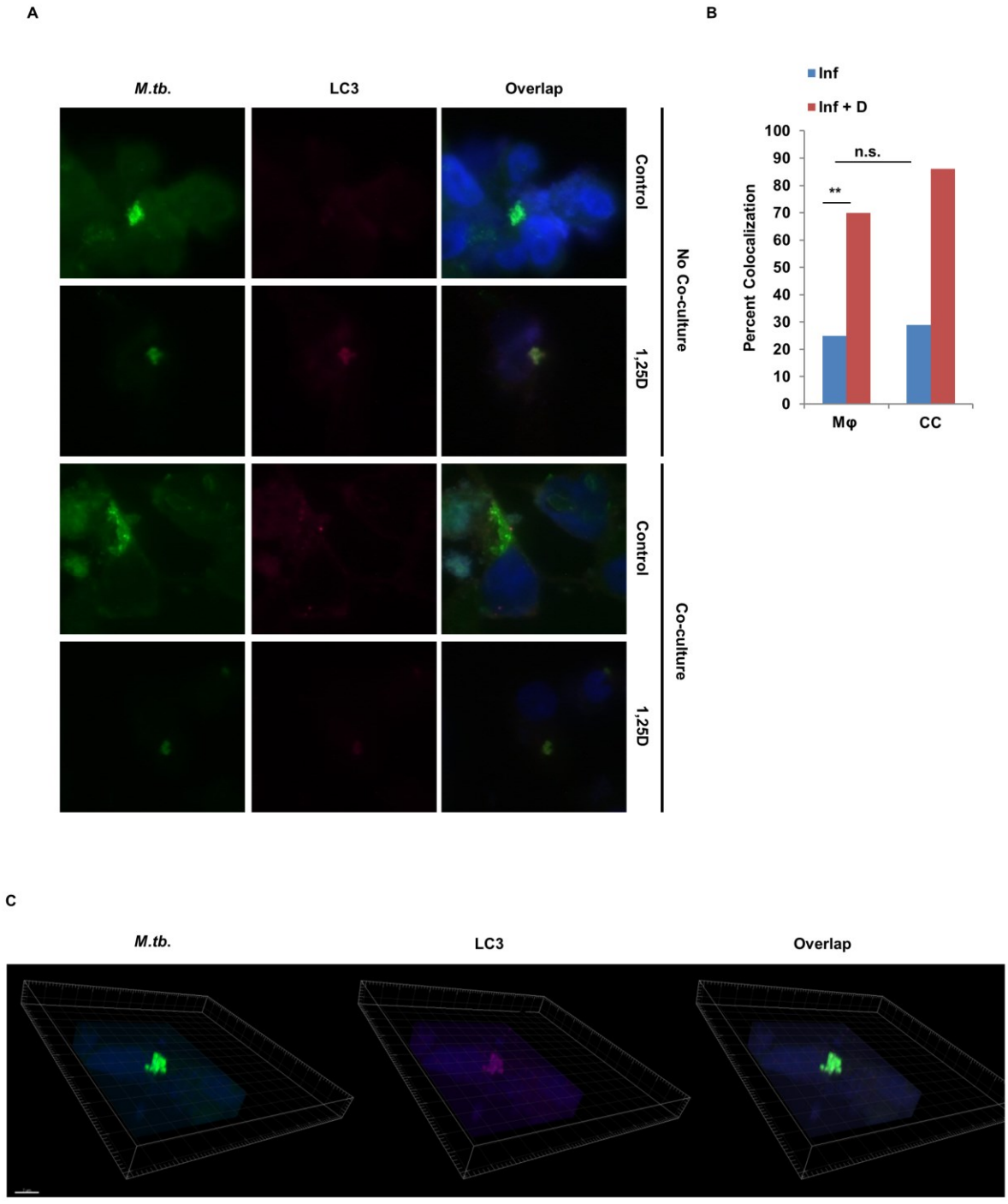
A
M.tb.
LC3
Overlap
Control
1,25D
No Co-culture
Control
1,25D
Co-culture
B
Inf
Inf + D
Percent Colocalization
100
90
80
70
60
50
40
30
20
10
0
n.s.
**
Mφ
CC
C
M.tb.
LC3
Overlap

Figure 3.5. Model of paracrine macrophage-epithelial cell signaling cascade driven by 1,25D and IL-1β.

IL1B gene expression is driven by infection and 1,25D, and pro-IL-1β maturation is dependent on the NLRP3 inflammasome. Released IL-1β signals via IL1R1 on adjacent epithelial cells to induce expression of *DEFB4*. The release of DEFB4 induced by IL-1β, in combination with 1,25D, leads to control of mycobacterial proliferation in the macrophage.

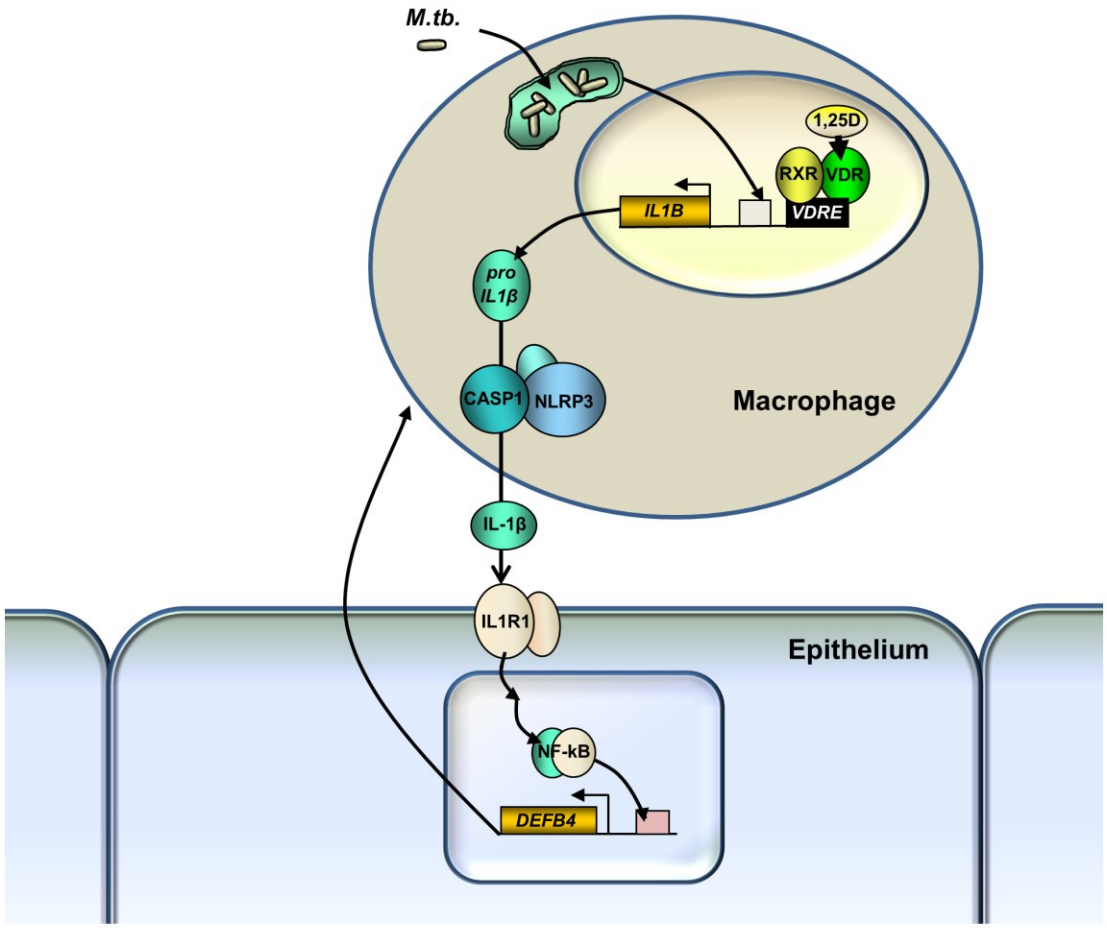
M.tb.
1,25D
RXR
VDR
VDRE
IL1B
pro
IL1β
CASP1
NLRP3
Macrophage
IL-1β
IL1R1
Epithelium
NF-kB
DEFB4

Figure S10 - IL-1β and 1,25D signaling induce the secretion of antimicrobial activity from lung epithelial cells.

(**A**) Expression of *DEFB4* and *CAMP* in Calu3 cells treated with 10ng/ml of recombinant IL-1β (I), 1,25D (D), or both (ID), relative to control (C) for 24 hour. (**B**) CFU quantification of *M.tb.* viability after 24-hour incubation in media supernatant filter-sterilized from (**A**). Data are from three experiments (mean and s.e.m.). (**C** and **D**) Expression of *DEFB4* and *CAMP* genes in CaLu3 lung epithelial cells incubated with conditioned media from uninfected (N) or H37Rv-infected (V) THP-1 cells treated with vehicle (-) or 100nM 1,25D (+) for 24h. Media was treated with vehicle control, neutralizing antibody against IL-1β, or normal serum IgG, as indicated, prior to incubation with CaLu3 cells. Values are expressed as a fold of the N- control. mRNA expression data (**A,C,D**) are from one experiment and representative of at least three (error bars, s.d.). *P<0.05, **P<0.01, ***P<0.001 as determined by Student's t-test relative to uninfected, untreated control unless otherwise indicated.

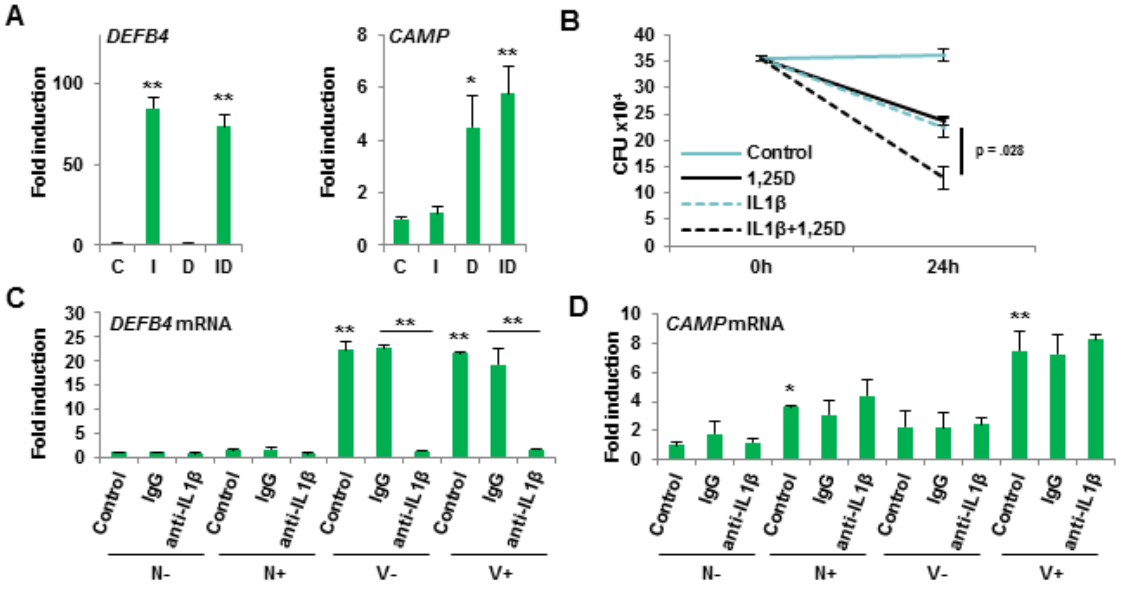

Figure S11 - IL-1β and 1,25D signaling reduce *Mtb* viability in coculture of macrophages and lung epithelial cells.

(**A**) Expression of *DEFB4* and *CAMP* in CaLu3 cells cocultured with H37Rv-infected THP-1 cells with vehicle (-) or 100nM 1,25D (+) after 5 days. mRNA expression data are from one experiment and representative of at least three (error bars, s.d.). *P<0.05, as determined by Student's t-test relative to uninfected, untreated control unless otherwise indicated. (**B**) CFU of THP-1 cells infected with H37Rv (V) and treated with vehicle (-) or 100nM 1,25D (+), with and without the presence of CaLu3 cells in transwell coculture (CaLu3). Data are from three experiments (mean and s.e.m.). Indicated p-value was calculated using one-way ANOVA.

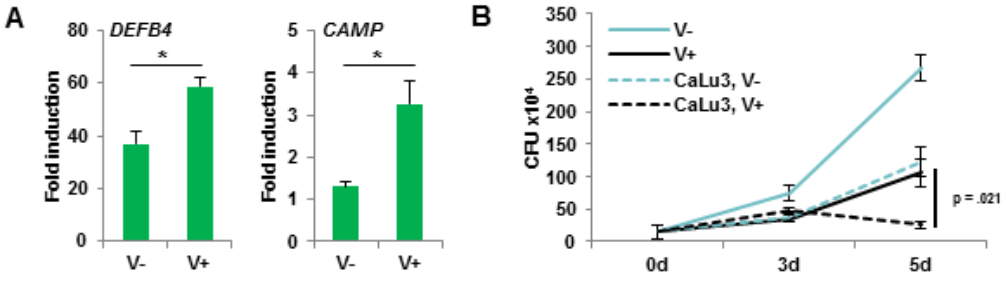

CHAPTER 4: Metformin controls *Mtb* infection in macrophages

4.0 Preface to Chapter 4

In the previous two chapters we investigated the effects of manipulating the host cell environment in *Mtb* infection by modulating the expression of inflammatory cytokines with 1,25D. This intervention demonstrated a protective effect both in macrophage cultures and our novel co-culture system between macrophages and epithelial cells. While these results may explain the clinical observations which show an inverse correlation between seasonal sunshine hours and incidence of TB, clinical trials which investigated the activity of vitamin D in the treatment of TB showed no benefit for patients. For this reason, we looked towards another strategy of changing the host macrophage environment so as to make it unfavorable for the bacteria.

Mtb is an obligate intracellular pathogen, and while it has its own metabolic capacity, it still requires host carbon sources to replicate and maintain virulence. From this, we hypothesized that in the same way that we were able to change the host environment and immune response by manipulating the host transcriptome with 1,25D, we would also be able to manipulate the host metabolic profile to expose the metabolic vulnerabilities of the bacteria. Many drugs have been developed and approved for use in humans for metabolic diseases such as diabetes, as we began this work by screening a panel of drugs which are commonly used to modulate a variety of metabolic pathways. From this screen we identified metformin as being able to limit bacterial replication *in vitro*, and proceeded to determine the mechanisms by which metformin was able to limit bacterial growth in macrophages and investigate its application in an *in vivo* model.

4.1 Abstract

Mycobacterium tuberculosis (*Mtb*) latently infects ~2 billion people and active tuberculosis (TB) represents the leading cause of death from a curable disease. Cases of drug resistant tuberculosis have increased in recent years, driving the demand for new therapies. While conventional antibiotics target critical bacterial processes, our goal was to characterize the host metabolic response to infection and to establish if drugs used for the modulation of human metabolism could impact *Mtb* infection for the benefit of the host. From a drug screen we identified metformin as being able to prolong survival of infected macrophages and control mycobacterial replication. From this, we have used the *in vitro* model of human macrophage infection with the virulent *Mtb* strain H37Rv to measure the effects of metformin on cytokine secretion, quantification of cell death and activation of cell death pathways, and bacterial proliferation. Additionally, we have performed GC-MS analysis to characterize the host metabolic response to infection. We have also performed *in vivo* experiments testing the effects of oral metformin administration in the low-dose aerosol model of murine tuberculosis on control of bacterial burden as compared to standard tuberculosis antibiotic therapy. We demonstrate that metformin treatment induces a variety of metabolic changes within the macrophages, such as an increase of glycolysis and depletion of TCA cycle intermediates. When macrophages are faced with mycobacterium, metformin treatment preferentially decreases palmitic acid and cholesterol availability in infected macrophages compared to uninfected controls. Treatment of infected human and mouse macrophages with metformin *in vitro* resulted in a skewing of cell death fate from necrosis to apoptosis, leading to a control of bacterial proliferation. In the *in vivo* model of infection, oral dose metformin did not have a significant effect on the course of infection. These results represent the first characterization of the host

macrophage metabolomic response to *Mtb*, as well as the successful manipulation *in vitro* of that response for the benefit of the host in the face of infection.

4.2 Introduction

Mycobacterium tuberculosis (*Mtb*) infects ~2 billion people[1] and active tuberculosis (TB) is the second leading cause of death from an infectious disease, being responsible for 1.4 million deaths in 2011[1]. This, in addition to the recent increase in clinical incidence of multi-drug resistant (MDR) and extremely drug resistant (XDR) strains[7], has spurred the search for a new vaccines and antibiotic therapies. While all existing anti-TB antibiotics function by directly interfering with a bacterial process critical for its survival, host-directed therapies (HDTs) have begun to emerge as possible adjunct therapies to the standard chemotherapy administered for the treatment of tuberculosis[238]. The principle behind HDTs is to exploit a pathway or cellular process, thus changing the host environment in a manner that disrupts the normal pathogenesis of the infection in a manner that aids in its clearance or resolution.

The metabolic pathways of *Mtb* have been extensively characterized in the search for new antibiotic therapies. From this we have learned that while the bacteria is able to synthesize some of its own amino acids and cellular structures, it still requires access to certain molecules from the host cell to remain viable. Studies investigating which molecules are essential for *Mtb* replication have focused on those which it is capable of using to replicate in culture[170,171], as well as on which are preferentially used while in the host macrophage[172]. From this we have an understanding of the metabolic demands of *Mtb*, and the implications of interfering with these pathways. For example, deletion of the mycobacterial cholesterol transporter encoded by mce4 severely limits the capacity of *Mtb* to form a stable infection[174], and under conditions where fatty acids (FAs), a principle carbon source for *Mtb*[172], are not available, byproducts of cholesterol metabolism can accumulate and become toxic to the bacteria[175].

Upon activation, the functional capacity of many immune cells changes dramatically, and these changes require a large shift in the production of metabolites to meet their new biosynthetic needs. Recent reports have demonstrated that certain immune cell subtypes display altered patterns of cellular metabolism when stimulated or undergoing expansion, and that ability to make these metabolic changes is critical for proper immune function[163]. In particular, pro-inflammatory M1 macrophages and macrophages stimulated with LPS have been shown to increase rates of glycolysis while decreasing the more efficient oxidative phosphorylation (OXPHOS)[164], similar to the Warburg effect seen in many forms of cancer. Furthermore, preventing macrophages from reprogramming their metabolism towards glycolysis by overexpressing CARKL has been shown to decrease in the capacity of the cell to produce inflammatory cytokines[165]. While cellular metabolism and immune responses to *Mtb* infection have been studied independently, no analysis of the host metabolic state of macrophages infected with *Mtb* has yet been undertaken.

In this study we begin by investigating the changes in cellular metabolism that occur in response to infection with *Mtb*. Finding that infection induces Warburg metabolic state in macrophages, we proceeded to test a panel of drugs routinely used to manipulate central metabolic pathways, and found that metformin, a drug commonly used for the management of diabetes and an inhibitor of complex I of the mitochondrial oxygen transport chain (OTC), limited bacterial replication. In performing the first large scale GC-MS analysis of the host metabolic response to *Mtb* infection we demonstrate that infection decreases TCA intermediates. Additionally, we identify two factors that could be contributing to this control of the bacteria by metformin, firstly that it increases the production of mitochondrial ROS (mROS), and secondly

that cholesterol and palmitate, molecules that have been shown to serve as important carbon sources for *Mtb*, were selectively limited in infected macrophages treated with the drug.

4.3 Results

Characterization of the metabolic response to *Mtb* infection in macrophages

Recently, a link has been demonstrated between the changes in cellular metabolism of macrophages and their functional immune responses[165,171]. To determine if *Mtb* infection was having an effect on the relative rates of glycolysis and OXPHOS in macrophages, we measured the oxygen consumption rate (OCR) and the extra-cellular acidification rate (ECAR) (**Figure 4.1A**). We found that increasing the magnitude of infection (MOI) produced a decrease in OCR (**Figure 4.1B**), with a corresponding increase in ECAR (**Figure 4.1C**), indicating that infection was shifting metabolic flux away from OXHPOS and towards glycolysis. This finding is consistent with previous reports which measured an increase in glycolysis in inflammatory, "classically activated", M1 macrophages[164] and in macrophages stimulated with LPS[165]. Furthermore, coupled ATP production decreased as the MOI increased (**Figure 4.1D**). We next measured total cellular ATP, and found that it also decreased in an MOI-dependent manner (**Figure 4.1E**).

To investigate the effect that this shift in energy production was having on the total pool of TCA intermediates, we used GC-MS to measure TCA intermediates in macrophages infected with H37Rv. This revealed a general decrease in TCA intermediates, with a significant decrease in citrate, cis-aconitate, α-ketoglutarate, and malate in *Mtb*-infected macrophages 24 hours after infection (**Figure 4.1F**). A comparison of TCA intermediates between cells infected with H37Ra or H37Rv showed no substantial differences at 24 hours after infection at the same MOI (**Figure S12**), suggesting that this metabolic response was not specific to infection with the virulent mycobacteria, but that it likely occurs as part of a generalized response to mycobacterial infection. Inhibition of TCA flow has been shown to result in ROS production from complex I

and III[239]. Additionally, the production of mROS has been linked to control of intracellular pathogens other than *Mtb* as mitochondria have been shown to co-localize with phagosomes[240], and in *Mtb*-infected macrophages it has been shown to be an important step in the signaling cascade that leads to the secretion of inflammatory cytokines[55]. For these reasons we next measured the levels of mitochondrial ROS (mROS), and found that they were elevated in response to infection (**Figure 4.1G**).

Metformin limits bacterial replication

As *Mtb* is an intracellular pathogen, it utilizes resources taken from its host cell to fuel its energetic and biosynthetic demands. A number of previous reports have focused on identifying the specific carbon sources which *Mtb* preferentially utilizes[170-172]. We thus hypothesized that manipulation of host metabolic pathways would be a useful method for understanding the changes that *Mtb* infection was having on the host cell, and serve as an opportunity to learn if modulation of these pathways presented any viable targets for control of the infection. To this end we tested a panel of drugs capable of inhibition or activation of the central regulators of cellular metabolism (**Figure S13**). This identified metformin, a complex I inhibitor, as being capable of controlling bacterial load down to a concentration of 10μM (10^{-5}M) as measured by colony forming unit (CFU) assay 3 days post-infection (**Figure 4.2A,B**), with the peak efficacy of treatment occurring at 1mM (10^{-3}M). (**Figure 4.2A**). In control experiments we added metformin to mid-log phase H37Rv culture grown in 7H9 media at a final concentration of 10^{-3}M and measured growth by OD_{600} after 24 and 48 hours. Metformin did not alter mycobacterial proliferation (data not shown), which revealed that it had no direct effect on mycobacterial viability.

Metformin shifts cell death fate towards apoptosis

Given the observation that bacterial load was controlled by metformin despite no direct effect on limiting the growth of bacteria in culture, we looked towards the changes that it was directing in the host cells. Firstly, there was a prominent visual difference in the number of adherent cells remaining after 24 hours (**Figure 4.3A**), with about 50% cells remaining adherent in the H37Rv-infected condition, while approximately 80% of the cells remained when treated with metformin (**Figure 4.3B**).

Changes in cell death program have been linked to the control of bacterial burden in macrophages[69], as macrophages which are able to die by apoptosis will also degrade phagocytosed bacteria along with their organelles, while uncontrolled cell death by necrosis allows for the escape of viable bacteria which can go on to infect other phagocytes. We analyzed the total changes in the rate of apoptosis and necrosis to understand if this was potentially contributing to the observed control of bacterial replication. In metformin-treated macrophages infected with H37Rv, 72 hours after infection we found that the rate of apoptosis was 4 times that of the control condition (**Figure 4.3C**). Importantly, metformin did not induce apoptosis in the uninfected control (**Figure 4.3C**). In addition, secretion of LDH into the media supernatant, a marker of plasma membrane disruption, and by extension necrosis and necroptosis, had decreased by approximately 20% after 72 hours (**Figure 4.3D**), even while there were relatively more cells viable in the metformin treated condition at this time point.

While this shift from necrosis to apoptosis could be contributing to the control of the mycobacteria, it was not clear if the cells were able to die by apoptosis because of a direct impact of metformin on cell death pathways, or because mycobacterial proliferation or virulence was

being limited by another mechanism. To address this, we tested a large panel proteins involved in cell death pathways, including members Bcl-2, Bcl-X, cleaved caspase-3, and cytochrome C of the intrinsic cell death pathway, and FADD, Fas, and the TRAIL receptors 1 and 2 of the extrinsic cell death pathway, and found that no particular target was being modulated (**Figure S14**). Furthermore, an analysis of the autophagy marker LC3-II, showed no differences between infected cells with and without metformin (**Figure S15**). These findings suggested that metformin was not acting by directly affecting the cell death program or autophagy, two processes which have been shown to be important for control of mycobacterial replication. Therefore we continued our analysis by investigating the changes in the production of secreted cytokines and chemokines.

We measured a broad range of cytokines in the media supernatant take from *Mtb*-infected macrophages treated with metformin at 24 hours to determine if metformin treatment altered the secretion of cytokines from macrophages, including IL-1β and TNF-α which have been directly implicated in control of *Mtb*. From this we observed that while TNF-α and IL-1β were elevated by metformin treatment in *Mtb*-infected mouse macrophages, there was no change in cytokine secretion in either uninfected or infected human macrophages (**Table S4, Figure S16**). Importantly, treatment with metformin did not induce an inflammatory response from uninfected cells (**Table S4, Figure S16**).

Metformin increases mROS in *Mtb*-infected macrophages

The level of ROS in *Mtb*-infected cells has been linked to the production of TNF-α [55,241], an inflammatory cytokine which is critical for the control of *Mtb* infection[43]. Furthermore, previous reports have demonstrated that an inhibition of TCA flow in macrophages, either

pharmacologically[164] or by activation with TLR ligands[165], generates mitochondrial ROS (mROS), which in combination with NADPH-derived ROS can have bactericidal activity[167]. To understand the impact of metformin on both ROS and mROS production in *Mtb*-infected cells, we incubated cells at 1, 2, and 24h with DCFDA, which labels several ROS species throughout the cell, or MitoSOX, which labels superoxide production at the mitochondria. Metformin treatment of infected cells had no impact on ROS or mROS production in the first few hours during the oxidative-burst phase of infection, although it did significantly increase ROS and mROS at 24 hours (**Figures 4.4A, 4.4B**).

Metformin reduces TCA intermediates in *Mtb*-infected macrophages

Given the observation that metformin treatment had increased levels of mROS, this would suggest that metformin was having an impact on oxygen consumption. We examined the effects of metformin on OXPHOS and glycolysis and observed that metformin decreased OCR (**Figure 4.5A**) and increased ECAR (**Figure 4.5B**) in both uninfected and infected cells. Treatment with metformin also reduced the proportion of coupled ATP production (**Figure 4.5C**), although surprisingly we did not observe any decrease in total ATP production in conditions treated with metformin relative to their respective controls (**Figure 4.5D**). This shift towards glycolysis is consistent with previous reports of metformin action in other cell lines and contexts[242]. To understand the impact that this further shift towards glycolytic energy production was having on carbon flow through the TCA, we incubated macrophages with uniformly labeled ^{13}C glucose or ^{13}C glutamine for 24 hours. The total abundance of TCA intermediates, specifically citrate, cis-aconitate, α-ketoglutarate, succinate, and fumarate, were further decreased in metformin treated conditions (**Figure 4.5E**). Despite changes in the total pool of a

number of the metabolic intermediates measured, an analysis of the proportion of either glucose- or glutamine-derived ^{13}C showed no notable changes in the relative proportion of label or the abundance of any specific isotopomer among the TCA intermediates and amino acids measured (**Figure S17**). In addition, a full analysis of amino acids at this time point showed no distinctive trends (**Figure S18**).

We also found that in infected cells treated with metformin, the amount of citrate was severely reduced, although the rate of ^{13}C incorporation into citrate from ^{13}C labeled glucose or ^{13}C labeled glutamine was largely unchanged (**Figure 4.5F**). Citrate can be processed via acetyl-CoA carboxylase (ACC) for the biosynthesis of cholesterol and fatty acids, molecules which are important carbon sources and are required for the virulence of the *Mtb*[174]. We next examined this pathway to understand if it was being modulated by metformin.

Metformin reduces cholesterol and palmitate levels

While *Mtb* has the capacity to utilize a number of carbon sources in vitro[170,171], it has been demonstrated that the major carbon during infection is a 2-carbon (2C) source derived from the breakdown of fatty acids (2C)[172]. Fatty acids and cholesterol are imported into bacteria where they are used to generate TCA intermediates, and build cell wall components[175,243]. The capacity of the bacteria to import cholesterol has also been shown to be critical for virulence, and as a possible carbon source[174].

Citrate can be exported from the mitochondria for to be used for the synthesis of fatty acids. To understand if the decrease in citrate seen in infected cells treated with metformin was impacting the production of fatty acids, we incubated infected macrophages with uniformly labeled ^{13}C glucose for 24 hours and measured the incorporation of ^{13}C into cholesterol and

palmitate. This revealed that less than 5% of the total palmitate and cholesterol pool carried any incorporation of the ^{13}C label (**Figure 4.6A,B**), despite it being present in high quantities in citrate when incubating cells with labeled glucose (**Figure 4.5F**). This would suggest that very little of the palmitate and cholesterol pool was being synthesized during this 24-hour period.

Metformin functions as an activator of AMPK[244]. When phosphorylated, AMPK phosphorylates ACC1, an enzyme that generates 2C subunits which are used for building long chain fatty acids and cholesterol[245], thus inactivating it and limiting the ability of the cell to synthesize fatty acids. For this reason, we looked to see if metformin was inducing AMPK phosphorylation in infected macrophages. Consistent with the known function of metformin, we found that phospho-AMPK signal increased in response to metformin or infection. However, the combination of the two did not result in a further increase 24 hours after infection (**Figure 4.6C**). Similarly, phospho-ACC increased during metformin treatment in uninfected cells, but did not increase when metformin was added to infected cells. This would suggest that any decrease of carbon flow from citrate into fatty acids would likely be due to a decrease in the total pool of citrate, and not because of the phosphorylation of AMPK and ACC.

To understand if metformin treatment was impacting the levels of fatty acids, we performed GC-MS of the total cellular pool of fatty acids in *Mtb*-infected macrophages. We identified the 20 most abundant fatty acids and found that their relative abundances were largely unchanged by infection or metformin treatment (**Table S5**). Two notable exceptions were cholesterol, which was reduced by metformin in infected cells by about 50% in only 3 hours after infection, and palmitate, the most abundant fatty acid, which was reduced in metformin treated conditions by about 20% relative to the control after 24 hours (**Figure 4.6D,E**).

As both palmitate and cholesterol can be imported by CD36 at the cell surface, we measured the surface expression of CD36 at 3 and 24 hours after infection and treatment by FACS but we observed no significant changes, indicating that differences in uptake are likely not the result of a differential expression of this surface transporter (**Figure S19**). Other mechanisms of uptake for cholesterol and palmitate have been identified. To understand if the global rate of uptake had changed in response to infection or metformin, we measured the rate of incorporation of NBD-labeled cholesterol at 1 and 3 hours (**Figure 4.6F**), and the rate of BODIPY-labeled palmitate uptake 24 hours after infection (**Figure 4.6G**). This revealed that the rate of cholesterol import had decreased in infected cells treated with metformin starting as soon as 1 hour after treatment and continued out to 3 hours. Additionally, the rate of palmitate at 24 hours had been reduced by about 20% in the infected, metformin treated condition relative to the uninfected, untreated control. This would suggest that the decrease observed in total abundance of these two molecules was due to an indirect effect on limiting uptake, or potentially the result of a compensatory consequence of increasing β-oxidation in order to maintain ATP levels under conditions where OXPHOS was severely limited (**Figure 4.7**).

Oral administration of metformin does not impact the progression of *Mtb* infection in mice

To understand if the benefits of bacterial control seen *in vitro* extended into an *in vivo* model of infection, we infected C57BL/6 mice with 20-30 CFU of H37Rv. After 14 days of infection, we added metformin to the drinking water, at a dose designed to deliver 6mg to each mouse per day. Water bottles were changed 3 times per week with fresh water and preparations of metformin. At 2 and 4 months after infection, total bacterial burden in the lung and spleen was measured (**Figure 4.8A**). We found no statistically significant difference in number of bacteria in

either organ. To understand if metformin was having an impact on the immune responses generated in response to infection, we performed FACS on cells prepared from the lungs of infected mice 21 days after infection (**Figure 4.8B**). No statistically significant difference was found in the number of cells participating in the innate immune responses (macrophages, neutrophils, dendritic cells), in the adaptive immune responses (total B-cells, $CD8^+$ T-cells, $CD4^+$ T-cells), or in the generation of antigen specific $CD8^+$ T-cell responses towards two epitopes common to *Mtb* (32C and TB10.4).

4.4 Discussion

In this study we have undertaken the first large scale analysis of the host macrophage response to *Mtb* infection, measuring the impact of it on host TCA intermediates, amino acids, and fatty acid levels. In an effort to understand if host metabolic pathways could be manipulated to limit the availability of *Mtb*'s essential and preferred carbon sources, we identified metformin, a drug which inhibits complex I of the ETC, as being capable of limiting bacterial proliferation by both increasing mROS and decreasing the availability of cholesterol and palmitate.

ROS has not been directly shown to induce bactericidal killing in *Mtb*-infected macrophages, although limited clinical evidence suggests that it may have a role[246]. Despite this, the role of ROS in cytokine signaling has been established[55,241]. A recent study in the zebrafish model of tuberculosis has demonstrated that TNF-α is able to induce ROS in vivo, and while the short term protective effects associated with elevated TNF-α can lead to control of the bacteria, at longer time points, an excess of TNF-α drives a secondary wave of necroptosis in infected macrophages[55]. The authors were also able to exploit the microbicidial effects associated with elevated TNF-α and mROS without the detrimental secondary necroptosis by pharmacologically inhibiting cell death. In our system we were able to directly influence the production of mROS by inhibiting complex I, but found no increase in the level of TNF-α. In the time period analyzed we found only a large increase in apoptosis and a decrease in LDH, a marker of necrosis and necroptosis, indicating that apoptosis was being heavily favored as a cell death pathway under these conditions. This could potentially lead to a safer mechanism of intervention, as we found that metformin was able to limit bacterial replication under conditions where both mROS and apoptosis were elevated, without the potentially negative effects resulting from elevated TNF-α.

A recent report identified the principle carbon source flowing into central metabolism of *Mtb* as a 2C source[172], which, in combination with previous reports[173,174], would suggest that it is likely from the the β-oxidation of fatty acids. Here we have demonstrated that treatment of infected macrophages with metformin selectively decreased levels of palmitate, a 16C saturated fatty acid, and the most abundance fatty acid present in the cells. *Mtb* can import palmitate which it uses for the synthesis of cell wall lipids[243,247], the neutralization of toxic metabolic intermediates from cholesterol metabolism[175], and to fuel its central metabolism by catabolism of palmitate into 2C subunits. Reducing the availability of palmitate in the host could be contributing to the control of bacterial replication seen in metformin-treated conditions for these reasons. Additionally, multiple reports have established that *Mtb* can accumulate and utilize cholesterol[183,184]. Infection with virulent *Mtb* is able to induce the formation of lipid-laden macrophages named 'foamy macrophages'. This dysregulation of cellular cholesterol and fatty acids is a critical component of *Mtb* virulence. The incidence of these cells in a granuloma is associated with more severe outcomes[39], and elevated cholesterol levels in patients has also been associated with a less favorable prognosis[186]. The decrease that we observed in *Mtb*-infected macrophages treated with metformin could led to control of infection by limiting it as a carbon source, and as a factor for virulence.

One limitation of this study is the use of the THP-1 cell line and not primary cultures of alveolar macrophages. However, THP-1 cells terminally differentiated with PMA have been routinely used in *Mtb* host-pathogen studies as they approximate the behavior of alveolar macrophages[248], while allowing for ease of scaling and portability of results, significant issues which occur with the use of primary cells due to the limited volume of blood draws and the high degree of variability seen donor to donor.

Host directed therapies are designed to modulate the host response to infection in combination with the normal treatment regimen. While administration of the currently available antibiotic therapies would be successful in the majority of TB cases for the elimination infection, HDTs are being developed in an effort to overcome the challenges associated with the length of treatment required (6-9 months), or the growing incidence of drug resistance. As metformin is already commonly prescribed for the management of type 2 diabetes, it might be possible that administration of metformin may be a safe adjunct therapy for the treatment of TB. Much remains to be done however, as the *in vitro* evidence we present would still need to validated in an *in vivo* setting. Statins, another drug commonly prescribed for diabetics for its ability to manage cholesterol levels, was recently analyzed in an *in vitro* model of tuberculosis and found to limit bacterial replication in macrophages by decreasing cholesterol levels by ~75%[249]. Unfortunately, a recently published retrospective cohort study of diabetics in India showed that the incidence of active tuberculosis was not associated with the prescription status of statins[250]. The undertaking of a similar study methodology with metformin would be a useful step in understanding its ability, if any, to aid in the host response to tuberculosis.

4.5 Materials and Methods

Ethics Statement

C57BL/6 mice were utilized as outlined in an animal use protocol approved by McGill University (Permit #2010-5860) according to Canadian Council on Animal Care guidelines.

Antibodies and Reagents

α-ACC (Cell Signalling), α-phospho-ACC (Cell Signalling), α-actin (Cell Signalling), α-AMPK (Cell Signalling), α-phospho-AMPK (Cell Signalling), α-LC3 (Novus Biologicals), metformin (Sigma). Unless otherwise specified, all experiments with metformin were performed at a final concentration of 1mM (10^{-3}M).

Cell Culture

THP-1 cells (TIB-202, ATCC) were cultured in RPMI-1640 (Wisent) with 10% FBS (Wisent). H37Rv and H37Ra were cultured to mid-log phase in a rolling incubator at 37°C in Middlebrook 7H9 (Difco) with .05% Tween-80 and 10% ADC enrichment (BD Biosciences).

Macrophage Infections

THP-1 cells were terminally differentiated by 2×10^{-8}M PMA for 24 hours in RPMI with 10% FBS, inducing cell cycle arrest. H37Rv or H37Ra cultures were centrifuged and pellets were resuspended in RPMI-1640 with 10% FBS and .05% Tween-80 and clumping was disrupted by repeated passage through a 27-gauge needle. Media was removed from THP-1 cells and replaced with media containing *Mtb* in the indicated multiplicity of infection (MOI) for 3 hours. THP-1 cells were then vigorously washed three times with RPMI to remove extracellular bacteria,

followed by incubation in RPMI with 10% FBS with or without metformin at a final concentration of 1mM, if not otherwise indicated.

CFU Assays

At the indicated time point, cells were scraped into the media supernatant and transferred to 50ml conical tubes for centrifugation at 4000rpm for 10 minutes. Media was carefully aspirated and macrophages were lysed with water for 5 min, after which an equal volume of 2x 7H9 with .1% Tween-80 was added. Samples were vigorously resuspended by and plated in serial dilution on Middlebrook 7H10 (Difco) with 10% OADC enrichment (BD Biosciences).

Extraction of Genomic DNA and qPCR of IS6110

Quantification of IS6110 by qPCR was performed essentially as described in [251]. In brief, 3 days after infection, the tissue culture plates were centrifuged for at 4000rpm for 10 minutes. The media supernatant was carefully removed, and 1ml of water was added to each well. The wells were scraped into the water volume, and the total volume was added to 1.5ml tubes containing 50ul of acid-washed glass beads. The tubes were then frozen at -80^{o}C overnight. The following day, the tubes were brought to room temperature and run on a Hybaid Ribolyzer for 45 seconds at 6.5m/s, followed by boiling at 95^{o}C for 20 minutes. Without any further processing or purification, these samples were then used directly for qPCR, using IS6110 primers sequences: GGAAGCTCCTATGACAATGCACTA and TCTTGTATAGGCCGTTGATCGTCT, as designed by [252].

Western Blots, Cell surface staining, Proteome Profiler

Protein extracts from THP-1 cells were prepared in lysis buffer (10 mMTris·HCl, 1 mM MgCl2, 1 mM EGTA, 0.5 mM CHAPS, 10% glycerol, 5 mM NaF) supplemented with the following protease additives: protease and phosphatase tablets (Roche), DTT (1μg/mL), and benzamidine (1μg/mL) and processed for Western blotting and separated on Tris-HEPES-SDS gradient protein gels (Pierce) using standard transfer and blotting protocols. Human cell death pathway proteome profiler array (R&D Systems, ARY009) was used as recommended by the manufacturer. In brief, cell lysates were prepared in an identical manner as described for western blots, and incubated with the membranes before developing with ECL and imaging. Mouse cytokine proteome profiler array (R&D Systems, ARY009) was used as recommended by the manufacturer. In brief, each panel was incubated with 2ml of media supernatant taken from BMDMs infected at an MOI of 5 and treated with 1mM of metformin for 24 hours.

Cell Death Assay, LDH

Cell-free media supernatant was collected from infected macrophages. Cytotoxicity Detection Kit (LDH) from Roche was used in accordance with the manufacturer's instructions. Apoptosis measurements were performed using the Cell Death Detection ELISA PLUS (Roche), as recommended by the manufacturer.

Microscopy

At the indicated time point, cell cultures were washed and media was replaced with an equal volume of trypan blue. Images were taken using an AMG Evos Core XL microscope. Cell counts were calculated according to three images taken of biological replicates of each condition by an individual blinded to the treatment conditions.

GC-MS Analysis of ^{13}C Metabolites and Fatty Acids.

For GC-MS analysis, protocols have been outlined previously[253]. Briefly, cells ($1.5x10^7$ per 10-cm dish) were collected in ice-cold 80% methanol. For isotopomer-labeling experiments, cells were treated with uniformly labeled ^{13}C glucose or ^{13}C glutamine (Cambridge Isotopes). For fatty acid profiles, triglycerides and other lipids were extracted using a modified Folch method[254] substituting methylene chloride for chloroform. Following extraction, the organic layer was isolated, dried in a warm N2 stream, and saponified in sodium hydroxide overnight at 60 °C. The fatty acids were re-extracted and dried, derivatized as tert-butyldimethylsilyl (TBDMS) esters, and analyzed on GC-MS. Metabolites from tissue culture cells were extracted from the aqueous phase of the modified Folch method, and prepared as described previously [253].

Seahorse XF96 Respirometry.

Respirometry oxygen consumption rate (OCR) and the extracellular acidification rate (ECAR) of cells were measured using an XF96 Extracellular Flux Analyzer (Seahorse Bioscience) as previously described[254]. In brief, cells were plated at 1×10^5 per well in 100μL of non-buffered DMEM containing 25mM glucose and 2mM glutamine. Cells were incubated in a CO_2-free incubator at 37 °C for 1 h to allow for temperature and pH equilibration before loading into the XF96 apparatus. XF assays consisted of sequential mix (2 minutes), and measurement (5 minutes) cycles, allowing for determination of OCR/ECAR every 7 min.

Quantification of ROS

Measurement of reactive oxygen species (ROS) was performed by incubating cells for 30 minutes prior to the indicated time point with 2′,7′–dichloro-fluorescein diacetate (DCF-DA) or

MitoSOX (Life Technologies). Cells were then lifted from the culture plate using Accutase (Millipore), followed by quantification using flow cytometry. All experiments for the measurement of ROS and mROS were performed in RPMI-1640 with 10% FBS but lacking phenol red (Wisent).

Cholesterol and Palmitate Uptake

For the measurement of cholesterol and palmitate uptake, 15 minutes prior to the indicated time point, NBD-cholesterol (Molecular Probes) or BODIPY-palmitate (Life Sciences) was added to the cells at a final concentration of 1μg/ml. After incubation, cells were lifted from the culture plate using Accutase (Millipore), followed by quantification using flow cytometry.

Flow Cytometry

Flow cytometry of THP-1s was conducted using a Gallios (Beckman Coulter) flow cytometer and analyzed with FlowJo software (Tree Star).

Cytokine Profiling

Cytokines were measured from the media supernatant 24 hours after infection as described previously[255].

Measurements of total ATP

Total ATP levels were measured using CellTiter-GLO Luminescent Assay (Promega) in accordance with the manufacturer's instructions. The reported luminescence was normalized first to cell count, and then expressed as relative to the uninfected, untreated control.

Pulmonary infection and metformin treatment

C57BL/6 mice were infected by aerosol with 20-30 bacteria of *M. tuberculosis* strain H37Rv. Quantification of the initial infectious was performed the following day. Bacterial burden was measured at different time points by serial dilution and plating on 7H11 plates supplemented with OADC and PANTA. After 14 days of infection, drinking water was supplemented with metformin at a concentration which would ensure a daily dose of 6mg per mouse. Water bottles were changed three times per week, with fresh preparations of metformin each time.

Assessment of innate and adaptive immune responses by FACS

At 21 days after infection, mouse lungs were digested in collagenase and cells were harvested and enumerated. Approximately 1×10^6 cells were seeded in 96-well U-bottom plates. Cells were blocked with FcBlock in 0.5% BSA/PBS for 15 min at 4^{oC}, then stained with the indicated antibodies against cell surface markers. Afterwards the cells were washed and fixed in 1% paraformaldehyde, and were run on a FACSCalibur (BD Pharmingen). The data was analyzed using FlowJo software (Tree Star).

Statistics

Student's t-test or one-way ANOVA with Tukey's post-test correction was performed where indicated using GraphPad software.

4.6 Figures

Figure 4.1 - Infection induces a glycolytic shift

A. Plot of ECAR against OCR for macrophages infected with H37Ra at an MOI of 5 for 24 hours, as measured on the Seahorse XF96. **B.** OCR measured in macrophages infected at the indicated MOI of H37Ra for 24 hours, as measured on the Seahorse XF96. **C.** ECAR measured in macrophages infected at the indicated MOI of H37Ra for 24 hours, as measured on the Seahorse XF96. **D.** Percent of oxygen consumption attributed to ATP production or proton leak in macrophages infected with H37Ra at the indicated MOI, as measured by Seahorse XF96. Seahorse XF96 data (A-D) are from one experiment and representative of three independent replicates (mean, s.d., n=4). **E.** ATP production in macrophages infected with H37Ra at an MOI of 5 for 24 hours, as measured using CellTiter Glo, and normalized to the number of cells in each condition. Data is from one experiment and representative of three independent experiments (mean, s.d., n=3). **F.** The relative fold expression of TCA intermediates in cells infected with H37Rv at an MOI of 5 for 24 hours. Data is the average of two independent biological experiments each measured in biological triplicate (mean, s.e.m. n=2) and levels of each metabolite have been normalized to the levels of that metabolite in the uninfected control. (**G**) Total ROS as measured by DCFDA labelling in macrophages infected with H37Ra at an MOI of 5 for 24 hours. Data is from one experiment and representative of three independent experiments (mean, s.d., n=3). *P<.05, **P<.01, ***P<.001, as determined by one-way ANOVA with Tukey post-test correction (B,C,D,E) or Student's t-test (F,G) relative to the uninfected control.

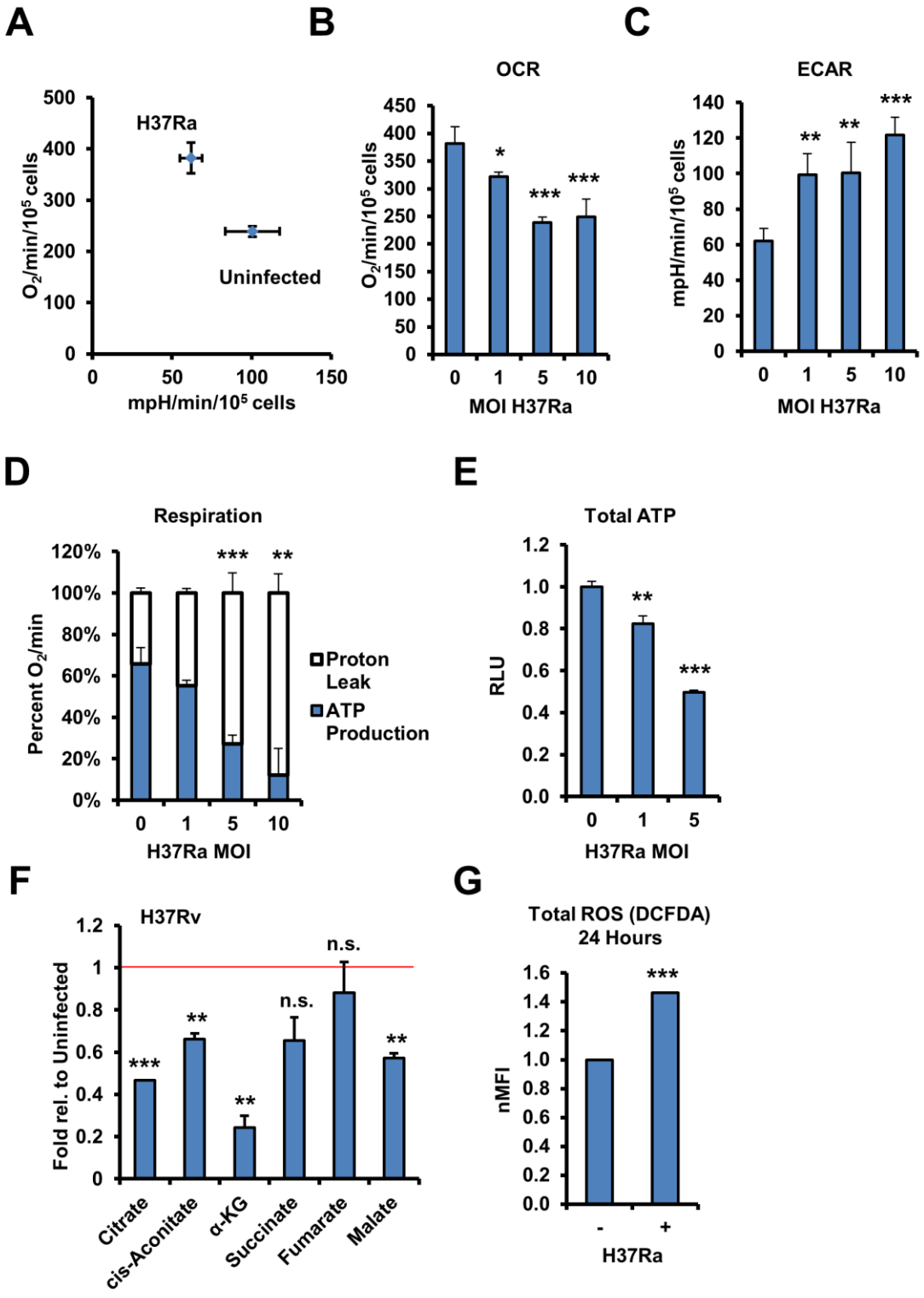
A
B
C
H37Ra
Uninfected
O2/min/10^5 cells
mpH/min/10^5 cells
OCR
ECAR
MOI H37Ra
mpH/min/10^5 cells
D
E
Respiration
Percent O2/min
Proton Leak
ATP Production
H37Ra MOI
Total ATP
RLU
H37Ra MOI
F
G
H37Rv
Fold rel. to Uninfected
Citrate
cis-Aconitate
α-KG
Succinate
Fumarate
Malate
n.s.
Total ROS (DCFDA) 24 Hours
nMFI
H37Ra

Figure 4.2 - Metformin controls *Mtb* replication in macrophages

A. Quantification of *Mtb* genomic DNA sequence IS6110 by qPCR from macrophages infected with H37Rv for 72 hours and treated with the indicated molar concentration of metformin. Values are expressed relative to a standard curve generated from a known quantity of *Mtb*, as measured by CFU. Data is the mean of two independent experiments, each performed in triplicate (mean, s.d., n=2) **B.** Quantification of *Mtb* by colony forming unit (CFU) assay, harvested from macrophages at the indicated time point after treatment with 1mM metformin. Data are from one experiment and representative of two independent experiments, each performed in technical quadruplicates of biological quadruplicates (mean, s.d. n=4). **P<.01, ***P<.001, as determined by one-way ANOVA with Tukey post-test correction (A) or one-way repeated measures ANOVA (B) as compared to the indicated control condition.

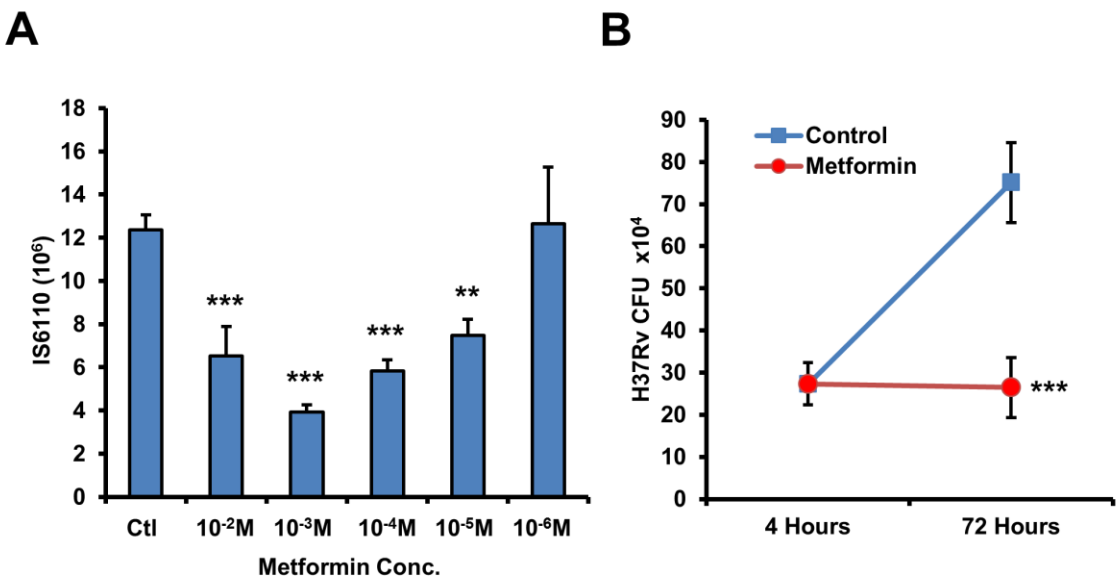
A
B
IS6110 (10^6)
18
16
14
12
10
8
6
4
2
0
***
***
***
**
Ctl
10-2M
10-3M
10-4M
10-5M
10-6M
Metformin Conc.
H37Rv CFU x10^4
90
80
70
60
50
40
30
20
10
0
Control
Metformin
***
4 Hours
72 Hours

Figure 4.3 - Metformin shifts the host cell death fate in *Mtb* infection to apoptosis

A. Representative phase-contrast microscopy of adherent macrophages 24 hours after infection with H37Rv at an MOI of 5, with and without 1mM metformin. Images are representative of three biological replicates imaged in quadruplicate. **B**. Adherent macrophages remaining after 24 hours of infection with H37Rv at an MOI of 5, with and without 1mM metformin. Values are expressed relative to the cell density of the uninfected, untreated control condition. (mean, s.d., n=4). **C.** Apoptosis in macrophages 72 hours after infection with H37Rv at an MOI of 5, with and without 1mM metformin. Values are expressed relative to the uninfected, untreated control. Data is from one experiment and representative of two independent experiments (mean, s.d., n=3). **D**. LDH secretion from macrophages 72 hours after infection with H37Rv at an MOI of 5, with and without 1mM metformin. Values are expressed relative to the uninfected, untreated control. Data are from one experiment and representative of four independent experiments (mean, s.d., n=3). **P<.01, ***P<.001, as determined by one-way ANOVA with Tukey post-test correction between the conditions indicated.

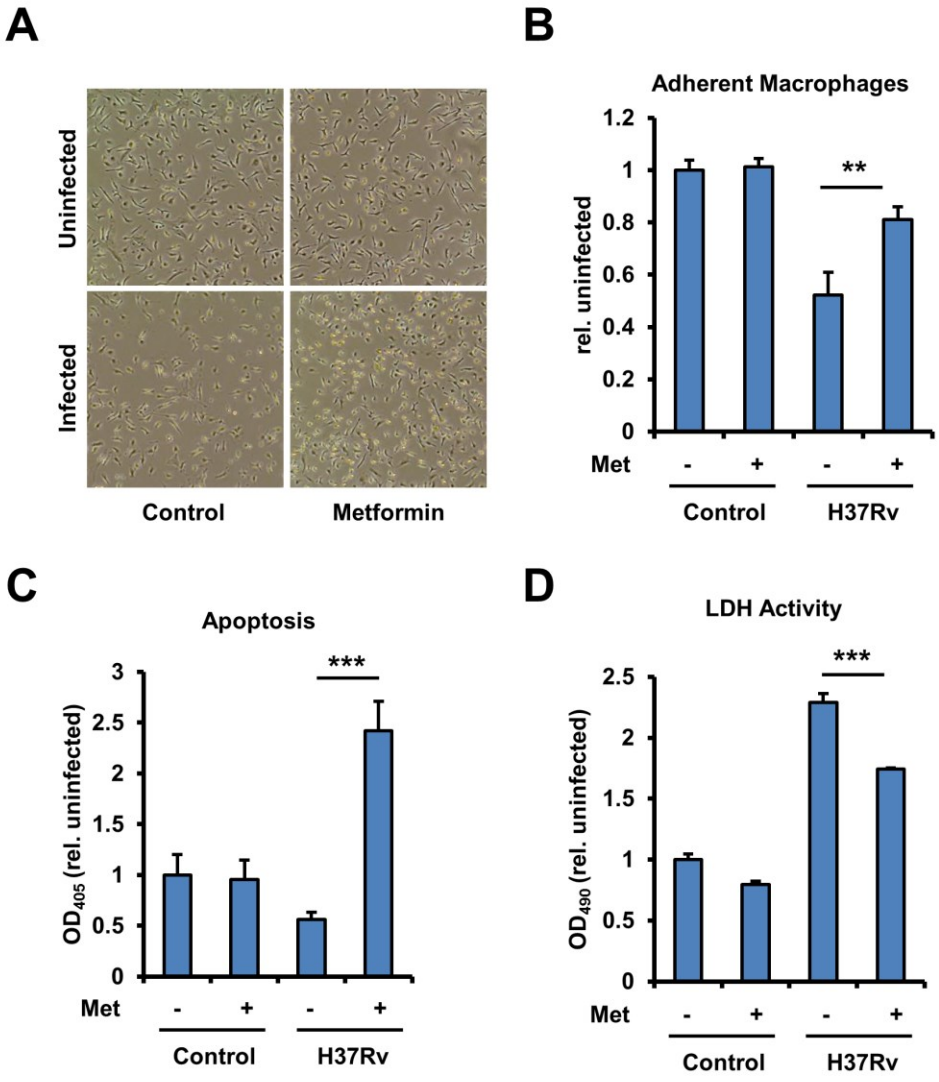
A
Uninfected
Infected
Control
Metformin
B
Adherent Macrophages
rel. uninfected
1.2
1
0.8
0.6
0.4
0.2
0
**
Met
-
+
-
+
Control
H37Rv
C
Apoptosis
OD405 (rel. uninfected)
3
2.5
2
1.5
1
0.5
0
***
Met
-
+
-
+
Control
H37Rv
D
LDH Activity
OD490 (rel. uninfected)
2.5
2
1.5
1
0.5
0
***
Met
-
+
-
+
Control
H37Rv

Figure 4.4 - Metformin induces ROS in macrophages

A and B. Time course of total ROS (A) and mitochondrial ROS (B) in macrophages infected with H37Ra at an MOI of 5, with and without 1mM metformin. Values are expressed relative to the MFI of the untreated, uninfected control. Data is from one experiment, and representative of 2 independent experiments (mean, s.d, n=3). **P<.01, ***P<.001, as determined by Student's t-test relative to the infected, untreated control for each time point.

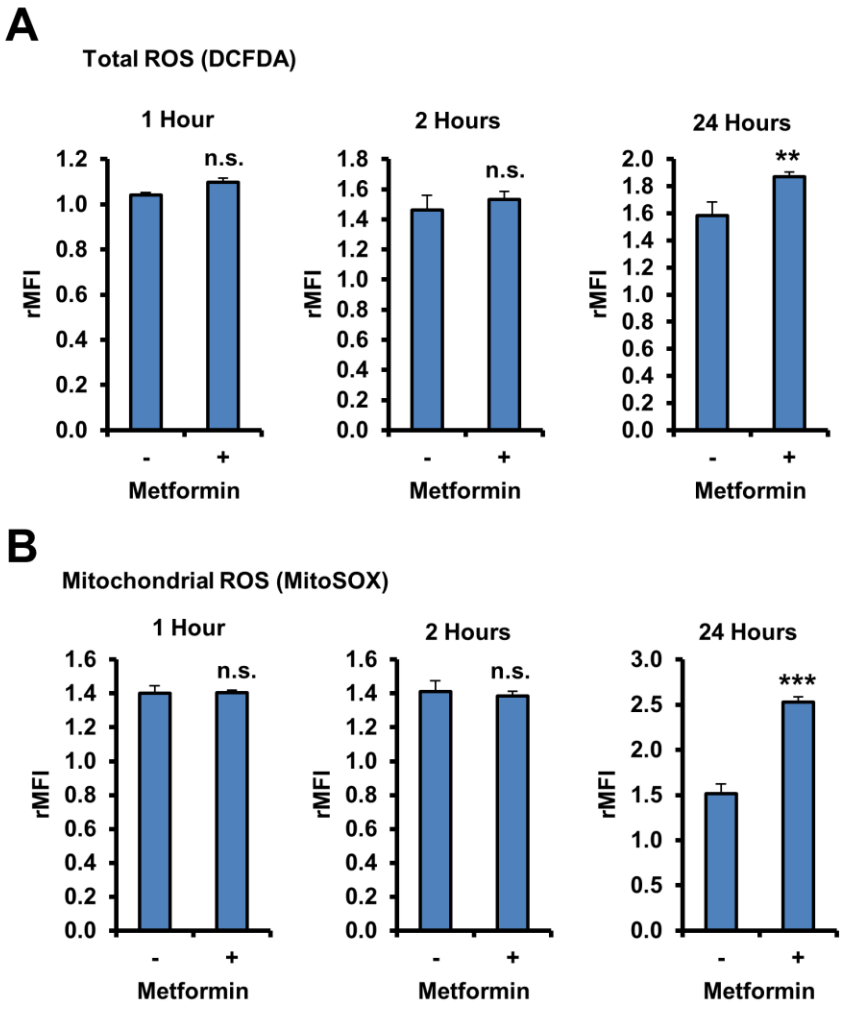
A
Total ROS (DCFDA)
1 Hour
2 Hours
24 Hours
rMFI
n.s.
n.s.
**
Metformin
B
Mitochondrial ROS (MitoSOX)
1 Hour
2 Hours
24 Hours
rMFI
n.s.
n.s.
***
Metformin

Figure 4.5 - Metformin increases the glycolytic shift in *Mtb* infected cells

A. OCR measured in macrophages infected with H37Ra at an MOI of 5 for 24 hours, with and without 1mM metformin as measured on the Seahorse XF96. **B.** ECAR measured in macrophages infected with H37Ra at an MOI of 5, with and without 1mM metformin for 24 hours, as measured on the Seahorse XF96. **C.** Percent of oxygen consumption attributed to ATP production or proton leak in macrophages infected with H37Ra at MOI of 5, with and without 1mM metformin, as measured by Seahorse XF96. Seahorse XF96 data (A-D) are from one experiment and representative of three independent (mean, s.d., n=8). **D.** ATP production in macrophages infected with H37Ra at an MOI of 5 for 24 hours with and without metformin, as measured using CellTiter Glo, and normalized in each condition to the number of cells in each condition. Data is from one experiment and representative of three independent experiments (mean, s.d., n=3). **E.** The relative fold expression of TCA intermediates in cells infected with H37Rv at an MOI of 5 and treated with 1mM metformin for 24 hours. Data is the average of two independent experiments each measured in biological triplicate (mean, s.e.m. n=2) and levels of each metabolite have been normalized to the levels of that metabolite in H37Rv-infected control. **F.** Relative abundance of citrate including the proportion of isotopomers containing ^{13}C derived from uniformly labeled ^{13}C glucose or^{13}C glutamine 24 hours after infection with H37Rv at an MOI of 5 and treatment with 1mM metformin. Data is from one experiment and representative of two independent experiments (mean, s.d., n=3). *P<.05, **P<.01, ***P<.001, as determined by one-way ANOVA with Tukey post-test correction (A,B,C,D) or Student's t-test (E) relative to the uninfected control, unless otherwise indicated.

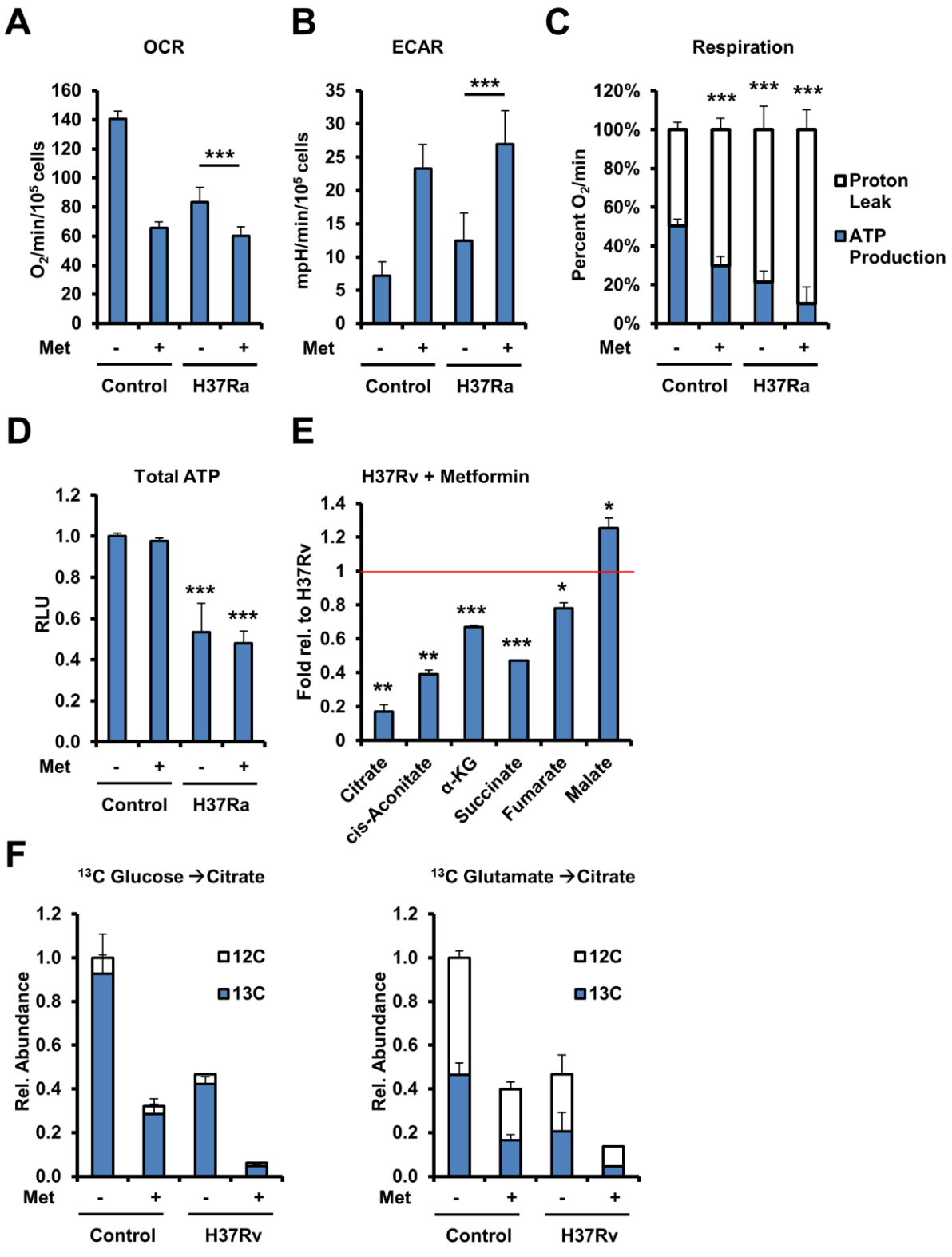
A
OCR
O2/min/10^5 cells
160
140
120
100
80
60
40
20
0
***
Met
-
+
-
+
Control
H37Ra
B
ECAR
mpH/min/10^5 cells
35
30
25
20
15
10
5
0
***
Met
-
+
-
+
Control
H37Ra
C
Respiration
Percent O2/min
120%
100%
80%
60%
40%
20%
0%
***
***
***
Proton Leak
ATP Production
Met
-
+
-
+
Control
H37Ra
D
Total ATP
RLU
1.2
1.0
0.8
0.6
0.4
0.2
0.0
***
***
Met
-
+
-
+
Control
H37Ra
E
H37Rv + Metformin
Fold rel. to H37Rv
1.4
1.2
1
0.8
0.6
0.4
0.2
0
**
**
***
***
*
*
Citrate
cis-Aconitate
α-KG
Succinate
Fumarate
Malate
F
13C Glucose →Citrate
Rel. Abundance
1.2
1.0
0.8
0.6
0.4
0.2
0.0
12C
13C
Met
-
+
-
+
Control
H37Rv
13C Glutamate →Citrate
Rel. Abundance
1.2
1.0
0.8
0.6
0.4
0.2
0.0
12C
13C
Met
-
+
-
+
Control
H37Rv

Figure 4.6 - Metformin selectively limits cholesterol and palmitate in *Mtb*-infected cells.

A. Percent mass incorporation of ^{13}C detected in cholesterol derived from uniformly labeled ^{13}C glucose in macrophages infected with H37Rv at an MOI of 5 and treated with 1mM metformin for 24 hours (mean, s.d., n=3). **B**. Percent mass incorporation of ^{13}C detected in palmitate derived from uniformly labeled ^{13}C glucose in macrophages infected with H37Rv at an MOI of 5 and treated with 1mM metformin for 24 hours (mean, s.d., n=3). **C**. Western blots of cell lysates from macrophages infected with H37Rv at an MOI of 5 with and without 1mM metformin for 24 hours. Images are from one experiment and representative of 3 independent experiments. **D, E**. Relative abundance of cholesterol (D) and palmitate (E) as detected by GC-MS. Samples were prepared from macrophages infected with H37Rv at an MOI of 5 with and without 1mM metformin for 3 (D) or 24 (E) hours. Abundance is expressed relative to the levels detected in the uninfected, untreated control. Data are from one experiment, and representative of two independent experiments (mean, s.d., n=3). **F**. Uptake of NBD-cholesterol in macrophages infected with H37Ra at an MOI of 5 with and without 1mM metformin for 1 and 3 hours. Values are expressed relative to the MFI of the uninfected, untreated control. Data are from one experiment and representative of 2 independent experiments (mean, s.d., n=3) **G**. Uptake of BODIPY-Palmitate in macrophages infected with H37Ra at an MOI of 5 with and without 1mM metformin for 24 hours. Values are expressed relative to the MFI of the uninfected, untreated control. Data are from one experiment and representative of 3 independent experiments (mean, s.d., n=3). **P<.01, ***P<.001, as determined by one-way ANOVA with Tukey post-test correction (A,B) or Student's t-test (D,E,F,G) relative to the uninfected control, unless otherwise indicated.

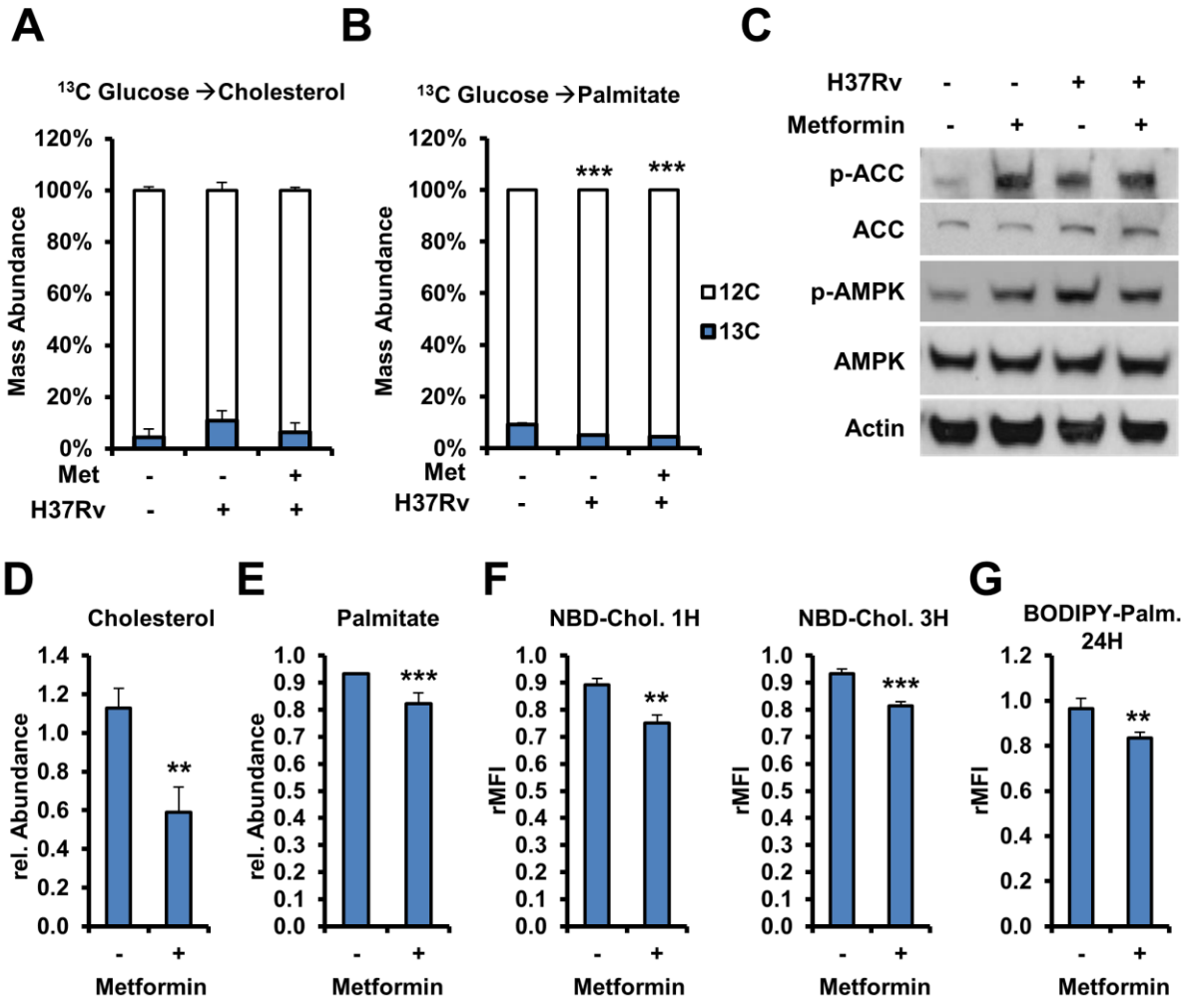
A
^{13}C Glucose →Cholesterol
Mass Abundance
120%
100%
80%
60%
40%
20%
0%
Met - - +
H37Rv - + +
B
^{13}C Glucose →Palmitate
***
***
12C
13C
C
H37Rv - - + +
Metformin - + - +
p-ACC
ACC
p-AMPK
AMPK
Actin
D
Cholesterol
rel. Abundance
**
Metformin
E
Palmitate
***
F
NBD-Chol. 1H
rMFI
**
NBD-Chol. 3H
***
G
BODIPY-Palm. 24H
**

Figure 4.7 - Model of metformin action in *Mtb*-infected macrophages.

Metformin treatment of infected macrophages inhibits TCA cycle flow, which results in increased lactate production and secretion and increased mROS production. A consequence of this is a decrease in cholesterol and palmitate uptake, and of their proportion in total intracellular lipid stores. *Mtb* has been shown to utilize cholesterol and fatty acids for virulence and to fuel its central metabolism. Decreasing the abundance of these fatty acids, along with increasing mROS, which has been shown to have bactericidal activity against intracellular bacteria., controls the replication of phagocytosed *Mtb*. Relative to infected control conditions, up-regulated pathways under metformin treatment are indicated in read, and down-regulated pathways are indicated in blue.

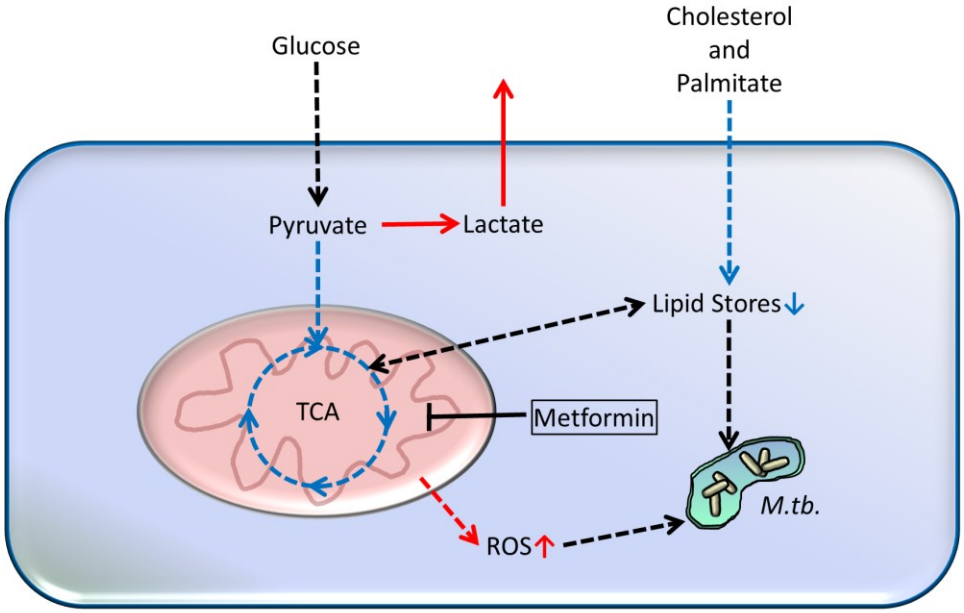
Glucose
Cholesterol
and
Palmitate
Pyruvate
Lactate
Lipid Stores
TCA
Metformin
M.tb.
ROS

Figure 4.8 - Oral Administration of metformin to mice infected with H37Rv

A. Quantification of *Mtb* in mice infected with 20-30 CFU of H37Rv in the lung and spleen after 2 and 4 months. Data are from the measurement of bacterial load in 5 mice, with total organs plated in serial dilution (mean, s.e.m., n=5) **B**. Quantification of cell types indicated, isolated from the lungs of mice 21 days after infection and measured by surface marker labeling and FACS. Data are from the measurement of cells isolated from the lungs of 4 mice. Box plots indicate mean and s.d.

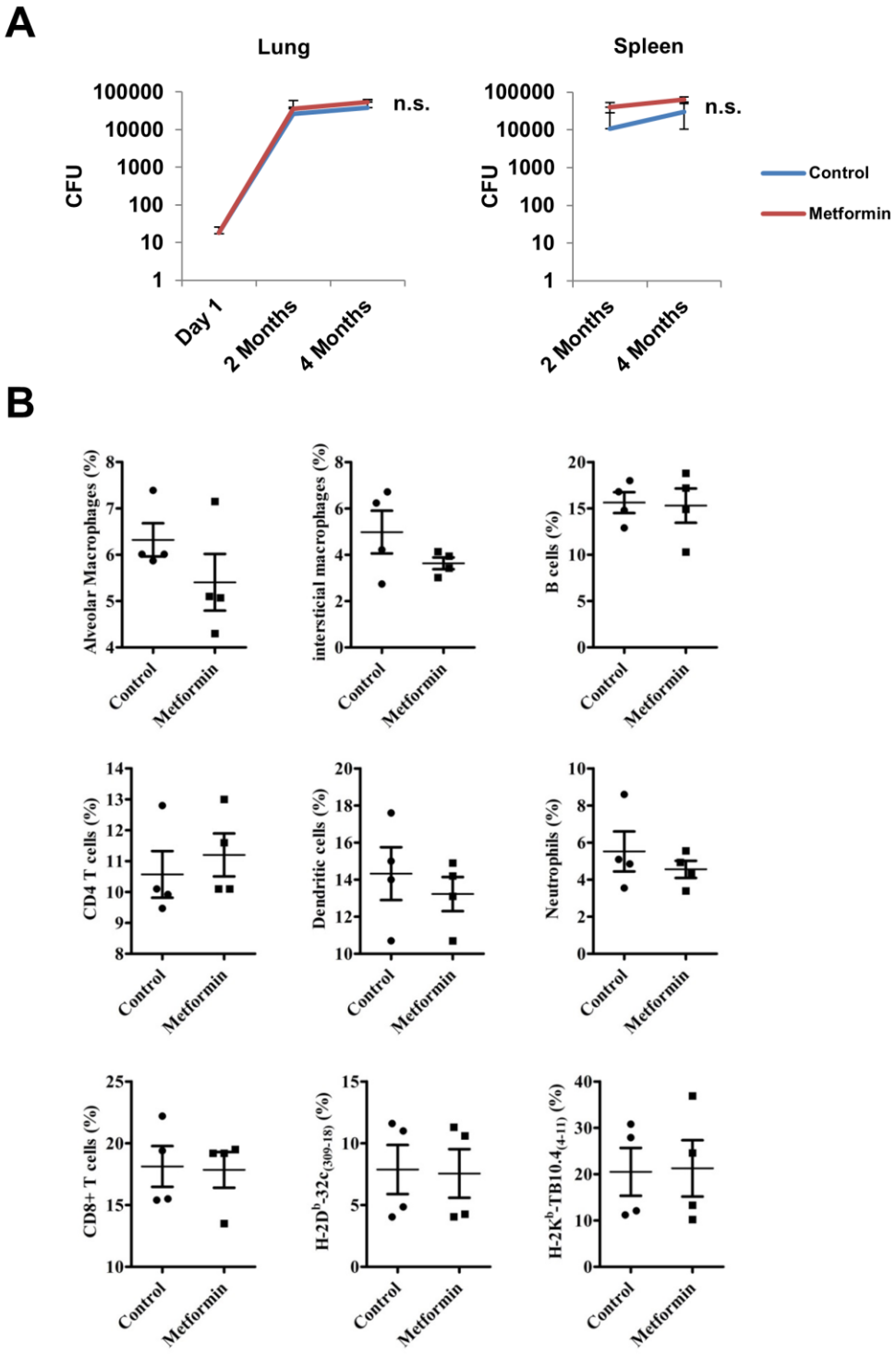
A
Lung
Spleen
CFU
100000
10000
1000
100
10
1
n.s.
Day 1
2 Months
4 Months
Control
Metformin
B
Alveolar Macrophages (%)
interstitial macrophages (%)
B cells (%)
CD4 T cells (%)
Dendritic cells (%)
Neutrophils (%)
CD8+ T cells (%)
H-2D^b-32c$_{(309-18)}$ (%)
H-2K^b-TB10.4$_{(4-11)}$ (%)
Control
Metformin

Figure S12 - TCA intermediates from macrophages, as detected by GC-MS.
Macrophages were collected 24 hours after infection with H37Ra or H37Rv. Value are expressed as a fold relative to the level detected in the macrophages infected with H37Rv. None of the comparisons are statistically significant, as determined by Student's t-test (mean, s.d., n=3).

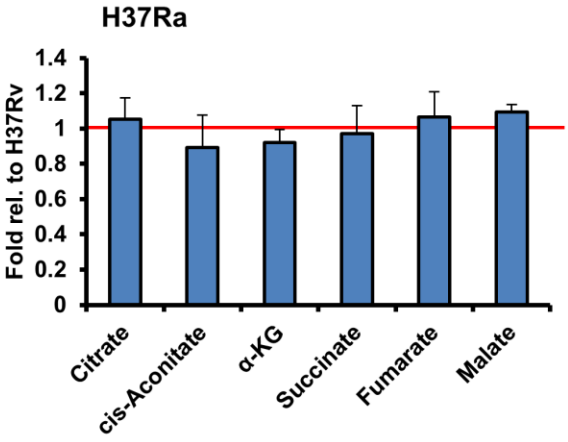

Figure S13 – LDH secretion from H37Rv-infected macrophages treated with drugs targeting central metabolic pathways.
LDH was measured in the media supernatant of macrophages infected with H37Rv at an MOI of 5, and treated with the drugs indicated for 24 hours. The threshold red bar is set at the level of LDH secretion detected from the infected control condition (mean, s.d., n=3).

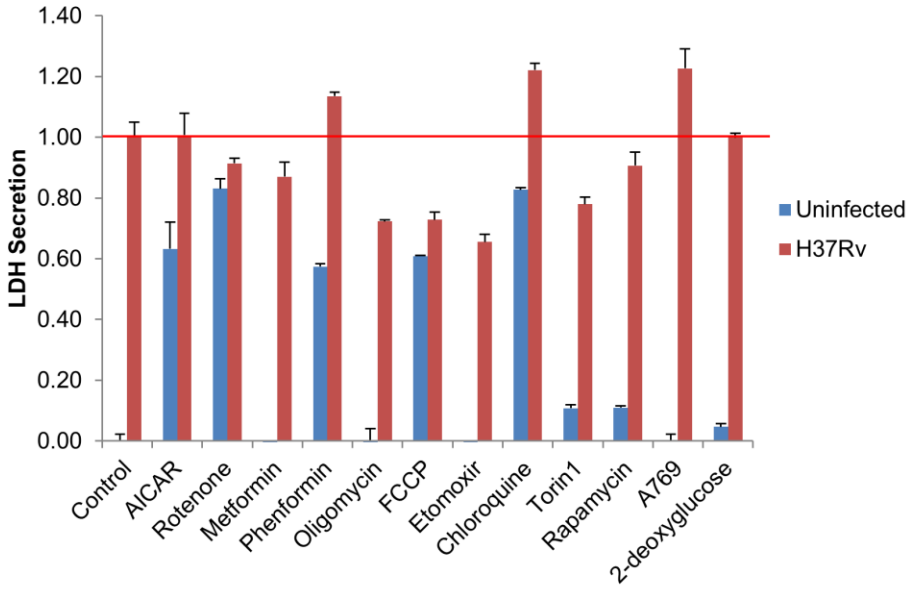

Figure S14 – Cell death pathway protein profile from H37Rv-infected macrophages.
Samples were collected 24 hours after infection with H37Rv at an MOI of 5 and treatment with 1mM metformin.

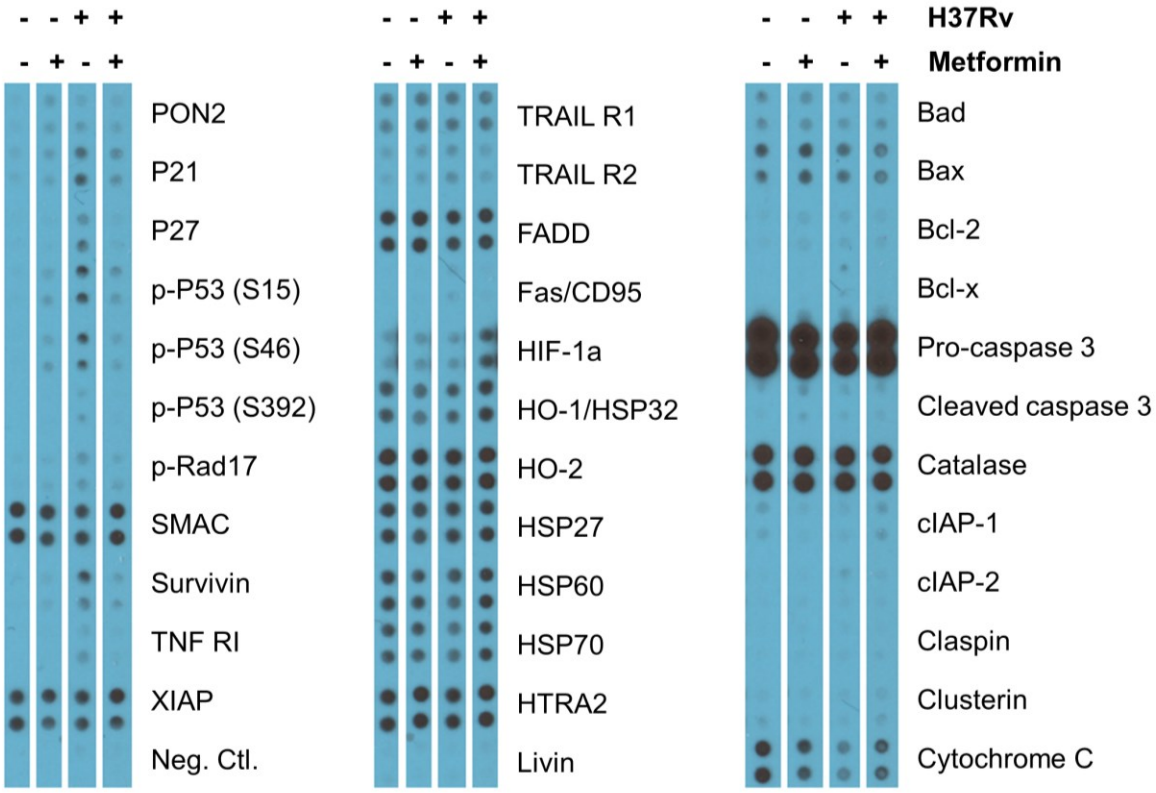

Figure S15 – Western blot of LC3-I and LC3-II from *Mtb*-infected macrophages.
Samples were collected 24 hours after infection and treatment. For loading control, refer to actin blot in Figure 4.6. Data are from one experiment and representative of three independent experiments.

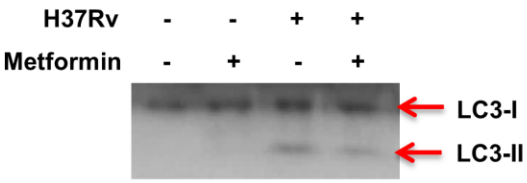

Table S4 – Cytokine Profile from THP-1 cells treated with metformin infected with H37Rv. Data are from one experiment and representative of three independent experiments (mean, s.d., n=3). The following cytokines were not detected above background: IL-2, IL-5, IL-7, IL-13, GM-CSF, and INF-γ.

	Uninfected		Uninfected + Metformin		Infected		Infected + Metformin	
Protein	average	s.d.	average	s.d.	average	s.d.	Average	s.d.
CCL3	238.4	31.1	255.5	126.3	1197.2	59.5	1153.6	33.8
CCL4	461.1	46.3	395.2	143.2	1461.4	174.9	1373.8	45.9
CCL5	1476.8	120.7	1334.8	375.2	1427.0	193.1	1412.2	39.0
Eotaxin	2.1	0.2	1.0	0.7	8.3	1.1	8.4	0.6
G-CSF	12.9	2.5	8.3	2.9	40.9	11.6	39.6	3.6
IL-1β	210.5	8.4	203.7	38.0	1426.8	41.0	1370.6	71.5
IL-1RA	13.6	0.6	11.3	1.4	22.6	2.7	24.1	0.3
IL-4	3.2	0.2	2.8	0.7	9.6	1.0	9.1	0.6
IL-6	2.8	0.2	2.4	0.3	10.9	1.4	10.6	0.0
IL-8	842.0	55.6	768.5	89.1	1202.8	24.3	1334.6	64.2
IL-9	12.6	0.5	9.3	1.9	42.4	3.1	49.4	1.8
IL-10	4.5	0.4	2.9	1.2	6.1	2.0	7.1	0.0
IL-12	9.6	0.6	7.3	0.9	12.4	2.0	11.7	1.1
IL-15	0.0	0.0	0.0	0.0	6.9	1.6	7.0	0.7
IL-17	3.4	0.4	2.2	1.6	17.2	1.6	17.0	1.9
IP-10	15.5	3.6	12.1	2.4	1229.2	51.4	729.6	73.0
MCP-1	53.1	2.5	41.5	6.6	862.6	22.8	648.5	10.9
PDGF	13.7	1.1	13.4	3.5	17.6	3.0	14.0	1.3
TNF-α	30.0	1.0	27.3	5.7	176.7	36.0	148.0	19.8
VEGF	157.8	11.7	135.8	28.0	142.7	30.7	134.8	7.3

Figure S16 – Cytokine Profile from mouse BMDMs.
Media supernatant was collected 24 hours after infection with H37Rv at an MOI of 5 and treatment with 1mM metformin.

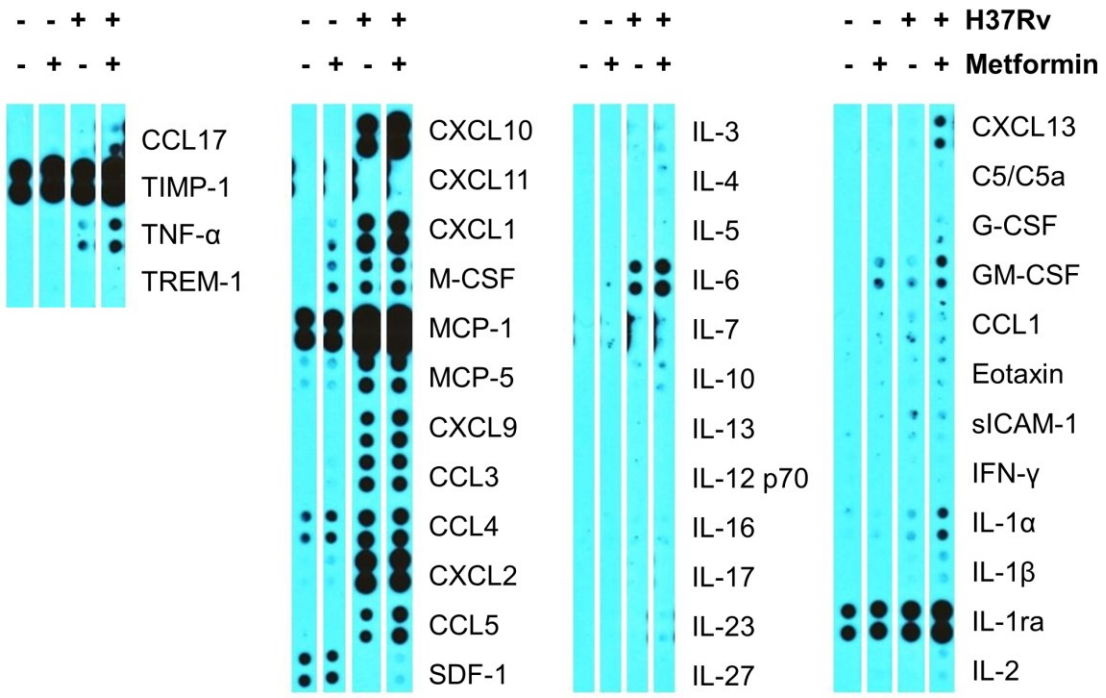

Figure S17 – TCA intermediates in Mtb-infected macrophages, as detected by GC-MS. Samples were collected 24 hours after infection, treatment, and incubation with uniformly labeled ^{13}C glucose or ^{13}C glutamine. (mean, s.d., n=3)

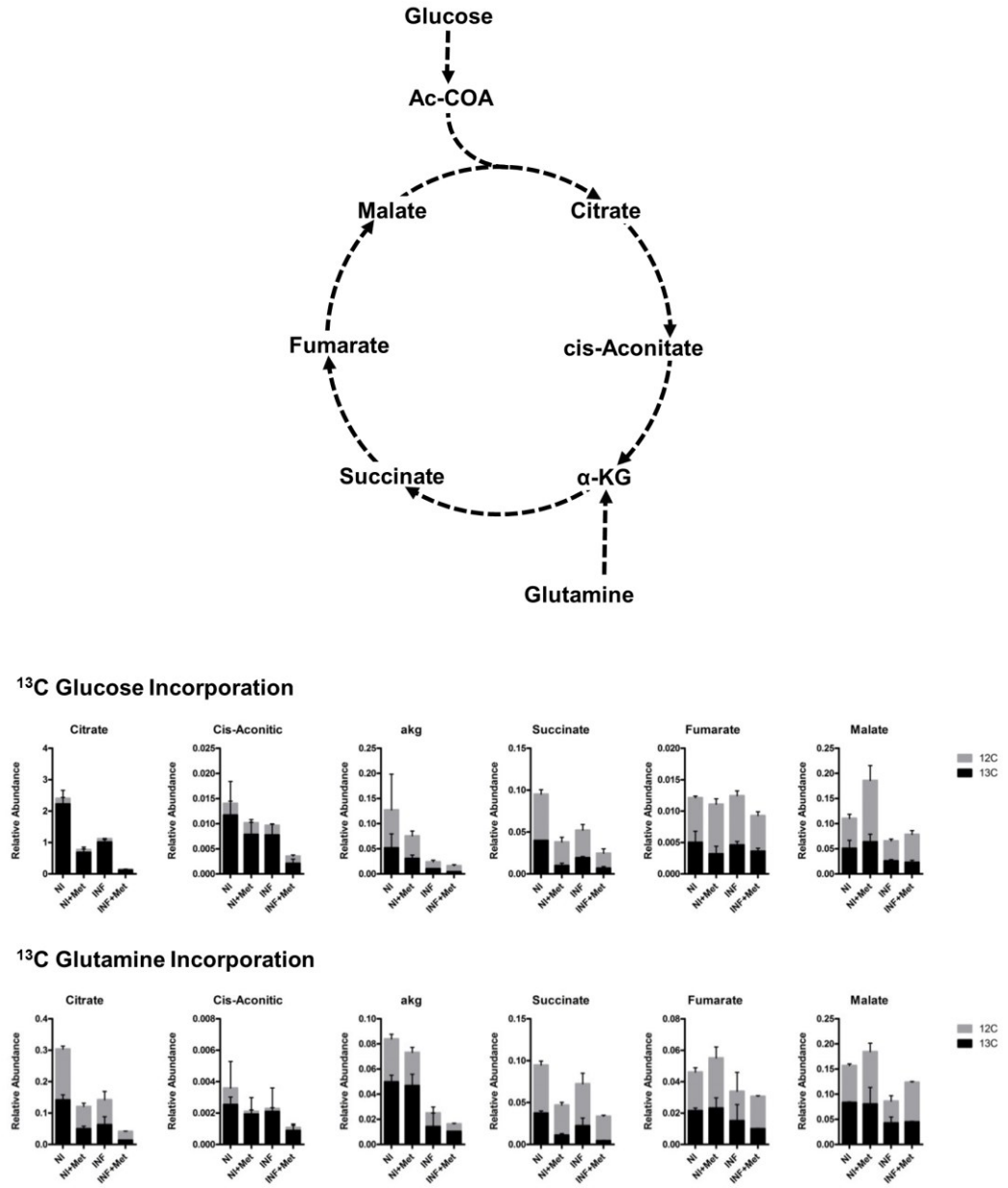

Figure S18 – Amino acids in *Mtb*-infected macrophages, as detected by GC-MS.
Samples were collected 24 hours after infection, treatment, and incubation with uniformly labeled ^{13}C glucose or glutamine (mean, s.d., n=3).

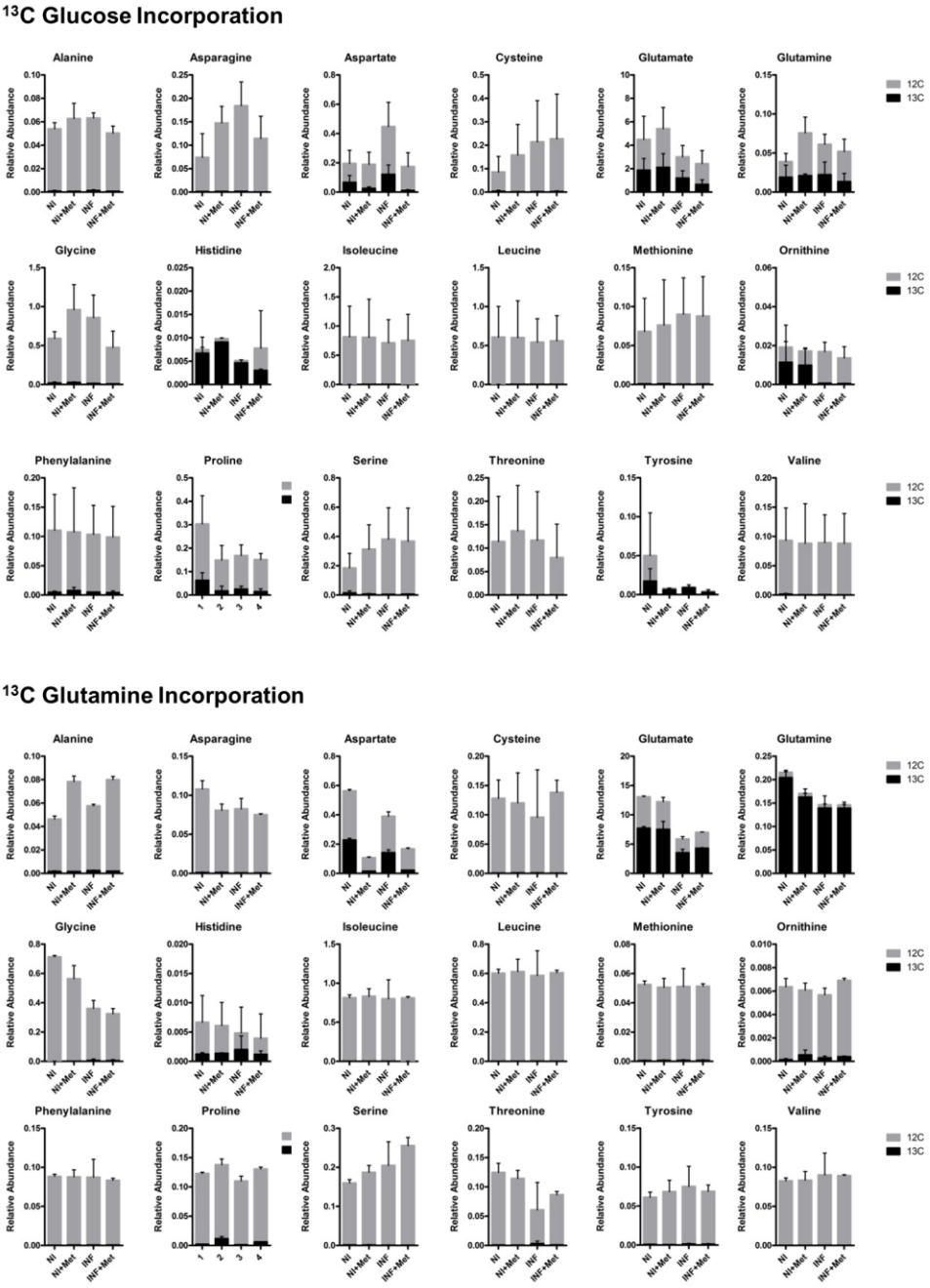

Table S5 – Fatty acids in *Mtb*-infected macrophages, as detected by GC-MS.
Samples were collected 24 hours after infection, treatment, and incubation with uniformly labeled ^{13}C glucose or glutamine (mean, s.d., n=3).

Compound Name	Uninfected		Uninfected + Met		H37Rv		H37Rv + Met	
	Average	SD	Average	SD	Average	SD	Average	SD
Dodecanoic acid	1.00	0.18	1.07	0.05	0.91	0.07	1.07	0.15
Tridecanoic acid	1.00	0.02	1.00	0.04	1.02	0.02	1.03	0.01
Palmitelaidic acid	1.00	0.03	1.07	0.06	0.96	0.02	1.00	0.03
Palmitoleic acid	1.00	0.05	0.96	0.05	1.01	0.02	0.99	0.03
cis-10-Heptadecenoic acid	1.00	0.06	0.97	0.04	0.93	0.02	0.95	0.02
Heptadecanoic acid	1.00	0.01	1.03	0.04	0.96	0.01	0.96	0.05
Linoleic acid	1.00	0.05	1.02	0.07	0.93	0.06	0.93	0.06
Oleic acid	1.00	0.03	1.06	0.03	0.91	0.01	1.01	0.01
Vaccenic acid	1.00	0.04	1.05	0.05	0.95	0.02	1.05	0.01
Stearic acid	1.00	0.14	0.96	0.03	0.99	0.07	0.88	0.04
cis-10-Nonadecenoic acid	1.00	0.03	1.04	0.09	0.96	0.06	0.94	0.04
Arachidonic acid	1.00	0.09	1.17	0.04	0.81	0.02	0.96	0.01
cis-5,8,11,14,17-eicosapentaenoic	1.00	0.08	0.97	0.05	0.77	0.04	0.79	0.01
cis-5,8,11-eicosatrienoic acid	1.00	0.08	1.05	0.10	0.88	0.08	0.91	0.09
cis-15-Tetracosanoic acid	1.00	0.20	0.94	0.04	0.89	0.04	0.93	0.15
Tetracosanoic acid	1.00	0.14	0.97	0.09	0.92	0.05	1.03	0.12
Tetradecanoic acid	1.00	0.02	0.96	0.09	1.05	0.02	1.03	0.05
Pentadecanoic acid	1.00	0.02	1.00	0.03	0.99	0.02	0.98	0.02

Figure S19 – Macrophage surface expression of CD36
Cells with infected with H37Ra and treated with metformin for 24 hours before staining and measurement by FACS Data are from one experiment and representative of two independent experiments (mean, s.d., n=3).

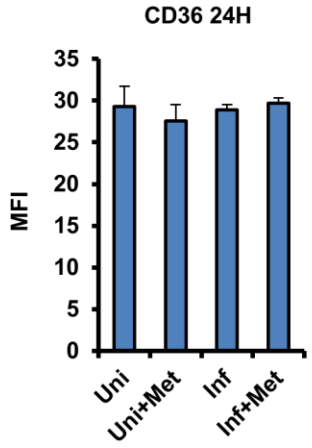

CHAPTER 5: General Discussion and Conclusion

Evaluation of Hypotheses

As stated Chapter 1, the principle hypothesis of this thesis was to determine if is possible to limit bacterial viability by changing the host environment with drugs that modulate the host transcriptome or metabolome. In the previous three chapters, we have characterized two methods for doing this *in vitro*, namely by using 1,25D and metformin.

Specifically, we sought to characterize the effect of 1,25D on the transcriptome of *Mtb*-infected macrophages and determine the secondary effects of 1,25D in the broader innate immune response to *Mtb*. In Chapter 2, we were able to achieve the first part of this by performing microarrays of *Mtb*-infected macrophages, and upon learning that the principle effect of 1,25D was to modulate the secretion profile of these cells, in Chapter 3 we used a novel co-culture system which simulated the alveolar environment to determine that the elevated production of IL-1β enhanced innate protection via the reciprocal secretion of DEFB4 from epithelial cells.

We also sought to characterize the metabolic response of the host macrophage to *Mtb*, and use this information to determine if modulation of host cell metabolism with metformin is effective at limiting bacterial replication *in vitro* and *in vivo*. From the data presented in Chapter 4, we were successfully able to characterize the host response. Furthermore, we were able to demonstrate the changes that metformin was having in this system, and suggest the possible mechanism by which bacterial proliferation was being attenuated. Unfortunately, this drug showed no effect in the murine model of TB infection, possible due to issues related to dosing or the method of drug delivery.

Vitamin D and Tuberculosis

As mentioned previously, clinical trials investigating the potential role of vitamin D supplementation in the treatment of active TB have shown no beneficial effect for the general population[152,153]. However, as the clinical incidence of active TB has been shown to inversely correlate with sunshine hours in a seasonal pattern[147] and serum concentration of vitamin D[125], the possibility remains that vitamin D sufficiency plays a prophylactic role in either the rate of the initial establishment of disease, insofar as that it would better enable innate responses to clear the infection, or that it reduces the rate of conversion from latent to active disease, potentially by modulating the dynamics of the granuloma to better contain infection.

The work presented in Chapters 2 and 3 substantially expands our understanding of the role of vitamin D in the early events of infection when a macrophage first encounters *Mtb*. In it we have undertaken the first genome-wide analysis of the effects of vitamin D on the transcriptome of an *Mtb*-infected macrophage. While previous reports on the mechanisms of vitamin D action in *Mtb* infection focused largely on the role of the induction of the AMPs CATH and DEFB4, our work demonstrated that these changes are but a minor part of the overall effect of vitamin D on the macrophage. In fact, we did not identify either of those genes as being regulated by vitamin D in an *Mtb*-infected macrophages by microarray or any follow-up qPCR study. Other cell lines have revealed these two genes to undoubtedly be transcriptional targets of the 1,25D-bound VDR, and in Chapter 3 we found that 1,25D and IL-1β stimulated the expression of both and the secretion of DEFB4 in CaLu3 cells and primary SAECs, cells types of lung epithelial origin.

The principle finding of Chapter 2 is that the largest impact that vitamin D is having on the *Mtb*-infected macrophage is in the modulation of a number of cytokines, including IL-1β,

TNF-α, CCL3, CCL4, and IL-8. As discussed in the introduction, IL-1β and TNF-α have been extensively studied in TB as they are critical for control of infection. Even though CCL3, CCL4, and IL-8 are important signaling mediators in other contexts, knockout mouse studies have demonstrated that CCL3 and CCL4 signaling pathways do not play a significant role in the initiation or long-term control of infection[256], and mice deficient in their capacity to recruit neutrophils are protected against *Mtb* infection[257]. With regard to IL-1β, *Mtb* has evolved a mechanism to interfere with active IL-1β secretion at the level of the inflammasome[214]. This report also demonstrated that elevated IL-1β secretion increased the rate of maturation of phagolysosomes containing *Mtb*. This would suggest that elevated secretion of IL-1β, as we observed in the context of 1,25D treatment, has the potential to improve the outcome of infection. At the time our study was conducted, the exact contribution of the 1,25D-driven elevation of IL-1β secretion could not be effectively addressed by siRNA- or shRNA-mediated knockdown, as totally removing IL-1β would severely limit the capacity of the macrophage to control infection, and would introduce a level of susceptibility in the control that does not accurately model normal conditions. With the advent of the CRISPR/Cas9 system allowing for selective genome editing, removal of the VDRE upstream of the IL-1β promoter would enable one to directly understand the contribution of elevated IL-1β to the protective effect of 1,25D in *Mtb*-infected macrophages.

We observed that 1,25D treatment in our *in vitro* model of infection generally enhanced the inflammatory cytokine and chemokine responses to infection. This has the potential to be both positive and negative, as increased IL-1β has been associated with maturation of phagolysosomes containing *Mtb*[214], although excessive inflammation can be deleterious to organs. This has been observed under conditions with increased TNF-α production, which was

associated with less favorable prognoses in cases of TB meningitis[56], as well as increased neutrophilia in the lungs, presumably the consequence of an over production of IL-8, which was also associated with a more severe disease outcome[258]. Despite these lines of speculation, an understanding of the balance between the potential positive and negative effects of vitamin D status in the face of *Mtb* infection requires an *in vivo* model. While non-human primates would serve as an effective model considering that they share the same distribution of VDREs, the costs associated with the purchase and maintenance of these animals represent a large barrier. A more viable alternative to this problem may be the use of mice with humanized immune systems[259]. These mice can be generated from the injection of hematopoietic stem cells into strains that have been genetically engineered to be severely immunocompromised. However, the challenges associated with this process make these mice expensive and difficult to generate. Another option is the use of *in vitro* granulomas, a method where unselected preparations of cells isolated from the buffy coat of whole blood are infected with *Mtb*. This has recently been developed and used to model the dynamics of lipid dysregulation in macrophages[260].

A sequence analysis of the VDREs proximal to the promoters of the cytokines modulated by 1,25D demonstrated that these sequences were only conserved evolutionarily in primates, and not in mice or rabbits, two commonly used models of TB infection. While these species do require vitamin D to maintain calcium and bone homeostasis, the varied distribution of VDREs between species means that the immune-modulating effects seen in human cells are not necessarily replicated in rodents. This lack of a readily available *in vivo* model severely limits our capacity to understand the impact of vitamin D on the total immune response to *Mtb*. For this reason, we developed a novel model of co-culture between macrophages and epithelial cells in Chapter 3 in order to model the microenvironment of the alveoli.

The evaluation of the effectiveness of vitamin D in the prevention or treatment of TB will ultimately be decided by clinical investigation. To date, clinical studies have demonstrated no benefit to vitamin D supplementation in the treatment of active disease[152,153]. Several studies have been conducted looking at the potential protective role of vitamin D supplementation in the prevention of pulmonary infections[136,137,139]. A similar study design would be required for the definitive evaluation of vitamin D in the prevention of TB. If proven successful, such a program of prophylaxis would obviously represent a benefit to the patients. Additionally, it would come at a large financial savings for health care services, as treating a single patient for tuberculosis can cost approximately $20,000, while vitamin D costs pennies per dose.

Metformin and Tuberculosis

The data presented in Chapter 4 represents the first full analysis of *Mtb* on the host macrophage metabolic program. In addition, we identify metformin as being capable of limiting the replication of *Mtb* in macrophages. The treatment of *Mtb*-infected macrophages with metformin skewed cell death fate towards apoptosis, increased mitochondrial ROS, and decreased the availability of cholesterol and palmitate, two important carbon sources for *Mtb.* The combination of these factors likely resulted in the observed control of bacterial replication.

Unfortunately, oral administration of metformin to *Mtb*-infected mice produced no effect in either bacterial burden or immune responses present in the lung. This may have been the result of a number of factors. Firstly, it is possible that the dose or PO method of delivery made the effective concentration in the lung insufficient to elicit the effects that we demonstrated at 10^{-3}M *in vitro*. An additional consideration on this point is that metformin uptake is relatively elevated in the liver, potentially reducing the bioavailability of it for other organs. Secondly, metformin

requires active transport to get into cells as it is not fat soluble, and this may pose a problem for penetrating the caseous matrix at the center of granulomas to get to the infected phagocytes. A potential solution to this is the use of phenformin. Phenformin is similar in molecular structure to metformin, but for the addition a phenyl group, allowing it to pass through membranes in the absence of active transport. Having a similar mechanism of action, it is substantially more potent than metformin. It was also prescribed for glycemic control, but was later discontinued from clinical use as a side effect of treatment was severe lactic acidosis. Phenformin was used in our initial screen of drugs, but was found to induce LDH secretion and cell death in uninfected cells. Despite this, a full dose-response curve was not performed, and it is possible that at a lesser dose it would be able to mimic the effects of metformin without these negative effects, while also having the ability to penetrate the lipid-rich environment of the granuloma. Lastly, metformin has been shown to have immunosuppressive effects in experimental autoimmune encephalitis, a mouse model of multiple sclerosis[261]. It is possible then that the benefit that metformin presented to the macrophage was balanced by its inhibitory effects on the adaptive immune system, resulting in no net effect on infection.

Given that cholesterol is an important component of *Mtb* virulence, reducing cholesterol levels serves as an attractive target for new HDTs. To this end, two other studies published recently have identified methods of reducing host cholesterol in macrophages as a method of controlling *Mtb*-infection *in vitro*[249,252]. One of these used statins, a class of drugs widely prescribed for decreasing serum cholesterol. In this study, the authors found that administering statins to mice did not have an effect on pulmonary bacterial burden, but mildly decreased the rate of extra-pulmonary dissemination of infection. Recently, a nation-wide retrospective cohort study from Korea was published addressing the potential of this[250]. They investigated the rates of

active TB in patients recently diagnosed with type 2 diabetes mellitus (T2DM), and analyzed these groups to understand if the prescription of statins had an impact on this. The authors found that the prescription of statins, after adjustment for covariates, did not have any impact on the rate of TB within that population. While this may limit the applicability of statins for TB, other methods for the targeted limitation of cholesterol may prove to be more beneficial.

While the most severe source of compromised immunity in cases of TB is the HIV/AIDS epidemic, other factors, including smoking and T2DM, also increase the risk of active disease[262]. Although drug delivery programs and field diagnostics for TB have improved in recent years, the number of cases has hit a relative plateau, largely due to the increasing rates of these factors in the developing world[263]. The association between T2DM and TB has been established for some time[264], and prior to the introduction of anti-TB antibiotics, patients with T2DM who did not die as a result of a diabetic coma were likely to die of TB[265]. Projections of current trends in the worldwide incidence of T2DM predict that ~440 million people will have the disease by 2030[266]. Metformin is commonly prescribed for the treatment of diabetes, and although we did not identify any protective effect with metformin treatment *in vivo*, more needs to be done to understand the impact of this drug, if any, on the progression of TB.

In the previously discussed Korean study of statins[250], the authors also included data on the drugs prescribed in each case for the management of T2DM. Interestingly, the authors included data on the medications that had been prescribed to the study population for the management of T2DM. Stratifying the study population by the anti-diabetic medication prescribed revealed that the patients given metformin, but not other anti-diabetic agents, were more likely to not have TB than have TB (Figure 5.1). In fact, the use of every other anti-diabetic medication identified was higher or no different in the population that acquired TB. While this is

far from demonstrating causation, correlation between the prescription of metformin and a decreased incidence of TB could be established by re-analyzing these groups while adjusting for the covariates used in the rest of the study, including the potential increase in risk of TB associated with co-prescribed anti-diabetic drugs.

The Future of HDTs

Existing HDTs for TB have been developed with the intent of treating active disease, and not for the prevention of disease in those who are uninfected or limiting the progression of disease in those latently infected. The deployment of HDTs is potentially complicated by the heterogeneity of hosts, in both genetics and environment. These variables would mean that HDTs will likely require additional diagnostic tests so that therapies can be optimized to each patient. On their own, these approaches will likely not be sufficient for the elimination of active disease, but they may provide an effective supporting measure in the absence of new front line antibiotics. HDTs show the most potential for the treatment of difficult cases of TB, including drug resistant and extra-pulmonary disease. Strategies that are able to reduce the duration of chemotherapy will be able to improve adherence, and reduce the evolutionary rate of drug-resistance. Even HDTs that are able to reduce inflammation and tissue damage, when given in combination with effective antibiotics, can reduce the inflammatory damage to infected organs and improve recovery time.

Challenges in The Future of TB Treatment

Even as the annual global rates of active TB have been falling in recent years, the massive global burden of disease and new MDR strains have elevated the need for new therapies

and vaccines. Ignoring the few percent of TB cases classified as drug resistant, ~96% of all cases of active disease should be treatable with current interventions. The prevalence of TB in the developing world therefore can largely be attributed to the lack of medical infrastructure and access to existing antibiotics. Current efforts to control the disease in endemic areas focus largely on the management of active cases, and not the treatment of latent TB.

There are two principle goals for the eradication of TB, the effective treatment of existing cases, and the prevention of future ones. Antibiotics are used for the former, and vaccinations are the most effective manner of managing the latter. A vaccine that reduces the rate of transmission will decrease the number of new cases and latent infections, but even if all transmission were stop today, ~2 billion people are currently infected, and in the event of progression to active disease they will need antibiotics to clear the infection. For this reason, progress on both of these fronts will be required for expedient global elimination of TB.

Compared to the treatment of other infectious diseases, the 6-9 month course of antibiotics prescribed for the treatment of TB is exceptionally long, and as a result of this, compliance with protocols is difficult to maintain. In addition, failure to complete the recommended course of antibiotics prescribed for bacterial infections in general has been associated with the increased incidence of drug-resistance in those bacteria. For these reasons, the World Health Organization formally launched its framework for effective TB control in 1994, which was rebranded as DOTS (Directly Observed Therapy, Short-course) in the following year. Effective implementation of DOTS programs has been associated with lower rates of MDR TB[28]. Fortunately, its popularity as a program has been growing. In its early stages of development, the treatment services that became the DOTS program were responsible for detecting and treating ~2% of cases of active TB worldwide, a number which has now grown in

recent years to ~60%. Since its official start, implementations of the DOTS program have successfully treated 41 million people, saving 6 million lives[267].

The development of a new vaccine that provides effective protection against active disease, if not latent disease, would greatly reduce the transmission rates of *Mtb*. With over a dozen candidates currently in clinical trials, this may soon be a reality. A single dose vaccine, especially one that is effective in adults, would provide a large benefit without necessarily requiring the long term development of medical infrastructure. Many new approaches are being tested, ranging from modified versions of the BCG vaccine, to other live attenuated mycobacteria, to recombinant versions of the common cold which have been engineered to express antigenic peptides common to *Mtb.*

Any vaccination strategy requires that individuals vaccinated possess a competent immune system capable of executing the adaptive memory formed by the vaccine, and this ability is severely jeopardized in the HIV positive population. Latent TB is almost completely ubiquitous in some parts of Africa, and TB is the leading cause of death in patients who have progressed to AIDS[1,194]. The AIDS epidemic in Africa represents another major hurdle to the elimination of TB. In cases of HIV and TB co-infection, rates of extra-pulmonary TB increase[268], and for this reason, although Africa is not responsible for the largest number of cases of TB worldwide, African countries are among those that have the highest rates of mortality (Figure 5.2). This means that any successful measure for the elimination of TB will come have to come hand in hand with the control of HIV.

Setting Goals for the Eradication of Tuberculosis

The target for elimination of TB established by the WHO is to reduce the global annual incidence of disease to one case per million by 2050, nearly a 1000-fold reduction in the current rate[263]. To achieve this goal, the annual rate must drop by 20% each year for the next 35 years. The viability of this model requires the development of new methods for diagnosis and treatment, as only a 10% annual reduction would be possible with the current tools[263]. In addition, it will require the treatment of cases of active and latent disease. Thirty-five countries have already entered the elimination phase, with less than 10 deaths per million occurring annually[263]. With aggressive management, substantially more could join that list in the next 10-20 years. Immigrant populations from the developing world are largely responsible for new cases reported in first world countries, in a proportion representative of their country of origin. Given the availability of travel, until global rates are managed, even first-world countries will not be able to completely eliminate disease.

Potential timelines for the worldwide elimination of TB have been modeled (Figure 5.3). Current global efforts to control TB focus largely on using the available resources to treat cases of active TB, representing the baseline shown. If large improvements are made globally in the detection and treatment of active TB (trace 1), mortalities associated with TB may be substantially mitigated in the next 15 years. If transmission were completely stopped today (trace 2), reactivation and relapse would still be responsible for 100 cases per million by 2050. Aggressive treatment of all cases of latent TB (trace 4) would have a substantial impact on reducing mortality and the total number of cases, as it would reduce both the potential for reactivation and transmission. In addition to this, by significantly decreasing the reservoir of latent infection, we would also hinder the capacity for *Mtb* to evolve drug resistance. In order to reach the goal of elimination by 2050 (trace 5), we will require a shift from just the treatment of

active disease to active prevention. This would mean building the capacity to quickly identify and treat all cases of TB, both active and latent. This will not be feasible with the DOTS program on its own, and thankfully other organizations and efforts have begun to support the WHO initiatives in order to realize elimination.

Building on DOTS

With the relative rarity of cases in the first world, TB has fallen out of the public consciousness. In most of the developed world, TB is largely an issue of the immigrants from the developing world and the homeless, and the availability of first and second line antibiotics means that almost every case of TB, including latent infection, is readily treatable. Unfortunately this is not the case in the rest of the world, and to address the resurgence of cases that was documented in the early 1990s, on April 23, 1993 The WHO declared TB a global emergency[28]. This was addressed in part with the development of DOTS, but the DOTS program on its own was not designed to manage drug resistant cases, and the cost of managing TB is ever increasing. In April 2003 the WHO's 'stop TB' program set a goal of detecting 70% of cases and successful treating 85% of these, at a projected cost of $1.2 billion annually[28]. Several programs now exist under the DOTS-Plus umbrella, which address the gaps left by the DOTS program, namely the delivery of the more expensive second-line antibiotics to the people diagnosed with MDR TB[28].

This effort has been further bolstered by the foundation of the Global Drug Facility (GDF). The GDF was founded 2001 in an effort to establish one large buyer of antibiotics which would be able to negotiate with pharmaceutical companies for reductions in pricing in exchange for purchasing volume. It has been successful in this regard, and in 2011 the GDF was responsible for the purchase of 35% of all drugs used for the treatment of TB that year[269]. In

addition to the contributions of the GDF, the Bill and Melinda Gates Foundation has brought significant financial resources to bear, having donated $1.3 billion to The Global Fund to Fight AIDS, Tuberculosis, and Malaria. Furthermore, they have funded the Aeras Global TB Vaccine Foundation, which produced a successful initiative to reduce the cost associated with the detection of *Mtb* in the field, with the added capacity to identify rifampicin resistance. Lastly, bedaquiline, the first new TB antibiotic in 40 years, has been approved by the FDA for the treatment of MDR TB. If this current rate of funding, progress, and discovery continues, after millennia of death and suffering, we have the strong potential of bringing TB into the global elimination phase within our lifetime.

	TB-negative *n* (%)	TB-positive *n* (%)	*P* value
Total, *n*	836 824	4075	
Initial DM drugs			
Sulfonylurea	460 674 (55.1)	2601 (63.8)	<0.01
Metformin	461 809 (55.2)	1868 (45.8)	<0.01
Meglitinide	18 161 (2.2)	116 (2.8)	<0.01
α-glucosidase inhibitor	56 711 (6.8)	364 (8.9)	<0.01
Thiazolidinediones	30 950 (3.7)	130 (3.2)	0.09
DPP-4 inhibitors	21 250 (2.5)	41 (1.0)	<0.01
GLP-1 analogues	3 (0.0)	0 (0.0)	>0.99
Insulin	129 842 (15.5)	1000 (24.5)	<0.01
Other DM drugs	54 119 (6.5)	293 (7.2)	0.06

Figure 5.1 – Incidence of TB among those prescribed drugs for the management of T2DM. Reproduced with modifications from Kang et al (2014)[250].

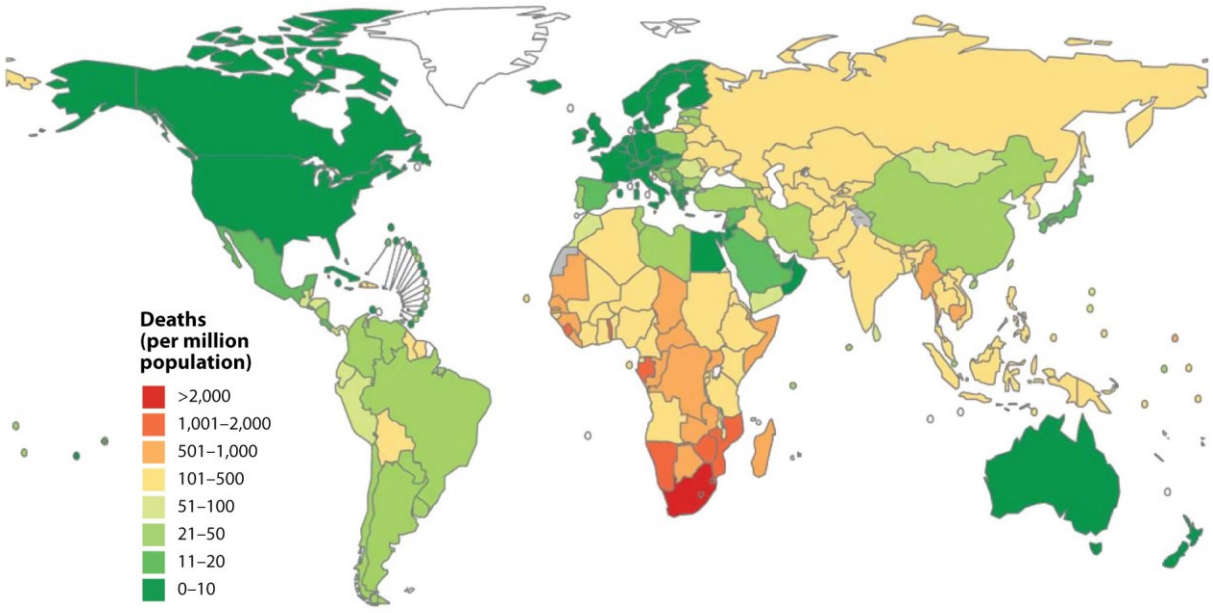

Figure 5.2 – TB mortality by country in 2012.
Reproduced from Dye et al (2013)[263].

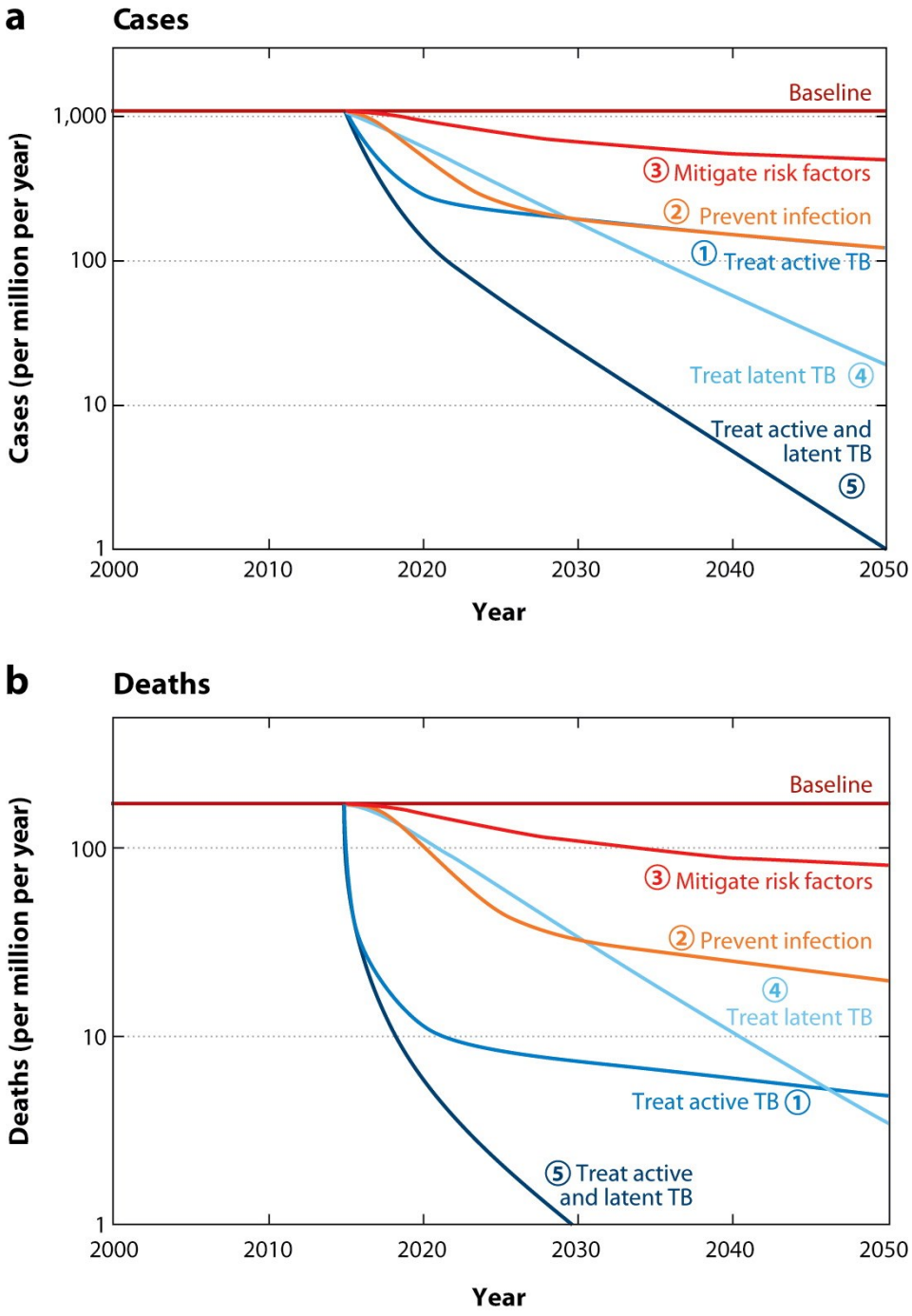

Figure 5.3 – Projections for the global elimination of TB.
Reproduced from Dye et al (2013)[263].

APPENDIX I - References

1. Floyd, K. *Global Tuberculosis Control 2011*, (WHO Pres, Geneva, Switzerland, 2011).
2. Keeler, E.*, et al.* Reducing the global burden of tuberculosis: the contribution of improved diagnostics. *Nature* (2006).
3. Dye, C.*, et al.* Global burden of tuberculosis: Estimated incidence, prevalence, and mortality by country. *JAMA* **282**, 677-686 (1999).
4. Nguyen, L. & Pieters, J. The Trojan horse: survival tactics of pathogenic mycobacteria in macrophages. *Trends in Cell Biology* **15**, 269-276 (2005).
5. Barry, C.E.*, et al.* The spectrum of latent tuberculosis: rethinking the biology and intervention strategies. *Nat Rev Micro* **7**, 845-855 (2009).
6. Modlin, R.L. & Bloom, B.R. TB or Not TB: That Is No Longer the Question. *Science Translational Medicine* **5**, 213sr216 (2013).
7. WHO. Multidrug-resistant tuberculosis (MDR-TB), 2013 update. (2013).
8. Gandhi, N.R.*, et al.* Extensively drug-resistant tuberculosis as a cause of death in patients co-infected with tuberculosis and HIV in a rural area of South Africa. *The Lancet* **368**, 1575-1580.
9. IoM. *Developing and Strengthening the Global Supply Chain for Second-Line Drugs for Multidrug-Resistant Tuberculosis: Workshop Summary*, (The National Academies Press, 2013).
10. Parida, S.K.*, et al.* Totally drug-resistant tuberculosis and adjunct therapies. *Journal of Internal Medicine*, n/a-n/a (2014).
11. Brewer, T.F. Preventing Tuberculosis with Bacillus Calmette-Guérin Vaccine: A Meta-Analysis of the Literature. *Clinical Infectious Diseases* **31**, S64-S67 (2000).
12. Fine, P.E.M. Variation in protection by BCG: implications of and for heterologous immunity. *The Lancet* **346**, 1339-1345 (1995).
13. Tameris, M.D.*, et al.* Safety and efficacy of MVA85A, a new tuberculosis vaccine, in infants previously vaccinated with BCG: a randomised, placebo-controlled phase 2b trial. *The Lancet* **381**, 1021-1028.
14. Ottenhoff, T.H.M. & Kaufmann, S.H.E. Vaccines against Tuberculosis: Where Are We and Where Do We Need to Go? *PLoS Pathog* **8**, e1002607 (2012).
15. Brosch, R.*, et al.* A new evolutionary scenario for the Mycobacterium tuberculosis complex. *Proceedings of the National Academy of Sciences* **99**, 3684-3689 (2002).
16. Gutierrez, M.C.*, et al.* Ancient Origin and Gene Mosaicism of the Progenitor of Mycobacterium tuberculosis. *PLoS Pathog* **1**, e5 (2005).
17. Gagneux, S.*, et al.* Variable host–pathogen compatibility in Mycobacterium tuberculosis. *Proceedings of the National Academy of Sciences of the United States of America* **103**, 2869-2873 (2006).
18. Sreevatsan, S.*, et al.* Restricted structural gene polymorphism in the Mycobacterium tuberculosis complex indicates evolutionarily recent global dissemination. *Proceedings of the National Academy of Sciences* **94**, 9869-9874 (1997).
19. Hirsh, A.E., Tsolaki, A.G., DeRiemer, K., Feldman, M.W. & Small, P.M. Stable association between strains of Mycobacterium tuberculosis and their human host populations. *Proceedings of the National Academy of Sciences of the United States of America* **101**, 4871-4876 (2004).
20. Pigrau-Serrallach, C. & Rodríguez-Pardo, D. Bone and joint tuberculosis. *Eur Spine J* **22**, 556-566 (2013).

21. Zimmerman, M.R. Pulmonary and osseous tuberculosis in an Egyptian mummy. *Bulletin of the New York Academy of Medicine: Journal of Urban Health* **55**, 604-608 (1979).
22. Nerlich, A.G., Haas, C.J., Zink, A., Szeimies, U. & Hagedorn, H.G. Molecular evidence for tuberculosis in an ancient Egyptian mummy [10]. *Lancet* **350**, 1404 (1997).
23. Cave, A.J.E. & Demonstrator, A. The evidence for the incidence of tuberculosis in ancient Egypt. *British Journal of Tuberculosis* **33**, 142-152 (1939).
24. Coar, T. *The Aphorisms of Hippocrates*, (Longman & Co.: London, 1822, 1822).
25. Meinecke, B. *Consumption (tuberculosis) in Classical Antiquity*, (P.B. Hoeber, Incorporated, 1927).
26. Koch, R. Die aetiologie der tuberculose, a translation by Berna Pinner and Max Pinner with an introduction by Allen K. Krause. *Am Rev Tuberc* **25**, pp. 285–323 (1932).
27. Daniel, T.M. Robert Koch and the pathogenesis of tuberculosis. *The international journal of tuberculosis and lung disease : the official journal of the International Union against Tuberculosis and Lung Disease.* **9**, 1181-1182 (2005).
28. Bynum, H. *Spitting Blood: The History of Tuberculosis*, (OUP Oxford, 2012).
29. Daniel, T.M. The history of tuberculosis. *Respiratory Medicine* **100**, 1862-1870 (2006).
30. Schatz, A., Bugle, E. & Waksman, S.A. Streptomycin, a Substance Exhibiting Antibiotic Activity Against Gram-Positive and Gram-Negative Bacteria.∗†. *Experimental Biology and Medicine* **55**, 66-69 (1944).
31. Weitzman, D., de Wend Cayley, F.E. & Wingfield, A.L. Streptomycin in the treatment of pulmonary tuberculosis. *British Journal of Tuberculosis and Diseases of the Chest* **44**, 98-104 (1950).
32. Russell, D.G., Barry, C.E. & Flynn, J.L. Tuberculosis: What We Don't Know Can, and Does, Hurt Us. *Science* **328**, 852-856 (2010).
33. Cooper, A.M., Mayer-Barber, K.D. & Sher, A. Role of innate cytokines in mycobacterial infection. *Mucosal Immunol* **4**, 252-260 (2011).
34. Riley, R.*, et al.* Aerial dissemination of pulmonary tuberculosis: a two-year study of contagion in a tuberculosis ward. *American Journal of Epidemiology* **70**, 185-196 (1959).
35. Cobat, A.*, et al.* Two loci control tuberculin skin test reactivity in an area hyperendemic for tuberculosis. *Journal of Experimental Medicine* **206**, 2583-2591 (2009).
36. Chackerian, A.A., Alt, J.M., Perera, T.V., Dascher, C.C. & Behar, S.M. Dissemination of Mycobacterium tuberculosis Is Influenced by Host Factors and Precedes the Initiation of T-Cell Immunity. *Infection and Immunity* **70**, 4501-4509 (2002).
37. Wolf, A.J.*, et al.* Initiation of the adaptive immune response to Mycobacterium tuberculosis depends on antigen production in the local lymph node, not the lungs. *The Journal of Experimental Medicine* **205**, 105-115 (2008).
38. Reiley, W.W.*, et al.* ESAT-6-specific CD4 T cell responses to aerosol Mycobacterium tuberculosis infection are initiated in the mediastinal lymph nodes. *Proceedings of the National Academy of Sciences* **105**, 10961-10966 (2008).
39. Russell, D.G., Cardona, P.-J., Kim, M.-J., Allain, S. & Altare, F. Foamy macrophages and the progression of the human tuberculosis granuloma. *Nat Immunol* **10**, 943-948 (2009).
40. Flynn, J.L., Chan, J. & Lin, P.L. Macrophages and control of granulomatous inflammation in tuberculosis. *Mucosal Immunol* **4**, 271-278 (2011).
41. Lin, P.L.*, et al.* Sterilization of granulomas is common in active and latent tuberculosis despite within-host variability in bacterial killing. *Nat Med* **20**, 75-79 (2014).

42. Flynn, J.L., *et al.* An essential role for interferon gamma in resistance to Mycobacterium tuberculosis infection. *The Journal of Experimental Medicine* **178**, 2249-2254 (1993).
43. Flynn, J.L., *et al.* Tumor necrosis factor-α is required in the protective immune response against mycobacterium tuberculosis in mice. *Immunity* **2**, 561-572 (1995).
44. Hunter, R.L., Jagannath, C. & Actor, J.K. Pathology of postprimary tuberculosis in humans and mice: Contradiction of long-held beliefs. *Tuberculosis* **87**, 267-278 (2007).
45. Kim, M.J., *et al.* Caseation of human tuberculosis granulomas correlates with elevated host lipid metabolism. *EMBO Mol Med* **2**, 258-274 (2010).
46. Grosset, J.H., Singer, T.G. & Bishai, W.R. New drugs for the treatment of tuberculosis: hope and reality. *The International Journal of Tuberculosis and Lung Disease* **16**, 1005-1014 (2012).
47. Rhoades, E.R., Frank, A.A. & Orme, I.M. Progression of chronic pulmonary tuberculosis in mice aerogenically infected with virulent Mycobacterium tuberculosis. *Tubercle and Lung Disease* **78**, 57-66 (1997).
48. Tsenova, L., Sokol, K., Victoria, H.F. & Kaplan, G. A Combination of Thalidomide plus Antibiotics Protects Rabbits from Mycobacterial Meningitis-Associated Death. *Journal of Infectious Diseases* **177**, 1563-1572 (1998).
49. Tsenova, L., Bergtold, A., Freedman, V.H., Young, R.A. & Kaplan, G. Tumor necrosis factor α is a determinant of pathogenesis and disease progression in mycobacterial infection in the central nervous system. *Proceedings of the National Academy of Sciences* **96**, 5657-5662 (1999).
50. Tsenova, L., *et al.* Virulence of Selected Mycobacterium tuberculosis Clinical Isolates in the Rabbit Model of Meningitis Is Dependent on Phenolic Glycolipid Produced by the Bacilli. *Journal of Infectious Diseases* **192**, 98-106 (2005).
51. Capuano III, S.V., *et al.* Experimental Mycobacterium tuberculosis infection of cynomolgus macaques closely resembles the various manifestations of human M. tuberculosis infection. *Infection and Immunity* **71**, 5831-5844 (2003).
52. Via, L.E., *et al.* Differential Virulence and Disease Progression following Mycobacterium tuberculosis Complex Infection of the Common Marmoset (Callithrix jacchus). *Infection and Immunity* **81**, 2909-2919 (2013).
53. Flynn, J.L. Lessons from experimental Mycobacterium tuberculosis infections. *Microbes and Infection* **8**, 1179-1188 (2006).
54. Tobin, D.M., *et al.* The lta4h Locus Modulates Susceptibility to Mycobacterial Infection in Zebrafish and Humans. *Cell* **140**, 717-730 (2010).
55. Roca, Francisco J. & Ramakrishnan, L. TNF Dually Mediates Resistance and Susceptibility to Mycobacteria via Mitochondrial Reactive Oxygen Species. *Cell* **153**, 521-534 (2013).
56. Tobin, David M., *et al.* Host Genotype-Specific Therapies Can Optimize the Inflammatory Response to Mycobacterial Infections. *Cell* **148**, 434-446 (2012).
57. Doz, E., *et al.* Acylation Determines the Toll-like receptor (TLR)-dependent Positive Versus TLR2-, Mannose Receptor-, and SIGNR1-independent Negative Regulation of Pro-inflammatory Cytokines by Mycobacterial Lipomannan. *Journal of Biological Chemistry* **282**, 26014-26025 (2007).
58. Noss, E.H., *et al.* Toll-Like Receptor 2-Dependent Inhibition of Macrophage Class II MHC Expression and Antigen Processing by 19-kDa Lipoprotein of Mycobacterium tuberculosis. *The Journal of Immunology* **167**, 910-918 (2001).

59. Means, T.K., *et al.* Differential Effects of a Toll-Like Receptor Antagonist on Mycobacterium tuberculosis-Induced Macrophage Responses. *The Journal of Immunology* **166**, 4074-4082 (2001).
60. Drennan, M.B., *et al.* Toll-Like Receptor 2-Deficient Mice Succumb to Mycobacterium tuberculosis Infection. *The American Journal of Pathology* **164**, 49-57 (2004).
61. Abel, B., *et al.* Toll-Like Receptor 4 Expression Is Required to Control Chronic Mycobacterium tuberculosis Infection in Mice. *The Journal of Immunology* **169**, 3155-3162 (2002).
62. Bafica, A., *et al.* TLR9 regulates Th1 responses and cooperates with TLR2 in mediating optimal resistance to Mycobacterium tuberculosis. *The Journal of Experimental Medicine* **202**, 1715-1724 (2005).
63. Hölscher, C., *et al.* Containment of aerogenic Mycobacterium tuberculosis infection in mice does not require MyD88 adaptor function for TLR2, -4 and -9. *European Journal of Immunology* **38**, 680-694 (2008).
64. Coulombe, F., *et al.* Increased NOD2-mediated recognition of N-glycolyl muramyl dipeptide. *The Journal of Experimental Medicine* **206**, 1709-1716 (2009).
65. Divangahi, M., *et al.* NOD2-Deficient Mice Have Impaired Resistance to Mycobacterium tuberculosis Infection through Defective Innate and Adaptive Immunity. *The Journal of Immunology* **181**, 7157-7165 (2008).
66. Schenk, M., *et al.* NOD2 triggers an interleukin-32-dependent human dendritic cell program in leprosy. *Nat Med* **18**, 555-563 (2012).
67. Netea, M.G., *et al. Mycobacterium tuberculosis* Induces Interleukin-32 Production through a Caspase- 1/IL-18/Interferon-γ-Dependent Mechanism. *PLoS Med* **3**, e277 (2006).
68. Bai, X., *et al.* IL-32 Is a Host Protective Cytokine against Mycobacterium tuberculosis in Differentiated THP-1 Human Macrophages. *The Journal of Immunology* **184**, 3830-3840 (2010).
69. Divangahi, M., *et al.* Mycobacterium tuberculosis evades macrophage defenses by inhibiting plasma membrane repair. *Nat Immunol* **10**, 899-906 (2009).
70. Divangahi, M., Desjardins, D., Nunes-Alves, C., Remold, H.G. & Behar, S.M. Eicosanoid pathways regulate adaptive immunity to Mycobacterium tuberculosis. *Nat Immunol* **11**, 751-758 (2010).
71. Hinchey, J., *et al.* Enhanced priming of adaptive immunity by a proapoptotic mutant of Mycobacterium tuberculosis. *The Journal of Clinical Investigation* **117**, 2279-2288 (2007).
72. Winau, F., *et al.* Apoptotic Vesicles Crossprime CD8 T Cells and Protect against Tuberculosis. *Immunity* **24**, 105-117 (2006).
73. Schaible, U.E., *et al.* Apoptosis facilitates antigen presentation to T lymphocytes through MHC-I and CD1 in tuberculosis. *Nat Med* **9**, 1039-1046 (2003).
74. Maertzdorf, J., *et al.* Human gene expression profiles of susceptibility and resistance in tuberculosis. *Genes Immun* **12**, 15-22 (2011).
75. Dinarello, C.A. Immunological and Inflammatory Functions of the Interleukin-1 Family. *Annual Review of Immunology* **27**, 519-550 (2009).
76. Latz, E., Xiao, T.S. & Stutz, A. Activation and regulation of the inflammasomes. *Nat Rev Immunol* **13**, 397-411 (2013).

77. Juffermans, N.P.*, et al.* Interleukin-1 Signaling Is Essential for Host Defense during Murine Pulmonary Tuberculosis. *Journal of Infectious Diseases* **182**, 902-908 (2000).
78. Walter, K., Hölscher, C., Tschopp, J. & Ehlers, S. NALP3 is not necessary for early protection against experimental tuberculosis. *Immunobiology* **215**, 804-811 (2010).
79. Schneider, B.E.*, et al.* A role for IL-18 in protective immunity against Mycobacterium tuberculosis. *European Journal of Immunology* **40**, 396-405 (2010).
80. Wieland, C.W., van der Windt, G.J.W., Florquin, S., McKenzie, A.N.J. & van der Poll, T. ST2 deficient mice display a normal host defense against pulmonary infection with Mycobacterium tuberculosis. *Microbes and Infection* **11**, 524-530 (2009).
81. Yamada, H., Mizumo, S., Horai, R., Iwakura, Y. & Sugawara, I. Protective Role of Interleukin-1 in Mycobacterial Infection in IL-1 α/β Double-Knockout Mice. *Lab Invest* **80**, 759-767 (2000).
82. Sugawara, I., Yamada, H., Hua, S.C. & Mizuno, S. Role of interleukin (IL)-1 type 1 receptor in mycobacterial infection. *Microbiol. Immunol.* **45**, 743-750 (2001).
83. Mayer-Barber, K.D.*, et al.* Cutting Edge: Caspase-1 Independent IL-1β Production Is Critical for Host Resistance to Mycobacterium tuberculosis and Does Not Require TLR Signaling In Vivo. *The Journal of Immunology* **184**, 3326-3330 (2010).
84. Bellamy, R.*, et al.* Assessment of the interleukin 1 gene cluster and other candidate gene polymorphisms in host susceptibility to tuberculosis. *Tubercle and Lung Disease* **79**, 83-89 (1998).
85. Gomez, L.M.*, et al.* Analysis of IL1B, TAP1, TAP2 and IKBL polymorphisms on susceptibility to tuberculosis. *Tissue Antigens* **67**, 290-296 (2006).
86. Koo, I.C.*, et al.* ESX-1-dependent cytolysis in lysosome secretion and inflammasome activation during mycobacterial infection. *Cellular Microbiology* **10**, 1866-1878 (2008).
87. TeKippe, E.M.*, et al.* Granuloma Formation and Host Defense in Chronic Mycobacterium tuberculosis Infection Requires PYCARD/ASC but Not NLRP3 or Caspase-1. *PLoS One* **5**, e12320 (2010).
88. Roach, D.R.*, et al.* TNF Regulates Chemokine Induction Essential for Cell Recruitment, Granuloma Formation, and Clearance of Mycobacterial Infection. *The Journal of Immunology* **168**, 4620-4627 (2002).
89. Keane, J.*, et al.* Tuberculosis Associated with Infliximab, a Tumor Necrosis Factor α–Neutralizing Agent. *New England Journal of Medicine* **345**, 1098-1104 (2001).
90. Trinchieri, G., Pflanz, S. & Kastelein, R.A. The IL-12 Family of Heterodimeric Cytokines: New Players in the Regulation of T Cell Responses. *Immunity* **19**, 641-644 (2003).
91. Filipe-Santos, O.*, et al.* Inborn errors of IL-12/23- and IFN-γ-mediated immunity: molecular, cellular, and clinical features. *Seminars in Immunology* **18**, 347-361 (2006).
92. Altare, F.*, et al.* Impairment of Mycobacterial Immunity in Human Interleukin-12 Receptor Deficiency. *Science* **280**, 1432-1435 (1998).
93. Khader, S.A.*, et al.* Interleukin 12p40 is required for dendritic cell migration and T cell priming after Mycobacterium tuberculosis infection. *The Journal of Experimental Medicine* **203**, 1805-1815 (2006).
94. Robinson, R.T.*, et al.* Mycobacterium tuberculosis infection induces il12rb1 splicing to generate a novel IL-12Rβ1 isoform that enhances DC migration. *The Journal of Experimental Medicine* **207**, 591-605 (2010).

95. Cooper, A.M., *et al.* Mice Lacking Bioactive IL-12 Can Generate Protective, Antigen-Specific Cellular Responses to Mycobacterial Infection Only if the IL-12 p40 Subunit Is Present. *The Journal of Immunology* **168**, 1322-1327 (2002).
96. Khader, S.A., *et al.* IL-23 Compensates for the Absence of IL-12p70 and Is Essential for the IL-17 Response during Tuberculosis but Is Dispensable for Protection and Antigen-Specific IFN-γ Responses if IL-12p70 Is Available. *The Journal of Immunology* **175**, 788-795 (2005).
97. Feng, C.G., *et al.* Maintenance of Pulmonary Th1 Effector Function in Chronic Tuberculosis Requires Persistent IL-12 Production. *The Journal of Immunology* **174**, 4185-4192 (2005).
98. Dalton, D., *et al.* Multiple defects of immune cell function in mice with disrupted interferon-gamma genes. *Science* **259**, 1739-1742 (1993).
99. Cooper, A.M., *et al.* Disseminated tuberculosis in interferon gamma gene-disrupted mice. *The Journal of Experimental Medicine* **178**, 2243-2247 (1993).
100. Ottenhoff, T.H.M., Kumararatne, D. & Casanova, J.-L. Novel human immunodeficiencies reveal the essential role of type-1 cytokines in immunity to intracellular bacteria. *Immunology Today* **19**, 491-494 (1998).
101. Ting, L.-M., Kim, A.C., Cattamanchi, A. & Ernst, J.D. Mycobacterium tuberculosis Inhibits IFN-γ Transcriptional Responses Without Inhibiting Activation of STAT1. *The Journal of Immunology* **163**, 3898-3906 (1999).
102. Feng, C.G., *et al.* NK Cell-Derived IFN-γ Differentially Regulates Innate Resistance and Neutrophil Response in T Cell-Deficient Hosts Infected with Mycobacterium tuberculosis. *The Journal of Immunology* **177**, 7086-7093 (2006).
103. Sada-Ovalle, I., Chiba, A., Gonzales, A., Brenner, M.B. & Behar, S.M. Innate Invariant NKT Cells Recognize Mycobacterium tuberculosis Infected Macrophages, Produce Interferon-γ, and Kill Intracellular Bacteria. *PLoS Pathog* **4**, e1000239 (2008).
104. D'Souza, C., *et al.* An anti-inflammatory role for gamma delta T lymphocytes in acquired immunity to Mycobacterium tuberculosis. *The Journal of Immunology* **158**, 1217-1221 (1997).
105. Junqueira-Kipnis, A.P., *et al.* NK Cells Respond to Pulmonary Infection with Mycobacterium tuberculosis, but Play a Minimal Role in Protection. *The Journal of Immunology* **171**, 6039-6045 (2003).
106. Manca, C., *et al.* Virulence of a Mycobacterium tuberculosis clinical isolate in mice is determined by failure to induce Th1 type immunity and is associated with induction of IFN-α/β. *Proceedings of the National Academy of Sciences* **98**, 5752-5757 (2001).
107. Ordway, D., *et al.* The Hypervirulent Mycobacterium tuberculosis Strain HN878 Induces a Potent TH1 Response followed by Rapid Down-Regulation. *The Journal of Immunology* **179**, 522-531 (2007).
108. Antonelli, L.R.V., *et al.* Intranasal Poly-IC treatment exacerbates tuberculosis in mice through the pulmonary recruitment of a pathogen-permissive monocyte/macrophage population. *The Journal of Clinical Investigation* **120**, 1674-1682 (2010).
109. Berry, M.P.R., *et al.* An interferon-inducible neutrophil-driven blood transcriptional signature in human tuberculosis. *Nature* **466**, 973-977 (2010).
110. Flynn, J.L. & Chan, J. Immunology of Tuberculosis. *Annual Review of Immunology* **19**, 93-129 (2001).

111. Srivastava, S. & Ernst, J.D. Cutting Edge: Direct Recognition of Infected Cells by CD4 T Cells Is Required for Control of Intracellular Mycobacterium tuberculosis In Vivo. *The Journal of Immunology* **191**, 1016-1020 (2013).
112. Lawn, S.D., Myer, L., Edwards, D., Bekker, L.-G. & Wood, R. Short-term and long-term risk of tuberculosis associated with CD4 cell recovery during antiretroviral therapy in South Africa. *AIDS* **23**, 1717-1725 (2009).
113. Jones, B.*, et al.* Relationship of the manifestations of tuberculosis to CD4 cell counts in patients with human immunodeficiency virus infection. *The American review of respiratory disease* **148**, 1292-1297 (1993).
114. Turner, J.*, et al.* CD8- and CD95/95L-Dependent Mechanisms of Resistance in Mice with Chronic Pulmonary Tuberculosis. *American Journal of Respiratory Cell and Molecular Biology* **24**, 203-209 (2001).
115. Turner, J. & Dockrell, H.M. Stimulation of human peripheral blood mononuclear cells with live Mycobacterium bovis BCG activates cytolytic CD8+ T cells in vitro. *Immunology* **87**, 339-342 (1996).
116. Tan, J.S.*, et al.* Human alveolar T lymphocyte responses to Mycobacterium tuberculosis antigens: role for CD4+ and CD8+ cytotoxic T cells and relative resistance of alveolar macrophages to lysis. *The Journal of Immunology* **159**, 290-297 (1997).
117. Kaufmann, S.H.E. CD8+ T lymphocytes in intracellular microbial infections. *Immunology Today* **9**, 168-174 (1988).
118. Martin, Constance J.*, et al.* Efferocytosis Is an Innate Antibacterial Mechanism. *Cell Host & Microbe* **12**, 289-300 (2012).
119. Bilaçeroglu, S., Perim, K., Büyükirin, M. & Çelikten, E. Prednisolone: a beneficial and safe adjunct to antituberculosis treatment? A randomized controlled trial. *The International Journal of Tuberculosis and Lung Disease* **3**, 47-54 (1999).
120. Wollis, R.S.*, et al.* A study of the safety, immunology, virology, and microbiology of adjunctive etanercept in HIV-1-associated tuberculosis. *AIDS.* **18**, 257-264 (2004).
121. Tramontana, J.M.*, et al.* Thalidomide treatment reduces tumor necrosis factor alpha production and enhances weight gain in patients with pulmonary tuberculosis. *Mol Med* **1**, 384-397 (1995).
122. Johnson, B.J.*, et al.* rhulL-2 adjunctive therapy in multidrug resistant tuberculosis: A comparison of two treatment regimens and placebo. *Tubercle and Lung Disease* **78**, 195-203 (1997).
123. Grahmann, P.R. & Braun, R.K. A new protocol for multiple inhalation of IFN- successfully treats MDR-TB: a case study. *The International Journal of Tuberculosis and Lung Disease* **12**, 636-644 (2008).
124. Deeb, K.K., Trump, D.L. & Johnson, C.S. Vitamin D signalling pathways in cancer: potential for anticancer therapeutics. *Nat Rev Cancer* **7**, 684-700 (2007).
125. White, J.H. Vitamin D Signaling, Infectious Diseases, and Regulation of Innate Immunity. *Infect Immun.* **76**, 3837-3843 (2008).
126. Tavera-Mendoza, L.a.W., J.H. Cell defenses and the sunshine vitamin. *Scientific American* **297**, 62-72 (2007).
127. Holick, M.F. Vitamin D Deficiency. *N Engl J Med* **357**, 266-281 (2007).
128. Cheng, J.B., Levine, M.A., Bell, N.H., Mangelsdorf, D.J. & Russell, D.W. Genetic evidence that the human CYP2R1 enzyme is a key vitamin D 25-hydroxylase. *Proc Natl Acad Sci U S A* **101**, 7711-7715 (2004).

129. Prosser, D.E. & Jones, G. Enzymes involved in the activation and inactivation of vitamin D. *Trends Biochem Sci* **29**, 664-673 (2004).
130. Shinkyo, R., Sakaki, T., Kamakura, M., Ohta, M. & Inouye, K. Metabolism of vitamin D by human microsomal CYP2R1. *Biochem Biophys Res Commun* **324**, 451-457 (2004).
131. Chawla, A., Repa, J.J., Evans, R.M. & Mangelsdorf, D.J. Nuclear receptors and lipid physiology: opening the X-files. *Science* **294**, 1866-1870 (2001).
132. Rochel, N., Wurtz, J.M., Mitschler, A., Klaholz, B. & Moras, D. The crystal structure of the nuclear receptor for vitamin D bound to its natural ligand. *Mol Cell* **5**, 173-179 (2000).
133. Lin, R. & White, J.H. The pleiotropic actions of vitamin D. *BioEssays* **26**, 21-28 (2004).
134. Tavera-Mendoza, L.*, et al.* Convergence of vitamin D and retinoic acid signalling at a common hormone response element. *EMBO Rep* **7**, 180-185 (2006).
135. Wayse, V., Yousafzai, A., Mogale, K. & Filteau, S. Association of subclinical vitamin D deficiency with severe acute lower respiratory infection in Indian children under 5[thinsp]y. *Eur J Clin Nutr* **58**, 563-567 (0000).
136. Urashima, M.*, et al.* Randomized trial of vitamin D supplementation to prevent seasonal influenza A in schoolchildren. *The American Journal of Clinical Nutrition* **91**, 1255-1260 (2010).
137. Li-Ng, M.*, et al.* A randomized controlled trial of vitamin D3 supplementation for the prevention of symptomatic upper respiratory tract infections. *Epidemiology & Infection* **137**, 1396-1404 (2009).
138. Muhe, L., Lulseged, S., Mason, K.E. & Simoes, E.A.F. Case-control study of the role of nutritional rickets in the risk of developing pneumonia in Ethiopian children. *The Lancet* **349**, 1801-1804 (1997).
139. Manaseki-Holland, S.*, et al.* Effect on the incidence of pneumonia of vitamin D supplementation by quarterly bolus dose to infants in Kabul: a randomised controlled superiority trial. *Lancet* **379**, 1419-1427 (2012).
140. Lai, Y. & Gallo, R.L. AMPed up immunity: how antimicrobial peptides have multiple roles in immune defense. *Trends in Immunology* **30**, 131-141 (2009).
141. Wang, T.-T.*, et al.* Cutting Edge: 1,25-Dihydroxyvitamin D3 Is a Direct Inducer of Antimicrobial Peptide Gene Expression. *J Immunol* **173**, 2909-2912 (2004).
142. Gombart, A., Borregaard, N. & Koeffler, H. Human cathelicidin antimicrobial peptide (CAMP) gene is a direct target of the vitamin D receptor and is strongly up-regulated in myeloid cells by 1,25-dihydroxyvitamin D3. *FASEB J* **19**, 1067 - 1077 (2005).
143. Liu, P.T.*, et al.* Toll-Like Receptor Triggering of a Vitamin D-Mediated Human Antimicrobial Response. *Science* **311**, 1770-1773 (2006).
144. Weber, G.*, et al.* Vitamin D Induces the Antimicrobial Protein hCAP18 in Human Skin. *J Investig Dermatol* **124**, 1080-1082 (2005).
145. Lapaquette, P., Glasser, A.-L., Huett, A., Xavier, R.J. & Darfeuille-Michaud, A. Crohn's disease-associated adherent-invasive E.coli are selectively favoured by impaired autophagy to replicate intracellularly. *Cellular Microbiology* **12**, 99-113 (2010).
146. Masten, A.R. Sunlight in Tuberculosis. *Chest* **1**, 8-23 (1935).
147. Chan, T.Y.K. Vitamin D Deficiency and Susceptibility to Tuberculosis. *Calcified Tissue International* **66**, 476-478 (2000).
148. Davies, P.D., Brown, R.C. & Woodhead, J.S. Serum concentrations of vitamin D metabolites in untreated tuberculosis. *Thorax* **40**, 187-190 (1985).

149. Sita-Lumsden, A., Lapthorn, G., Swaminathan, R. & Milburn, H.J. Reactivation of tuberculosis and vitamin D deficiency: the contribution of diet and exposure to sunlight. *Thorax* **62**, 1003-1007 (2007).
150. Nnoaham, K.E. & Clarke, A. Low serum vitamin D levels and tuberculosis: a systematic review and meta-analysis. *International Journal of Epidemiology* **37**, 113-119 (2008).
151. Chen, C., Liu, Q., Zhu, L., Yang, H. & Lu, W. Vitamin D Receptor Gene Polymorphisms on the Risk of Tuberculosis, a Meta-Analysis of 29 Case-Control Studies. *PLoS ONE* **8**, e83843 (2013).
152. Martineau, A.R., Honecker, F.U., Wilkinson, R.J. & Griffiths, C.J. Vitamin D in the treatment of pulmonary tuberculosis. *The Journal of Steroid Biochemistry and Molecular Biology* **103**, 793-798 (2007).
153. Martineau, A.R.*, et al.* High-dose vitamin D3 during intensive-phase antimicrobial treatment of pulmonary tuberculosis: a double-blind randomised controlled trial. *The Lancet* **377**, 242-250 (2011).
154. Wang, T.-T.*, et al.* Direct and Indirect Induction by 1,25-Dihydroxyvitamin D3 of the NOD2/CARD15-Defensin β2 Innate Immune Pathway Defective in Crohn Disease. *Journal of Biological Chemistry* **285**, 2227-2231 (2010).
155. White, J.H. Vitamin D metabolism and signaling in the immune system. *Reviews in Endocrine & Metabolic Disorders* **13**, 21-29 (2012).
156. Szeles, L.*, et al.* 1,25-Dihydroxyvitamin D(3) Is an Autonomous Regulator of the Transcriptional Changes Leading to a Tolerogenic Dendritic Cell Phenotype. *Journal of Immunology* **182**, 2074-2083 (2009).
157. Kisich, K.O., Heifets, L., Higgins, M. & Diamond, G. Antimycobacterial Agent Based on mRNA Encoding Human β-Defensin 2 Enables Primary Macrophages To Restrict Growth ofMycobacterium tuberculosis. *Infection and Immunity* **69**, 2692-2699 (2001).
158. Martineau, A.R.*, et al.* Neutrophil-mediated innate immune resistance to mycobacteria. *The Journal of Clinical Investigation* **117**, 1988-1994 (2007).
159. Liu, P.T., Stenger, S., Tang, D.H. & Modlin, R.L. Cutting Edge: Vitamin D-Mediated Human Antimicrobial Activity against Mycobacterium tuberculosis Is Dependent on the Induction of Cathelicidin. *J Immunol* **179**, 2060-2063 (2007).
160. Fabri, M.*, et al.* Vitamin D Is Required for IFN-γ–Mediated Antimicrobial Activity of Human Macrophages. *Science Translational Medicine* **3**, 104ra102 (2011).
161. Locasale, Jason W. & Cantley, Lewis C. Metabolic Flux and the Regulation of Mammalian Cell Growth. *Cell Metab.* **14**, 443-451 (2011).
162. Vander Heiden, M.G., Cantley, L.C. & Thompson, C.B. Understanding the Warburg effect: the metabolic requirements of cell proliferation. *Science (New York, N.Y.)* **324**, 1029-1033 (2009).
163. Pearce, Erika L. & Pearce, Edward J. Metabolic Pathways in Immune Cell Activation and Quiescence. *Immunity* **38**, 633-643 (2013).
164. Rodríguez-Prados, J.-C.*, et al.* Substrate Fate in Activated Macrophages: A Comparison between Innate, Classic, and Alternative Activation. *The Journal of Immunology* **185**, 605-614 (2010).
165. Haschemi, A.*, et al.* The Sedoheptulose Kinase CARKL Directs Macrophage Polarization through Control of Glucose Metabolism. *Cell Metab.* **15**, 813-826 (2012).
166. Aktan, F. iNOS-mediated nitric oxide production and its regulation. *Life Sciences* **75**, 639-653 (2004).

167. West, A.P., *et al.* TLR signalling augments macrophage bactericidal activity through mitochondrial ROS. *Nature* **472**, 476-480 (2011).
168. Sorbara, M.T. & Girardin, S.E. Mitochondrial ROS fuel the inflammasome. *Cell Res* **21**, 558-560 (2011).
169. Tschopp, J. & Schroder, K. NLRP3 inflammasome activation: the convergence of multiple signalling pathways on ROS production? *Nat Rev Immunol* **10**, 210-215 (2010).
170. Beste, D.J.V., *et al.* 13C Metabolic Flux Analysis Identifies an Unusual Route for Pyruvate Dissimilation in Mycobacteria which Requires Isocitrate Lyase and Carbon Dioxide Fixation. *PLoS Pathog* **7**, e1002091 (2011).
171. de Carvalho, L.P.S., *et al.* Metabolomics of Mycobacterium tuberculosis Reveals Compartmentalized Co-Catabolism of Carbon Substrates. *Chemistry & Biology* **17**, 1122-1131 (2010).
172. Beste, Dany J.V., *et al.* 13C-Flux Spectral Analysis of Host-Pathogen Metabolism Reveals a Mixed Diet for Intracellular Mycobacterium tuberculosis. *Chemistry & Biology* **20**, 1012-1021 (2013).
173. Munoz-Elias, E.J. & McKinney, J.D. Mycobacterium tuberculosis isocitrate lyases 1 and 2 are jointly required for in vivo growth and virulence. *Nat Med* **11**, 638-644 (2005).
174. Pandey, A.K. & Sassetti, C.M. Mycobacterial persistence requires the utilization of host cholesterol. *Proceedings of the National Academy of Sciences* **105**, 4376-4380 (2008).
175. Lee, W., VanderVen, B.C., Fahey, R.J. & Russell, D.G. Intracellular Mycobacterium tuberculosis Exploits Host-derived Fatty Acids to Limit Metabolic Stress. *Journal of Biological Chemistry* **288**, 6788-6800 (2013).
176. Watanabe, S., *et al.* Fumarate Reductase Activity Maintains an Energized Membrane in Anaerobic Mycobacterium tuberculosis. *PLoS Pathog* **7**, e1002287 (2011).
177. Tullius, M.V., Harth, G. & Horwitz, M.A. Glutamine Synthetase GlnA1 Is Essential for Growth of Mycobacterium tuberculosis in Human THP-1 Macrophages and Guinea Pigs. *Infection and Immunity* **71**, 3927-3936 (2003).
178. Hondalus, M.K., *et al.* Attenuation of and Protection Induced by a Leucine Auxotroph of Mycobacterium tuberculosis. *Infection and Immunity* **68**, 2888-2898 (2000).
179. Smith, D.A., Parish, T., Stoker, N.G. & Bancroft, G.J. Characterization of Auxotrophic Mutants ofMycobacterium tuberculosis and Their Potential as Vaccine Candidates. *Infection and Immunity* **69**, 1142-1150 (2001).
180. Lee, S., *et al.* Protection Elicited by Two Glutamine Auxotrophs of Mycobacterium tuberculosis and In Vivo Growth Phenotypes of the Four Unique Glutamine Synthetase Mutants in a Murine Model. *Infection and Immunity* **74**, 6491-6495 (2006).
181. Awasthy, D., *et al.* Inactivation of the ilvB1 gene in Mycobacterium tuberculosis leads to branched-chain amino acid auxotrophy and attenuation of virulence in mice. *Microbiology* **155**, 2978-2987 (2009).
182. McAdam, R.A., *et al.* In vivo growth characteristics of leucine and methionine auxotrophic mutants of Mycobacterium bovis BCG generated by transposon mutagenesis. *Infection and Immunity* **63**, 1004-1012 (1995).
183. Brzostek, A., Pawelczyk, J., Rumijowska-Galewicz, A., Dziadek, B. & Dziadek, J. Mycobacterium tuberculosis Is Able To Accumulate and Utilize Cholesterol. *Journal of Bacteriology* **191**, 6584-6591 (2009).

184. Griffin, Jennifer E.*, et al.* Cholesterol Catabolism by Mycobacterium tuberculosis Requires Transcriptional and Metabolic Adaptations. *Chemistry & Biology* **19**, 218-227 (2012).
185. Singh, V.*, et al.* Mycobacterium tuberculosis-Driven Targeted Recalibration of Macrophage Lipid Homeostasis Promotes the Foamy Phenotype. *Cell Host & Microbe* **12**, 669-681 (2012).
186. Martens, G.W.*, et al.* Hypercholesterolemia Impairs Immunity to Tuberculosis. *Infection and Immunity* **76**, 3464-3472 (2008).
187. Owen, M.R., Doran, E. & Halestrap, A.P. Evidence that metformin exerts its anti-diabetic effects through inhibition of complex 1 of the mitochondrial respiratory chain. *Biochemical Journal* **348**, 607-614 (2000).
188. El-Mir, M.Y.*, et al.* Dimethylbiguanide inhibits cell respiration via an indirect effect targeted on the respiratory chain complex I. *Journal of Biological Chemistry* **275**, 223-228 (2000).
189. Chan, N.N., Brain, H.P.S. & Feher, M.D. Metformin-associated lactic acidosis: a rare or very rare clinical entity? *Diabetic Medicine* **16**, 273-281 (1999).
190. Gong, L., Goswami, S., Giacomini, K., Altman, R. & Klein, T. Metformin pathways: pharmacokinetics and pharmacodynamics. *Pharmacogenetics and Genomics* **22**, 820-827 (2012).
191. Shu, Y.*, et al.* Effect of genetic variation in the organic cation transporter 1 (OCT1) on metformin action. *The Journal of Clinical Investigation* **117**, 1422-1431 (2007).
192. Jeon, C.Y. & Murray, M.B. Diabetes Mellitus Increases the Risk of Active Tuberculosis: A Systematic Review of 13 Observational Studies. *PLoS Med* **5**, e152 (2008).
193. Sullivan, T. & Ben Amor, Y. The Co-Management of Tuberculosis and Diabetes: Challenges and Opportunities in the Developing World. *PLoS Med* **9**, e1001269 (2012).
194. WHO. Global Tuberculosis Report 2012. (2012).
195. Nunes-Alves, C.*, et al.* In search of a new paradigm for protective immunity to TB. *Nat Rev Micro* **12**, 289-299 (2014).
196. O'Neill, L.A.J., Golenbock, D. & Bowie, A.G. The history of Toll-like receptors [mdash] redefining innate immunity. *Nat Rev Immunol* **13**, 453-460 (2013).
197. Behar, S.M.*, et al.* Apoptosis is an innate defense function of macrophages against Mycobacterium tuberculosis. *Mucosal Immunol* **4**, 279-287 (2011).
198. Lamkanfi, M. Emerging inflammasome effector mechanisms. *Nat Rev Immunol* **11**, 213-220 (2011).
199. Behar, S.M., Martin, C.J., Nunes-Alves, C., Divangahi, M. & Remold, H.G. Lipids, apoptosis, and cross-presentation: links in the chain of host defense against Mycobacterium tuberculosis. *Microbes and Infection* **13**, 749-756 (2011).
200. O'Neill, L.A.J. & Hardie, D.G. Metabolism of inflammation limited by AMPK and pseudo-starvation. *Nature* **493**, 346-355 (2013).
201. Viollet, B.*, et al.* Cellular and molecular mechanisms of metformin: an overview. *Clinical Science* **122**, 253-270 (2012).
202. Dye, C. Global epidemiology of tuberculosis. *The Lancet* **367**, 938-940 (2006).
203. Keeler, E.*, et al.* Reducing the global burden of tuberculosis: the contribution of improved diagnostics. *Nature* **444 Suppl 1**, 49-57 (2006).

204. Fremond, C.M., *et al.* IL-1 Receptor-Mediated Signal Is an Essential Component of MyD88-Dependent Innate Response to Mycobacterium tuberculosis Infection. *The Journal of Immunology* **179**, 1178-1189 (2007).
205. Hornung, V., *et al.* AIM2 recognizes cytosolic dsDNA and forms a caspase-1-activating inflammasome with ASC. *Nature* **458**, 514-518 (2009).
206. Tsuchiya, K., *et al.* Involvement of Absent in Melanoma 2 in Inflammasome Activation in Macrophages Infected with Listeria monocytogenes. *J Immunol* **185**, 1186-1195 (2010).
207. Warren, S.E., *et al.* Cutting Edge: Cytosolic Bacterial DNA Activates the Inflammasome via Aim2. *J Immunol* **185**, 818-821 (2010).
208. Fernandes-Alnemri, T., *et al.* The AIM2 inflammasome is critical for innate immunity to Francisella tularensis. *Nat Immunol* **11**, 385-393 (2010).
209. Rathinam, V.A.K., *et al.* The AIM2 inflammasome is essential for host defense against cytosolic bacteria and DNA viruses. *Nat Immunol* **11**, 395-402 (2010).
210. Ogura, Y., *et al.* Nod2, a Nod1/Apaf-1 Family Member That Is Restricted to Monocytes and Activates NF-κB. *Journal of Biological Chemistry* **276**, 4812-4818 (2001).
211. Hsu, L.-C., *et al.* A NOD2–NALP1 complex mediates caspase-1-dependent IL-1β secretion in response to Bacillus anthracis infection and muramyl dipeptide. *Proceedings of the National Academy of Sciences* **105**, 7803-7808 (2008).
212. Yang, C.-S., Shin, D.-M. & Jo, E.-K. The Role of NLR-related Protein 3 Inflammasome in Host Defense and Inflammatory Diseases. *Int Neurourol J* **16**, 2-12 (2012).
213. Campbell, G.R. & Spector, S.A. Vitamin D Inhibits Human Immunodeficiency Virus Type 1 and Mycobacterium tuberculosis Infection in Macrophages through the Induction of Autophagy. *PLoS Pathog* **8**, e1002689 (2012).
214. Master, S.S., *et al.* Mycobacterium tuberculosis Prevents Inflammasome Activation. *Cell Host & Microbe* **3**, 224-232 (2008).
215. Wang, T.-T., *et al.* Large-Scale in Silico and Microarray-Based Identification of Direct 1,25-Dihydroxyvitamin D3 Target Genes. *Mol Endocrinol* **19**, 2685-2695 (2005).
216. Zella, L.A., Kim, S., Shevde, N.K. & Pike, J.W. Enhancers Located within Two Introns of the Vitamin D Receptor Gene Mediate Transcriptional Autoregulation by 1,25-Dihydroxyvitamin D3. *Mol Endocrinol* **20**, 1231-1247 (2006).
217. Kent, W.J., *et al.* The Human Genome Browser at UCSC. *Genome Research* **12**, 996-1006 (2002).
218. Gupta, U.D. & Katoch, V.M. Animal models of tuberculosis. *Tuberculosis* **85**, 277-293 (2005).
219. Bryan, N.B., Dorfleutner, A., Rojanasakul, Y. & Stehlik, C. Activation of Inflammasomes Requires Intracellular Redistribution of the Apoptotic Speck-Like Protein Containing a Caspase Recruitment Domain. *The Journal of Immunology* **182**, 3173-3182 (2009).
220. Matsushita, K., *et al.* A Splice Variant of ASC Regulates IL-1β Release and Aggregates Differently from Intact ASC. *Mediators of Inflammation* **2009**(2009).
221. Schroder, K. & Tschopp, J. The Inflammasomes. *Cell* **140**, 821-832 (2010).
222. TeKippe, E.M., *et al.* Granuloma Formation and Host Defense in Chronic Mycobacterium tuberculosis Infection Requires PYCARD/ASC but Not NLRP3 or Caspase-1. *PLoS One* **5**(2010).

223. Brooks, M.N., *et al.* NOD2 controls the nature of the inflammatory response and subsequent fate of Mycobacterium tuberculosis and M. bovis BCG in human macrophages. *Cellular Microbiology* **13**, 402-418 (2011).
224. Ippagunta, S.K., *et al.* The inflammasome adaptor ASC regulates the function of adaptive immune cells by controlling Dock2-mediated Rac activation and actin polymerization. *Nat Immunol* **12**, 1010-1016 (2011).
225. Calderon, M.R., *et al.* Ligand-dependent Corepressor (LCoR) Recruitment by Krüppel-like Factor 6 (KLF6) Regulates Expression of the Cyclin-dependent Kinase Inhibitor CDKN1A Gene. *Journal of Biological Chemistry* **287**, 8662-8674 (2012).
226. Marks, S.M., *et al.* Outcomes of contact investigations of infectious tuberculosis patients. *American Journal of Respiratory and Critical Care Medicine* **162**, 2033-2038 (2000).
227. Holt, P.G., Strickland, D.H., Wikstrom, M.E. & Jahnsen, F.L. Regulation of immunological homeostasis in the respiratory tract. *Nat Rev Immunol* **8**, 142-152 (2008).
228. Li, Y., Wang, Y. & Liu, X. The Role of Airway Epithelial Cells in Response to Mycobacteria Infection. *Clinical and Developmental Immunology* **2012**, 11 (2012).
229. Singh, P.K., *et al.* Production of β-defensins by human airway epithelia. *Proceedings of the National Academy of Sciences* **95**, 14961-14966 (1998).
230. Corrales-Garcia, L., Ortiz, E., Castañeda-Delgado, J., Rivas-Santiago, B. & Corzo, G. Bacterial expression and antibiotic activities of recombinant variants of human β-defensins on pathogenic bacteria and M. tuberculosis. *Protein Expression and Purification*.
231. Thompson, A., *et al.* Immunological functions of the pulmonary epithelium. *European Respiratory Journal* **8**, 127-149 (1995).
232. Liu, P.T., *et al.* Convergence of IL-1β and VDR Activation Pathways in Human TLR2/1-Induced Antimicrobial Responses. *PLoS ONE* **4**, e5810 (2009).
233. Xia, Y. & Zhai, Q. IL-1β enhances the antibacterial activity of astrocytes by activation of NF-κB. *Glia* **58**, 244-252 (2010).
234. Yuk, J.-M., *et al.* Vitamin D3 Induces Autophagy in Human Monocytes/Macrophages via Cathelicidin. **6**, 231-243 (2009).
235. Kolls, J.K., McCray, P.B. & Chan, Y.R. Cytokine-mediated regulation of antimicrobial proteins. *Nat Rev Immunol* **8**, 829-835 (2008).
236. Abreu, M.T. Toll-like receptor signalling in the intestinal epithelium: how bacterial recognition shapes intestinal function. *Nat Rev Immunol* **10**, 131-144 (2010).
237. Coussens, A.K., *et al.* Vitamin D accelerates resolution of inflammatory responses during tuberculosis treatment. *Proceedings of the National Academy of Sciences* (2012).
238. Zumla, A., *et al.* Inflammation and tuberculosis: host-directed therapies. *Journal of Internal Medicine*, n/a-n/a (2014).
239. Sena, Laura A. & Chandel, Navdeep S. Physiological Roles of Mitochondrial Reactive Oxygen Species. *Molecular Cell* **48**, 158-167 (2012).
240. Matsumoto, A., Bessho, H., Uehira, K. & Suda, T. Morphological Studies of the Association of Mitochondria with Chlamydial Inclusions and the Fusion of Chlamydial Inclusions. *Journal of Electron Microscopy* **40**, 356-363 (1991).
241. Miller, J.L., Velmurugan, K., Cowan, M.J. & Briken, V. The Type I NADH Dehydrogenase of Mycobacterium tuberculosis Counters Phagosomal NOX2 Activity to Inhibit TNF-α-Mediated Host Cell Apoptosis. *PLoS Pathog* **6**, e1000864 (2010).

242. Fendt, S.-M.*, et al.* Metformin Decreases Glucose Oxidation and Increases the Dependency of Prostate Cancer Cells on Reductive Glutamine Metabolism. *Cancer Research* **73**, 4429-4438 (2013).
243. Daniel, J., Maamar, H., Deb, C., Sirakova, T.D. & Kolattukudy, P.E. <italic>Mycobacterium tuberculosis</italic> Uses Host Triacylglycerol to Accumulate Lipid Droplets and Acquires a Dormancy-Like Phenotype in Lipid-Loaded Macrophages. *PLoS Pathog* **7**, e1002093 (2011).
244. Hardie, D.G. AMPK: A Target for Drugs and Natural Products With Effects on Both Diabetes and Cancer. *Diabetes* **62**, 2164-2172 (2013).
245. Hardie, G., Carling, D. & Sim, A. The AMP-activated protein kinase: a multisubstrate regulator of lipid metabolism. *Trends in Biochemical Sciences* **14**, 20-23 (1989).
246. Deffert, C., Cachat, J. & Krause, K.-H. Phagocyte NADPH oxidase, chronic granulomatous disease and mycobacterial infections. *Cellular Microbiology* **16**, 1168-1178 (2014).
247. Takayama, K., Wang, C. & Besra, G.S. Pathway to Synthesis and Processing of Mycolic Acids in Mycobacterium tuberculosis. *Clinical Microbiology Reviews* **18**, 81-101 (2005).
248. Riendeau, C.J. & Kornfeld, H. THP-1 Cell Apoptosis in Response to Mycobacterial Infection. *Infection and Immunity* **71**, 254-259 (2003).
249. Parihar, S.P.*, et al.* Statin Therapy Reduces the Mycobacterium tuberculosis Burden in Human Macrophages and in Mice by Enhancing Autophagy and Phagosome Maturation. *Journal of Infectious Diseases* **209**, 754-763 (2014).
250. Kang, Y.A.*, et al.* The effects of statin use on the development of tuberculosis among patients with diabetes mellitus. *The International Journal of Tuberculosis and Lung Disease* **18**, 717-724 (2014).
251. Pathak, S., Awuh, J.A., Leversen, N.A., Flo, T.H. & Åsjø, B. Counting Mycobacteria in Infected Human Cells and Mouse Tissue: A Comparison between qPCR and CFU. *PLoS ONE* **7**, e34931 (2012).
252. Wheelwright, M.*, et al.* All-Trans Retinoic Acid–Triggered Antimicrobial Activity against Mycobacterium tuberculosis Is Dependent on NPC2. *The Journal of Immunology* **192**, 2280-2290 (2014).
253. Faubert, B.*, et al.* AMPK Is a Negative Regulator of the Warburg Effect and Suppresses Tumor Growth In Vivo. *Cell Metab.* **17**, 113-124 (2013).
254. Faubert, B.*, et al.* Loss of the tumor suppressor LKB1 promotes metabolic reprogramming of cancer cells via HIF-1α. *Proceedings of the National Academy of Sciences* **111**, 2554-2559 (2014).
255. Verway, M.*, et al.* Vitamin D Induces Interleukin-1β Expression: Paracrine Macrophage Epithelial Signaling Controls M. tuberculosis Infection. *PLoS Pathog* **9**, e1003407 (2013).
256. Badewa, A.P., Quinton, L.J., Shellito, J.E. & Mason, C.M. Chemokine receptor 5 and its ligands in the immune response to murine tuberculosis. *Tuberculosis* **85**, 185-195 (2005).
257. Nouailles, G.*, et al.* CXCL5-secreting pulmonary epithelial cells drive destructive neutrophilic inflammation in tuberculosis. *The Journal of Clinical Investigation* **124**, 1268-1282 (2014).
258. Lowe, D.M., Redford, P.S., Wilkinson, R.J., O'Garra, A. & Martineau, A.R. Neutrophils in tuberculosis: friend or foe? *Trends in Immunology* **33**, 14-25 (2012).

259. Ito, R., Takahashi, T., Katano, I. & Ito, M. Current advances in humanized mouse models. *Cell Mol Immunol* **9**, 208-214 (2012).
260. Peyron, P.*, et al.* Foamy Macrophages from Tuberculous Patients' Granulomas Constitute a Nutrient-Rich Reservoir for M. tuberculosis Persistence. *PLoS Pathog* **4**, e1000204 (2008).
261. Nath, N., Khan, M., Paintlia, M.K., Hoda, M.N. & Giri, S. Metformin Attenuated the Autoimmune Disease of the Central Nervous System in Animal Models of Multiple Sclerosis. *The Journal of Immunology* **182**, 8005-8014 (2009).
262. Fox, G.J. & Menzies, D. Epidemiology of tuberculosis immunology. *Advances in experimental medicine and biology* **783**, 1-32 (2013).
263. Dye, C., Glaziou, P., Floyd, K. & Raviglione, M. Prospects for Tuberculosis Elimination. *Annual Review of Public Health* **34**, 271-286 (2013).
264. Morton, R. & White, R. *Phthisiologia: or, a treatise of consumptions.*, (printed for W. and J. Innys, 1720).
265. Root, H.F. The Association of Diabetes and Tuberculosis. *New England Journal of Medicine* **210**, 1-13 (1934).
266. Chen, L., Magliano, D.J. & Zimmet, P.Z. The worldwide epidemiology of type 2 diabetes mellitus - present and future perspectives. *Nat Rev Endocrinol* **8**, 228-236 (2012).
267. WHO. The Millennium Development Goals Report 2011. (2011).
268. Leeds, I.L.*, et al.* Site of Extrapulmonary Tuberculosis is Associated with HIV Infection. *Clinical Infectious Diseases* (2012).
269. Arinaminpathy, N., Cordier-Lassalle, T., Vijay, A. & Dye, C. The Global Drug Facility and its role in the market for tuberculosis drugs. *The Lancet* **382**, 1373-1379.

APPENDIX II – Copyright Permissions